GEORGIA DOT RESEARCH PROJECT 14-20

FINAL REPORT

IMPACT OF LRFD SEISMIC BRIDGE DESIGN FOR GEORGIA

OFFICE OF PERFORMANCE-BASED MANAGEMENT AND RESEARCH
15 KENNEDY DRIVE
FOREST PARK, GA 30297

TECHNICAL REPORT STANDARD TITLE PAGE

1. Report No.: FHWA-GA-19-1420	2. Government Accession No.:	3. Recipient's Catalog No.:
4. Title and Subtitle: Impact of LRFD Seismic Bridge Design for Georgia		5. Report Date: November 2018
		6. Performing Organization Code:
7. Authors: Reginald DesRoches, Ph.D.; Iris Tien, Ph.D.; CS Walter Yang, Ph.D.; Piyush Sood; Yijian Zhang; and Borja Zarco.		8. Performing Organ. Report No.:
9. Performing Organization Name and Address: School of Civil and Environmental Engineering Georgia Institute of Technology 790 Atlantic Drive Atlanta, GA 30332-0355		10. Work Unit No.:
		11. Contract or Grant No.: P.I. NO. 0013421
12. Sponsoring Agency Name and Address: Georgia Department of Transportation 600 Peachtree St NW, Atlanta, GA 30308		13. Type of Report and Period Covered: Final; January 2015–November 2018
		14. Sponsoring Agency Code:
15. Supplementary Notes:		

16. Abstract:

The objectives of this study were to evaluate the impact of AASHTO LRFD seismic detailing on Georgia bridges under various seismic hazards. Significant findings from this study are the following:

1. The analytical results show significant influences of lap-splice length, rebar size, and transverse reinforcement (TR) spacing on the ductility behavior of lap-spliced columns.
2. For multi-span simply supported concrete girder bridges, results for Site Classes A, B, and C show a lower than 25% probability of exceeding Limit State 1 with non-seismic TR spacing. For Site Class D, 3-in. TR spacing is recommended in Regions 1 and 2 to reduce the risk of exceeding Limit State 1 (initial longitudinal rebar yield) from 40.15% to 13.16% and 29.38% to 8.07%, respectively. For Site Class E, 3-in. TR spacing is recommended in Regions 1, 2, and 3 to reduce the risk of exceeding Limit State 1 from 68.53% to 33.87%, 51.39% to 19.88%, and 42.37% to 14.36%, respectively.
3. For multi-span continuous steel girder bridges, the 9-ft lap splice can be provided at the base of the column. 3-in. TR spacing is recommended to reduce the risk of exceeding Limit State 1 by 20-30% for Seismic Zone 2. Lap splice is not recommended for Zone 2.
4. For multi-span simply supported steel girder bridges, having one stirrup in each direction (two total legs in each plane) compared to two stirrups in each direction (four total legs in each plane) show less than a 2% difference in probability of exceeding defined limit states. Regions 1 and 2 for Site Classes B and C; Regions 1-3 for Site Class D; Regions 1-5 for Site Class E show relatively high risk values (>25%) of exceeding Limit State 1, and based on parametric studies of seismic risk from other bridge classes, reducing TR spacing is recommended.
5. For pile bents, for Seismic Zone 1, at least 12-in. embedment of piles into bents is the only requirement. The pile embedment length does not significantly affect the pile lateral strength.

6. The results of the seismic risk assessment on columns with varying TR spacing showed similar responses. The risk probabilities for the #3 @ 3 in., #6 @ 4 in., and #6 @ 6 in. cases for Georgia bridges are similar, with a difference of approximately 5% under the maximum factored peak ground acceleration of 0.35 g in Georgia.			
17. Key Words: AASHTO LRFD design, lap splice, pile-to-bent connections, seismic hazard and risk analyses, MSSS concrete bridges, MSC steel bridges, MSSS steel bridges, and MSSS slab bridges		18. Distribution Statement:	
19. Security Classification (of this report): Unclassified	20. Security Classification (of this page): Unclassified	21. Number of Pages: 120	22. Price:

Form DOT 1700.7 (8-69)

GDOT Research Project No. 14-20

Final Report

IMPACT OF LRFD SEISMIC BRIDGE DESIGN FOR GEORGIA

By

Reginald DesRoches, Ph.D., Principal Investigator
Iris Tien, Ph.D., co-Principal Investigator
Chuang-Sheng Walter Yang, Ph.D., P.E., Research Engineer
Piyush Sood, Graduate Research Assistant
Yijian Zhang, Graduate Research Assistant
Borja Zarco, Graduate Research Assistant

School of Civil and Environmental Engineering
Georgia Institute of Technology

Contract with

Georgia Department of Transportation
In Cooperation with
U.S. Department of Transportation
Federal Highway Administration

November 2018

TABLE OF CONTENTS

LIST OF TABLES

LIST OF FIGURES

EXECUTIVE SUMMARY

Before the switch in design specifications from Standard Specifications to the fifth edition of the American Association of State Highway and Transportation Officials (AASHTO) Load and Resistance Factor Design (LRFD) Bridge Design Specifications in 2010, few bridges in the state of Georgia were designed with seismic detailing. Recent 2014 LRFD specifications increased the number of Georgia bridges requiring seismic design and details, with the state of Georgia being identified as a region with seismic activity leading to estimated maximum peak ground accelerations of 0.34 g in Site Class E. The purpose of this study is to investigate the need for these increased seismological design requirements for bridges in the state of Georgia based on their dynamic characteristics, local soil conditions, and ground motion frequency contents. Three of the most common factors for a possible deficiency in performance in a possible seismic event arise from lap splice at column bases, inadequate transverse reinforcement in the column hinge zones, and insufficient embedded length of piles into bents. Therefore, these design parameters and their influences on seismic risk are investigated in detail in this study.

In this study, the performance of representative bridges from different bridge classes in Georgia is investigated to estimate the expected seismic behavior considering the latest AASHTO LRFD Bridge Design Specifications [1]. The responses are compared with the previously used design practices in Georgia's Bridge and Structures Design Manual. Different cases of varying lap splice length, seismic and non-seismic transverse reinforcement spacing, and seismic and non-seismic pile bents are compared based on nonlinear time history analyses. Probabilistic analysis is performed through analyzing these bridges under a suite of 48 ground motions to compare the component capacity against the imposed demand of the columns and piles. Seismic damage risk

estimates computed through the probabilistic analyses for different seismic site classes and for different regions in the state are used to make recommendations on the bridges to be built in the future in the state of Georgia. The primary conclusions from this study are given below. Conclusions 3-6 are based on results from analyses conducted by bridge type.

1. The analytical results show significant influences of lap-splice length, rebar size, and transverse reinforcement (TR) spacing on the ductility behavior of lap-spliced columns.

2. For all bridge classes, lap splice at the base of the column with 12-in. TR spacing is acceptable for the lowest Seismic Zone 1A (SD1<0.10). (Note: SD1 = the design spectral response acceleration parameter at 1-s period)

3. For multi-span simply supported concrete girder bridges, results for Site Classes A, B, and C show a lower than 25% probability of exceeding Limit State 1 with non-seismic TR spacing. For Site Class D, 3-in. TR spacing is recommended in Regions 1 and 2 to reduce the risk of exceeding Limit State 1 (initial longitudinal rebar yield) from 40.15% to 13.16% and 29.38% to 8.07%, respectively. For Site Class E, 3-in. TR spacing is recommended in Regions 1, 2, and 3 to reduce the risk of exceeding Limit State 1 from 68.53% to 33.87%, 51.39% to 19.88%, and 42.37% to 14.36%, respectively.

4. For multi-span continuous steel girder bridges, the 9-ft lap splice can be provided at the base of the column. 3-in. TR spacing is recommended to reduce the risk of exceeding Limit State 1 by 20-30% for Seismic Zone 2. Lap splice is not recommended for Zone 2.

5. For multi-span simply supported steel girder bridges, the risk values comparing the case of one stirrup in each direction (two total legs in each plane) and two stirrups in each direction (four total legs in each plane) with #6 at 6-in. transverse reinforcement are investigated.

The results show that there is less than 2% difference in probability of exceeding defined limit states between the two cases. Regions 1 and 2 for Site Classes B and C; Regions 1-3 for Site Class D; Regions 1-5 for Site Class E show relatively high risk values (>25%) of exceeding Limit State 1, and based on parametric studies of seismic risk from other bridge classes, reducing transverse spacing is recommended.

6. For pile bents, for Seismic Zone 1, at least 12-in. embedment of piles into bents is the only requirement. The specifications do not include the pile sizes and corresponding embedment lengths, which are consistent with the experimental results, if bents are designed appropriately. The pile embedment length does not significantly affect the pile lateral strength.

7. The results of the seismic risk assessment on columns with varying TR spacing showed similar responses. The risk probabilities for the #3 @ 3-in., #6 @ 4-in., and #6 @ 6-in. cases for Georgia bridges are similar, with a difference of approximately 5% under the maximum factored PGA of 0.35 g in Georgia

ACKNOWLEDGEMENTS

The authors thank the Georgia Department of Transportation (GDOT) for support of this research under Research Project 14-20. The authors also thank Bill DuVall and Steven Gaston for providing drawings of bridges in Georgia and their valuable insights on bridge design practices.

LIST OF VARIABLES

p	Perimeter of the characteristic concrete block for rectangular and circular column
s_l	Center-to-center spacing between the longitudinal bars
d_b	Diameter of the longitudinal bars
c	Clear concrete cover
n	Number of evenly distributed longitudinal bars around the core
D	Diameter of the core concrete
T_b	Maximum force developed in the longitudinal reinforcement bar
f_t	Concrete tensile strength
A_b	Cross-sectional area of longitudinal bar
l_s	Length of lap splice
f_s	Maximum stress capacity developed in lap splice section
f_r	Residual stress of lap splice section
μ	Frictional factor
n_l	Number of transverse reinforcement legs perpendicular to the cracked plane
n_t	Number of transverse reinforcement bars crossing the cracked plane
A_h	Crack surface area

f_h Yield strength of the transverse reinforcement

u Slip displacement

ε_s Total strain at the peak stress

E_S Elastic modulus of the rebar

l_{ss} Fictitious length

ε_r Residual strain of lap splice section

PGA Peak ground acceleration

S_S Short-period spectral acceleration

S_1 Long-period spectral acceleration

F_{PGA} Site adjustment factors for PGA

F_a Site adjustment factors for short-period spectral acceleration

F_v Site adjustment factors for long-period spectral acceleration

A_S Peak seismic ground acceleration coefficient modified by short-period site factor

S_{DS} Horizontal response spectral acceleration coefficient at 0.2-s period modified by short-period site factor

S_{D1} Horizontal response spectral acceleration coefficient at 1.0-s period modified by short-period site factor

S_a Spectral acceleration in unit of gravitational acceleration g

C_{sm} Elastic seismic response coefficient for the m^{th} mode of vibration

T_m Period of vibration for m^{th} mode (s)

T_o Reference period used to define shape of acceleration response spectrum (s)

T_s Corner period at which acceleration response spectrum changes from being independent of period to being inversely proportional to period (s)

F Fragility function

D Demand of the structural component

C Capacity of the component

IM Intensity measure of the hazard

$\Phi(\cdot)$ Standard normal cumulative distribution function

S_d Median parameter of the demand random variable

S_c Median parameter of the capacity random variable

β_d Lognormal standard deviation of the demand random variable

β_c Lognormal standard deviation of the capacity random variable

I_f Indicator function that tracks the number of failed samples

LS Limit state

N	Number of random sample generated from capacity and demand distributions
$\mu_{\emptyset}$	Curvature ductility
κ_{max}	Maximum curvature observed in the column under seismic shaking
κ_{yield}	Column yield curvature
EDP	Engineering demand parameters
a, b	Coefficients obtained from the linear regression analysis of the model
k_0	Initial stiffness of the bearing
h_r	Height of the bearing pad
μ_f	Frictional coefficient
σ_m	Normal stress on the bearing pad due to the superstructure
V_{fuse}	Fuse capacity for steel bearings
ϕ	Strength reduction factor
F_u	Ultimate tensile strength of the material
A_{bs}	Effective cross-sectional area of the shear element
$f_{ys}\ (or\ f_y)$	Yield stress of steel.

CHAPTER 1 INTRODUCTION

1.1 Problem Description

The AASHTO LRFD Bridge Design Specifications [1] include extensive seismic design provisions. While earthquakes are considered primarily a problem on the West Coast of the United States, geologists have observed ongoing tectonism in the southeastern region [2]. The southeastern United States has historically seen some of the largest earthquakes, e.g. the 1811–1812 New Madrid earthquakes and the 1886 Charleston earthquake. Because Georgia lies in the vicinity of this active seismic region, potential seismic hazard is identified in the state with estimated maximum peak ground accelerations of 0.34 g in Site Class E. Recent studies [3] have shown that seismic risk in Georgia, even though low, can impose significant demands on some bridges depending on their dynamic characteristics. Furthermore, seismic provisions of the 2014 AASHTO LRFD Bridge Design Specifications [1] have been integrated with Georgia's Bridge and Structures Design Manual [4] as part of the design specifications. This combination has led to an increase in the number of bridges affected in Georgia by the LRFD Specifications. However, there has not been significant practical experience with damage or failure to bridges from seismic events to demonstrate the necessity of this change. Therefore, there is the need to evaluate the seismic performance and associated damage risk of Georgia's bridges to the seismic hazard present in the state. This is done through studying the impact of the latest developments in the LRFD Specifications on these structures.

The latest 2014 AASHTO LRFD Bridge Design Specifications [1] recognize the seismic hazard return period to be equal to 1000 years instead of the previously adopted return period of 500 years. This has resulted in a shift of boundaries of seismic performance zones. According to

the latest code, the upper boundary for spectral acceleration (at 1.0 second) for Seismic Zone 1 is 0.15 g as opposed to 0.10 g in the previous AASHTO Specifications (2011). The code has increased seismic design requirements defined for Seismic Zones 2, 3, and 4. However, the change in the spectral acceleration boundaries has led to some ambiguity regarding the seismic detailing requirements, specifically for lap splice and transverse reinforcement spacing, for Seismic Zone 1 when the spectral acceleration is between 0.10 and 0.15 g.

Lap splices are an essential part of reinforced concrete structures as they help to maintain the continuity between the structural members. It has been customary to provide lap splices at the bottom of the bridge columns to maintain continuity of the connection with the foundations. During earthquake events, column connections with other bridge components, such as foundations and bent caps, are subjected to significant moments that lead to tensile stresses in the longitudinal reinforcement. If a lap splice is present at these locations, it results in splitting bond failure due to stiffness degradation and low deformation capacity [5,6]. Furthermore, inadequate lap splice length combined with widely spaced transverse reinforcement worsens the seismic performance of these columns. Adequate transverse confinement is necessary to develop a bond between the longitudinal bars and surrounding concrete, so that the transfer of force between the two spliced bars happens effectively. Previous research has shown that the lack of adequate transverse reinforcement leads to low flexural strength, low shear strength, and low ductility, which result in a higher damage risk.

In recent decades, seismic fragility curves have been used extensively to evaluate the damage risk associated with bridge components and the structure as a whole [7–10]. Fragility curves depict the conditional probability of a structural component reaching or exceeding a limit state given the intensity measure of the earthquake. Researchers have developed several ways to

quantify the vulnerability of structures [9,10]. Analytical fragility curves are utilized in this study to assess the impact of the latest AASHTO LRFD Bridge Design Specifications [1] on highway bridges in Georgia. These curves are used to estimate the associated seismic damage risk as a function of seismic hazard levels in various regions in the state.

1.2 Objectives and Scope of Research

The goal of this research is to evaluate the seismic performance and fragility of multi-span highway bridges of varying classes in Georgia considering the latest AASHTO LRFD seismic design provisions. Based on the results, the study aims to provide recommendations to the Georgia Department of Transportation (GDOT) regarding seismic detailing for multi-span bridges to be built in the future.

The following are the specific tasks that have been completed in this research:

1. Review commonly used detailing practices in the Bridge and Structures Design Manual [4] in the current design codes and compare them with the latest seismic design provisions in AASHTO LRFD Bridge Design Specifications [1].

2. Perform a literature review of previous research on seismic detailing, including the impacts of lap splice and transverse reinforcement on column performance. To analyze the effect of lap splices, develop a stress–strain curve for the lap-spliced section based on the truss-based force transfer mechanism model to evaluate its impact on columns.

3. Develop seismic hazard maps and design response spectra for various regions in the state of Georgia to estimate the expected peak ground accelerations (PGA) in these regions.

4. Develop three-dimensional analytical models of selected multi-span bridges based on Georgia bridge plans and models of lap splice and transverse reinforcement to assess their seismic performance.

5. Perform deterministic seismic analyses considering the current practices used in Georgia and the latest AASHTO LRFD Bridge Design Specifications [1] to assess the performance differences between the two sets of design guidance.

6. Generate probabilistic seismic demand models and fragility curves as a function of lap splice length and transverse reinforcement spacing to estimate the associated seismic damage risk.

7. Provide recommendations to GDOT for bridges to be built in the future based on the obtained results.

1.3 Outline

The report is organized into eight chapters:

Chapter 2 presents an overview of past research conducted on seismic detailing highlighting the importance of providing adequate lap splice and transverse reinforcement, especially in columns in seismically active regions. This chapter also presents the stress–strain formulation used to study the lap splice behavior and effects of various geometric parameters on the lap splice strength.

Chapter 3 presents assessments of the seismic hazard for Site Classes A, B, C, D, and E in the state of Georgia. The state is divided into six regions based on the potential peak ground

acceleration in these regions. This chapter further provides an overview of the bridge inventory in the state of Georgia.

Chapter 4 summarizes the mathematical framework employed to formulate the analytical fragility curves in the study, along with the limit state capacity and probabilistic seismic demand model definitions.

Chapter 5 presents the characteristics of the representative bridges investigated for each of the three bridge classes analyzed in the study: (1) multi-span simply supported concrete girder bridges, (2) multi-span continuous steel girder bridges, (3) and multi-span simply supported steel girder bridges. This chapter further explores the effect of lap splice and transverse reinforcement spacing on the columns and bearings of the bridge.

Chapter 6 presents the seismic fragility curves for each of the bridge classes. It evaluates the site-specific fragility damage risk estimates for columns to determine the appropriate seismic detailing requirements in terms of lap-splice and pile-bent specifications for various regions in the state of Georgia.

Chapter 7 presents the effects of the AASHTO LRFD required transverse reinforcement spacings on column responses.

Chapter 8 presents the key contributions of the research, along with recommendations based on the analysis results.

CHAPTER 2 LAP SPLICE REINFORCEMENT AND TRANSVERSE REINFORCEMENT

Studies on lap splices began in the mid-1970s when several bridge columns suffered severe damage and collapse during moderate-intensity earthquakes. Researchers conducted experimental tests to investigate the impact of lap-splice lengths and transverse detailing on column strength and ductility. Following an introductory section, this chapter provides a summary of those studies and highlights the impacts of lap splice lengths and transverse reinforcement detailing on column strength and ductility. The third section of this chapter presents a lap splice formulation that is used in assessing the bridge fragilities. Finally, a parametric study is presented to investigate the effects of variables that affect the strength of a seismically detailed section compared to a non-seismically detailed section.

2.1 Introduction

This study focuses on seismic detailing of highway bridges located in the state of Georgia. Many of these bridges were built before specifications for seismic design such that lap splices were often at the column bases and transverse reinforcement was widely spaced. Therefore, these factors lead to increased potential seismic risk for bridges built before 1970. The first instance of the need for seismic detailing was recognized in the San Fernando earthquake in 1971. Despite being considered an earthquake of moderate intensity, it led to the collapse of five freeways. More recent examples include the upper deck failure of the Cypress viaduct of Interstate 880 after the Loma Prieta earthquake in 1989. As shown in Figure 2.1, the columns of the viaduct could not support the superstructure, leading to the death of 42 people by falling roadway. Most of the other bridges

that collapsed in the Loma Prieta earthquake were constructed before 1971 and lacked seismic detailing requirements [11].

Figure 2.1 – Column Failure Leading to Substructure Collapse of Cypress Viaduct in Oakland, California.

A similar type of failure was identified in the 1995 Kobe, Japan, earthquake in which a 630 m intermediate segment of the Hanshin Expressway supported by 18 circular columns failed, as shown in Figure 2.2. Post-earthquake investigations revealed that poor transverse column reinforcement, improper anchorage of longitudinal reinforcement, and lack of study of soil-structure interactions led to overturning of the complete bridge in the transverse direction [12]. Investigators also found that the longitudinal reinforcement bars joined together using butt welding at the base of the columns lacked flexural strength, which was a cause of failure.

(a) **(b)**

Figure 2.2 – Overturning Failure of Bridge Segment on Hanshin Expressway due to Inadequate Transverse Reinforcement, Improper Longitudinal Reinforcement Anchorage, and Soil-Structure Interactions.

The substructure for any bridge plays an important role in transferring all types of loads imposed on the bridge to the ground. Failure of seismically inadequate columns has led to severe damage or collapse of bridges in the past. Of course, the seismic hazard in the state of Georgia differs from these cases. However, the risk in Georgia and recent LRFD Specifications warrant an in-depth analysis of column detailing in Georgia relative to the seismic risk of bridges.

2.2 Literature Review

The earliest experimental research on lap splices was conducted by Orangun et al. [13], who developed an empirical design equation for development and lap splice length in terms of steel stress, concrete strength, bar diameter, concrete cover, and transverse reinforcement. This

equation was adopted into the 1989 American Concrete Institute (ACI) Building Codes. These equations were later revised by experimental tests carried out by Sozen and Moehle [14].

In the same decade, Cairns and Arthur carried out an experimental test in which they evaluated responses from 51 columns with smooth and roughened longitudinal bars under lateral cyclic loading [15]. The conclusion from their research was that lap-spliced sections in tension and compression have significantly different responses. Further, columns with roughened bars performed significantly better than columns with smooth bars.

Studies by Paulay et al. revealed the importance of confinement by transverse reinforcement in spliced column sections [16]. They performed experimental tests on 12 specimens and found that despite insufficient lap splice length, well-confined columns could develop tensile yield stress in the longitudinal reinforcement and maintain their lateral load capacity up to high displacement ductility of about 4.

Lynn et al. investigated the impact of longitudinal reinforcement ratio and transverse spacing on lap-spliced columns from pre-1970 [17]. The test specimens included eight 18-inch-square columns out of which five had continuous reinforcement and three had lap splices at the bottom of the columns. These columns were subjected to reversed cyclic lateral displacements under a vertical load. The findings of the research revealed that the columns with a low reinforcement ratio subjected to low axial stresses showed a ductile response with a displacement ductility up to 4.2. However, ultimately the columns with a lap splice failed in shear due to cracks developed along the lap splice. On the other hand, the columns subjected to high axial stresses showed brittle failure, irrespective of the presence of a lap splice, shortly after reaching the yield strength.

Melek and Wallace [18] conducted a similar study to examine the effects of lap-splices on short columns through experimental tests. The columns in their experiments were subjected to lateral cyclic loading while under axial compression, as shown in Figure 2.3. Their findings revealed that inadequate confining reinforcement led to bond deterioration between reinforcement bars and surrounding concrete. This led to steep degradation in the strength of columns at lateral drift ratios of 1.0% to 1.5%. Later, Cho and Pincheira proposed an analytical modeling approach using different bond–slip relationships [19] to match the experimental results by Melek and Wallace [18].

Figure 2.3 – Test Setup Used by Melek and Wallace [18] for Lateral Cyclic Loading of Columns.

Another study to investigate the effect of lap splices on beams was conducted by Harajli et al. [20]. They evaluated the stress–strain relationship based on the bond–slip behavior between steel and concrete when the beams were subjected to a four-point flexural test with the lap splice in the middle. Wu et al. conducted a similar study on lap-spliced beam sections with enamel-coated reinforcing bars and found that enamel coating increases the bond strength of deformed rebars in normal strength concrete [21].

Recently, studies have been conducted to evaluate the response of lap-spliced sections in high-strength concrete members [22–24]. These studies show a similar response to earlier specimens and highlight the importance of adequate lap splice lengths and transverse detailing for improved column performance. While these studies mostly focus on the strength evaluation in the lap splice sections, several studies have been carried out to improve the strength of lap-spliced columns and beams through steel and fiber-reinforced polymer (FRP) jacketing [25–27].

All of these studies reveal a significant need for adequate lap splice length and transverse detailing to improve the response of columns under lateral cyclic loading. The objective of this study is to assess the impacts of these parameters on seismic performance for highway bridges in Georgia with non-seismic details compared to the latest AASHTO LRFD Bridge Design Specifications [1] by the means of fragility curves.

2.3 Lap Splice Formulation

The force transfer phenomenon in a lap-spliced section follows a complex mechanism (Figure 2.4(a)). However, simplifications can be made based on mechanistic principles to model its behavior. Traditionally, two mechanisms have been used to do this: bond mechanism and truss mechanism [28]. In a structural member, both mechanisms act together. For modeling purposes, it is fair to assume that either of the mechanisms dominates.

The basic principle of the bond mechanism is that the lugs on the reinforcement bar exert a bearing force on the surrounding concrete at an angle. The component of this force parallel to the axis of the rebar causes shearing stress in the concrete, and the normal component of this force exerts a radial stress on concrete causing splitting of concrete. When the resultant stress exceeds

the tensile capacity of concrete, the concrete is no longer able to take the bearing force exerted by the reinforcement lugs, and failure of the section occurs.

In the truss mechanism, a simple truss model is used to calculate the force transfer between the lap-spliced bars and the surrounding concrete. Priestley et al. [29] proposed the truss system methodology to model the approximate response of the longitudinal reinforcement in a lap-spliced section in tension. Tariverdilo et al. [30] used the truss mechanism model to evaluate the fragility functions for reinforced concrete (RC) frames with lap-spliced columns and matched the results with the experimental work done by Aboutaha et al. [25] and Melek and Wallace [18]. They concluded that the truss model adequately captures the maximum strength and post-peak softening behavior of spliced sections. Canbay and Frosch suggested a similar approach to evaluate the lap splice behavior. Their model, however, also included some empirical factors [31]. The model used in this study is based on the analytical formulation and as suggested by Priestley et al. [29].

Figure 2.4(b) represents the stress–strain model behavior of the truss system to model the approximate response of the lap-spliced bars. In this model, the lap splice section reaches the maximum peak strength, $f_{s,max}$, until the surrounding concrete splits. At that point, the section experiences a steep softening behavior due to splitting of surrounding concrete until it reaches the point of constant frictional stress, f_r, developed across the failure interface. The corresponding strain values are ε_s and ε_r, respectively.

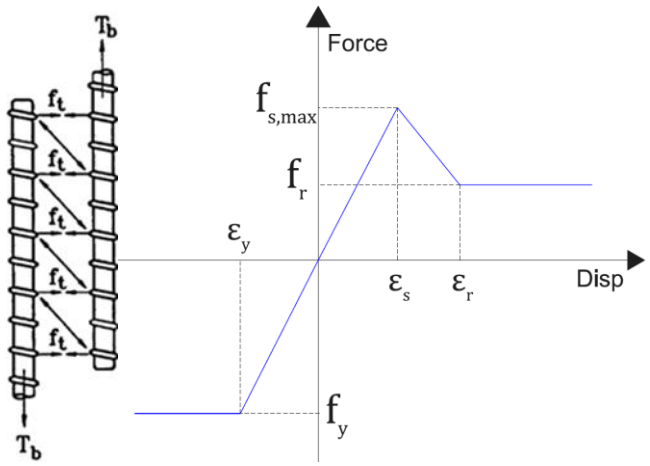

(a) **(b)**

Figure 2.4 – Lap Splice Reinforcement: (a) Mechanism, and (b) Stress–Strain Curve for a Numerical Model.

The truss analogy assumes development of a uniform compressive field across the spliced bars at an angle approximately equal to 45°. The concrete surrounding the lap splice acts as compression struts to transfer the load between the bars. The mechanism considers the lap splice failure by considering the formation of fracture surfaces perpendicular to the column surface to allow the relative movement between bars. With each longitudinal bar, an associated characteristic concrete block, as depicted in Figure 2.5, of length equal to the lap splice length, l_s, and perimeter, p, is assumed to contribute to the splice strength.

The perimeter, p, of the characteristic concrete block for rectangular and circular column cross section can be calculated as follows:

$$p = \frac{s_l}{2} + 2(d_b + c) \leq 2\sqrt{2}\,(d_b + c) \qquad (1)$$

where s_l is the center-to-center spacing between the longitudinal bars, d_b is the diameter of the longitudinal bars, and c is the clear concrete cover. For a circular column cross section, the perimeter of the characteristic block can be written as:

$$p = \frac{\pi D}{2n} + 2(d_b + c) \leq 2\sqrt{2}\,(d_b + c) \tag{2}$$

where n is the number of evenly distributed longitudinal bars around the core of diameter, D, of the column. MacKay et al. concluded that the confined concrete did not add much to the lap splice strength in the case of cyclic loading; hence, the derivation ignores the strength contribution to the lap splice section due to the confined concrete [32].

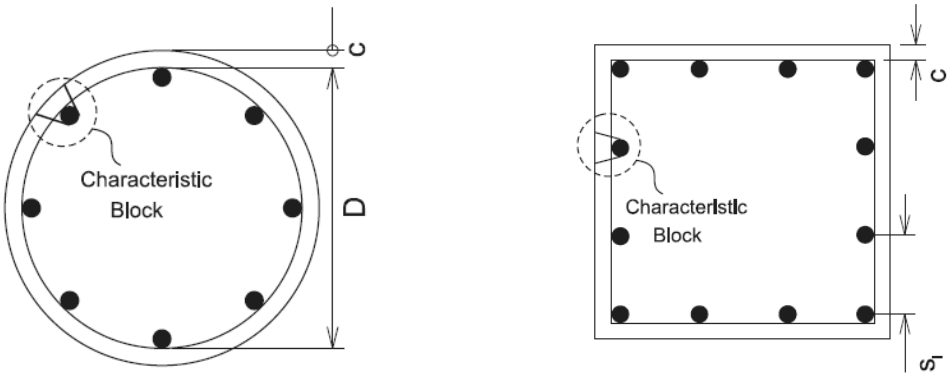

(a) **(b)**

Figure 2.5 – Characteristic Block for (a) Circular, and (b) Square Column.

Thus, satisfying the equilibrium of the free body diagram of the system, the maximum force, T_b, in the longitudinal reinforcement bar can be expressed in terms of concrete tensile strength, f_t, as follows:

$$T_b = A_b\, f_s = f_t\, p l_s \tag{3}$$

where A_b is cross-sectional area of longitudinal bar, p is perimeter of cylindrical block, and l_s is length of lap splice. Once the lap splice section reaches its maximum stress capacity, f_s, the stress drops down to a constant value of residual stress, f_r. The residual stress can be calculated by the shear-friction concept by estimating the shear force contribution by the transverse reinforcement crossing the cracked plane as follows:

$$\mu n_l n_t A_h f_h = n A_b f_r \tag{4}$$

where μ is frictional factor, which is taken as 1.4, n_l denotes the number of transverse reinforcement legs perpendicular to the cracked plane, n_t the number of transverse reinforcement bars crossing the cracked plane, A_h the crack surface area, f_h the yield strength of the transverse reinforcement, and n the number of longitudinal rebars in the tension side of the column.

The strain can be taken equal to the elastic yield strain of the bar; however, Tariverdilo et al. assumed an additional slip displacement, u, equal to 1 mm at yield point that must be added to the elastic strain [30]. This additional displacement is assumed to occur due to the bar slip over a fictitious length, l_{ss}. This length is different from the lap splice length. Tariverdilo evaluated the impact of lap splice on estimated risk of reinforced concrete columns assuming that the slip occurs over a length equal to the depth of the column section [30]. Thus, the total strain at the peak stress can be written as:

$$\varepsilon_s = \frac{f_s}{E_S} + \frac{u}{l_{ss}} \quad (5)$$

where E_S is the elastic modulus of the rebar.

At residual stress, f_r, the strain, ε_r, is calculated by assuming a slip, u, equal to 10 mm that is approximately equal to the lug distance on the bar and can be written as:

$$\varepsilon_r = \frac{u}{l_{ss}} \quad (6)$$

2.4 Effects of Variables on the Strength of Lap Splice Reinforcement

From the equations discussed in Section 2.3, the lap splice strength is a function of several variables, such as lap splice length, column cross section, reinforcement ratio, etc. Therefore, it is desirable to investigate the impacts of these variables on the lap splice strength. The following subsections present a parametric study on the strength of the lap splice due to each of these variables. To isolate the effect of one variable, other variables are kept constant and equal to the most commonly used values in Georgia bridge columns.

2.4.1 Effect of Lap Splice Length

An adequate lap splice length is required to transfer the force from one rebar to another in a spliced section. While most of the experimental tests on lap splice lengths show that it has an important role to play in the splice strength, Paulay stated that increasing length of a lap splice in columns in case of cyclic loading is of very little benefit because of the “unzipping” effect [33].

Despite the plethora of research on the impact of lap splices, there is no clear agreement between the relation of the lap splice length and column capacity. In this study, this relation is investigated using a numerical analysis.

From Equation 3, the maximum stress developed in the lap splice is directly proportional to its length. In the present study, the effect of length of the spliced section is evaluated for the range of commonly used splice spacing in the state of Georgia. The inventory analysis revealed that older highway bridge columns in Georgia used lap splices as short as 4.5-ft However, the most commonly used lap splice lengths are 6.5-ft and 9-ft. Figure 2.6 shows the stress–strain plot for these two lap splice lengths for a typical bridge column layout used in Georgia. This column has a height of 18-ft and cross-sectional dimensions of 3-ft by 3-ft. The transverse reinforcement spacing is 12-in.

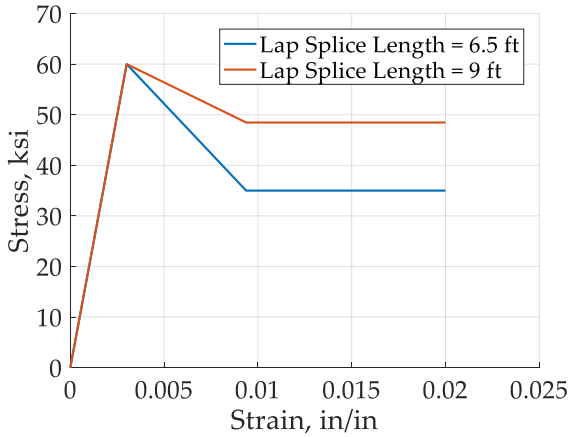

Figure 2.6 – Lap Splice Stress–Strain Plot for Commonly Used Splice Lengths of 6.5-ft and 9-ft in Georgia.

Figure 2.7 also shows the impact of the lap splice lengths ranging from 4-ft to 14-ft. on the peak stress and residual stress of the lap splice of the same column. Interestingly, the peak stress is not affected by the change in length of the spliced section. On the other hand, the residual stress

shows a steep increase as the length of the lap splice increases. For this column configuration, the residual strength of the spliced section matches the peak strength at about a lap splice length of 11-ft. Note that f_{ys} is yield strength of steel.

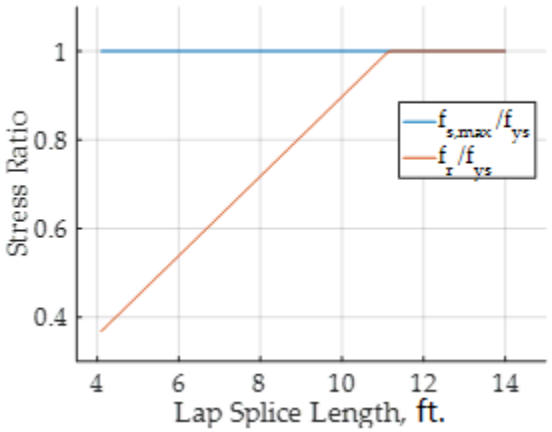

Figure 2.7 – Effect of Change in Lap Splice Length on Peak and Residual Stress of Spliced Section.

2.4.2 Effect of Transverse Reinforcement

Hamad and Najjar have documented the effects of transverse reinforcement on a spliced section through experimental tests [22]. Their research revealed that the presence of adequate transverse reinforcement helps reduce cracking along the lap splice length, significantly improving the ductility of the columns. This is in agreement with the findings of many other researchers who used experimental results to assess the effect of confinement on lap splices [24,34].

Adequate transverse reinforcement spacing not only helps to confine the core concrete in a structural member but also allows the lap splice section to develop enough shear friction after its strength goes past the peak strength. This effect depends on the type (such as hoops, spiral, or ties) and shape (such as circular, square, or rectangular) of confining transverse reinforcement. To

model the effect of confinement on concrete, a widely accepted stress–strain model of concrete formulated by Mander et al. is used in this study [35]. The effect of confinement on the post-peak lap splice strength is evaluated using Equation 4.

Before the introduction of the AASHTO LRFD Bridge Design Specifications [1] into the GDOT manual [4], the most commonly used reinforcement spacing for Georgia bridge columns was 12-in. (see Figure 2.8). However, the latest seismic design provisions suggest that the transverse spacing should not exceed one-quarter of the minimum member dimension or 4-in. center-to-center. In the present study, the effect of transverse reinforcement spacing is studied for the lap splice length of 6.5-ft. The column reinforcement detailing for this case is as it was in Section 2.4.1.

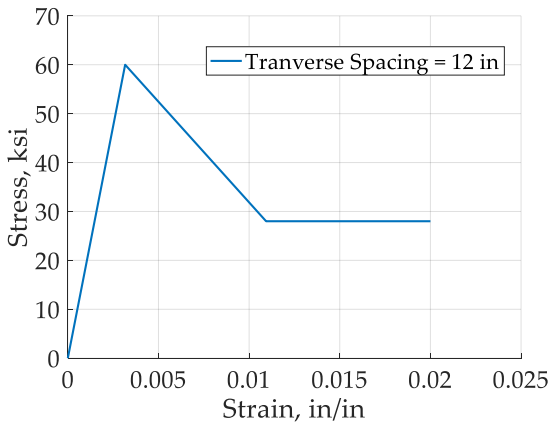

Figure 2.8 – Lap Splice Stress–Strain Plot for Commonly Used Transverse Spacing of 12-in. in Georgia.

Figure 2.9 depicts the effect of transverse spacing on the lap splice behavior. Similar to the effect of the lap splice length, the peak strength is not affected by the change in transverse reinforcement spacing. On the other hand, the residual strength of the lap splice drops considerably as the transverse reinforcement spacing exceeds about 5.5-in. for this cross section.

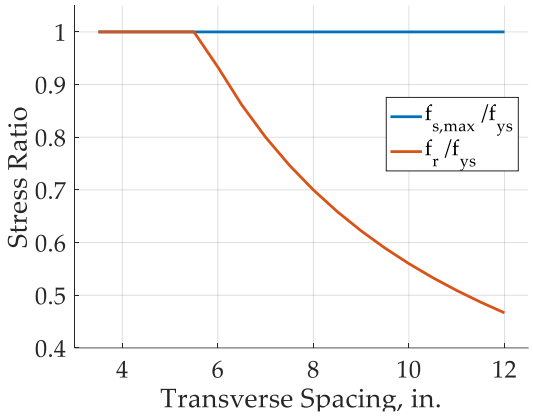

Figure 2.9 – Effect of Change in Transverse Reinforcement Spacing on Peak and Residual Stress of Spliced Section.

2.4.3 Effect of Steel Yield Strength

According to Equation 4, the steel yield strength plays an important role in development of the bond between the steel rebars and the surrounding concrete. The steel strength governs the level of forces that can be transferred through the steel–concrete interface in a spliced section. Moreover, the stress–strain curve of the steel reinforcement also governs the bond slip and strength characteristics, which can lead to splitting and shear failures.

The commonly used longitudinal steel rebars in Georgia bridge columns have yield strengths of either 40 ksi or 60 ksi. Figure 2.10 shows the variation of stress and strain for varying yield strengths.

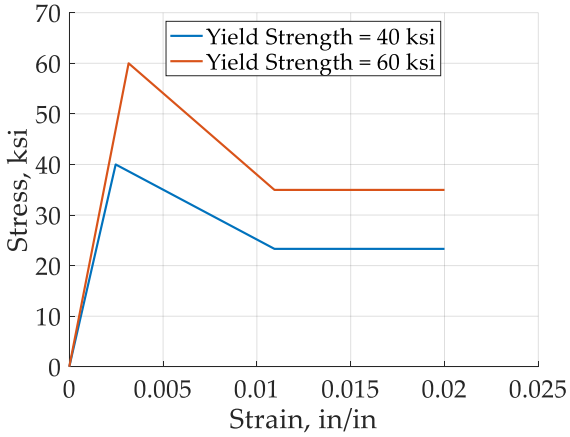

Figure 2.10 – Lap Splice Stress–Strain Plot for Commonly Used Steels in Georgia.

2.4.4 Effect of Rebar Diameter

In addition to the yield strength, the diameter of the reinforcement bars also affects the stress–strain curve of a spliced section. The ratio of cross-sectional to surface area of the rebar is directly proportional to the diameter of the rebar. This ratio impacts the bond stress concentration in the rebar.

The most commonly used rebar size for Georgia bridges is #11. Figure 2.11 shows the stress–strain curve for a typical Georgia column when 12 equally spaced #11 rebars are used as longitudinal reinforcement.

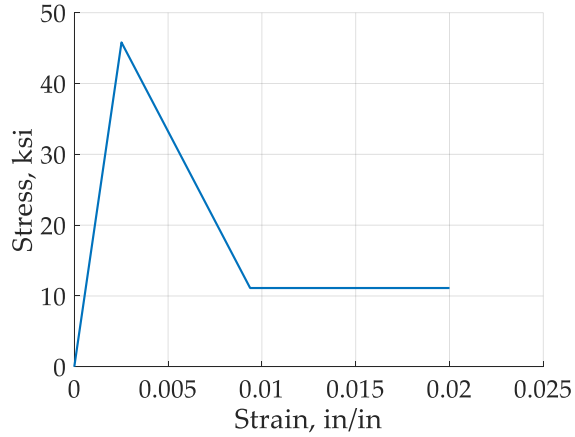

Figure 2.11 – Lap Splice Stress–Strain Plot for Commonly Used #11 Rebar in Georgia.

Additionally, Figure 2.12 shows the effect of the rebar diameter on the lap splice. Larger diameters for spliced sections show a steep reduction in residual stress that could lead to ductility degradation of the structural member. The steep reduction in the post-peak strength is due to larger bond stress concentrations resulting from a greater cross-section area to surface area ratio for larger diameter rebars.

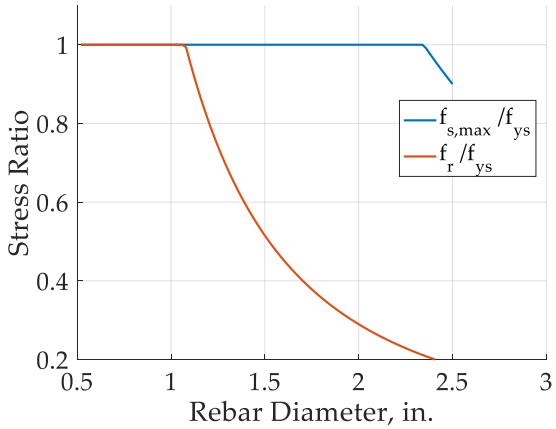

Figure 2.12 – Effect of Change in Longitudinal Rebar Diameter on Peak and Residual Stress of Spliced Section.

2.5 Effects of Transverse Reinforcement on Concrete and Reinforcement

The provisions 5.10.11.4.1d and e in the 2014 AASHTO LRFD Bridge Design Specifications [1] specify that the cores of columns and pile bents must be confined by transverse reinforcement in the expected plastic hinge regions. The spacing of the transverse reinforcement must be taken as specified in provision 5.10.11.4.1e. The main function of the transverse reinforcement specified in these provisions is: (1) to ensure that the axial load carried by the column after spalling of the concrete cover will at least equal the load carried before spalling, and (2) to ensure that buckling of the longitudinal reinforcement is prevented.

In this section, seismic-designed columns (#5 bars @ 4-in. o.c. transverse reinforcement) are compared to non-seismic-designed columns (#4 bars @ 12-in. o.c. transverse reinforcement), in both square and circular configurations. The columns used are based on typical Georgia bridges, using a concrete strength of 3500 psi and steel yield strength of 60,000 psi. Column details are shown in Figure 2.13, and all columns are 192-in. (16-ft) in height.

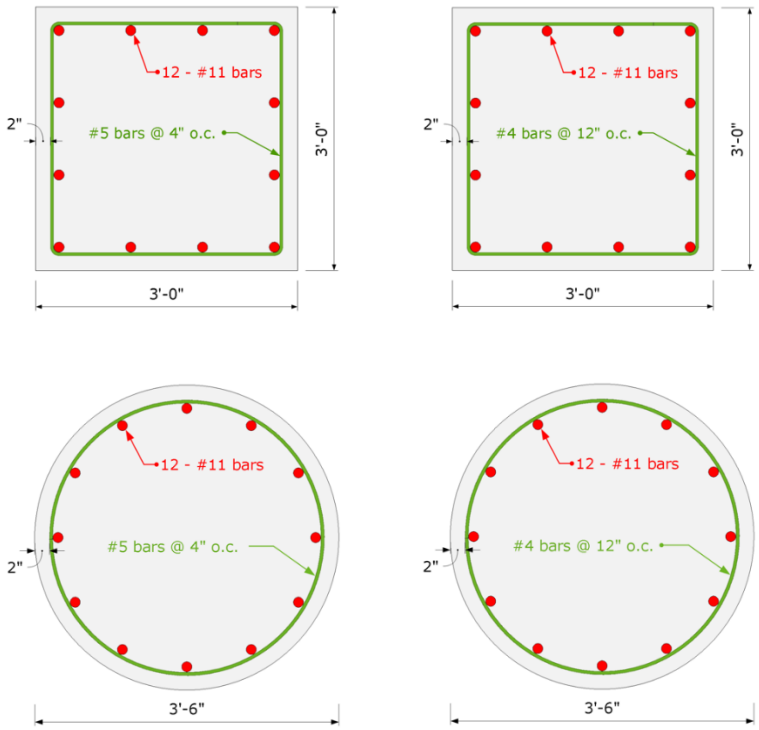

Figure 2.13 – Typical GA Columns with 4-in. vs. 12-in. Spacings.

First, a material analysis was performed, as shown in Figure 2.14. Confinement provided by the transverse reinforcement is clearly represented, and circular sections show better confinement than squared sections, as expected. The impact of the transverse reinforcement spacing on the longitudinal steel's buckling behavior on the compression side is evident. Additional analyses comparing performance of columns with various transverse reinforcement spacings in the plastic hinges, including #3 @ 3-in., #6 @ 4-in., and #6 @ 6-in., are presented in Chapter 7.

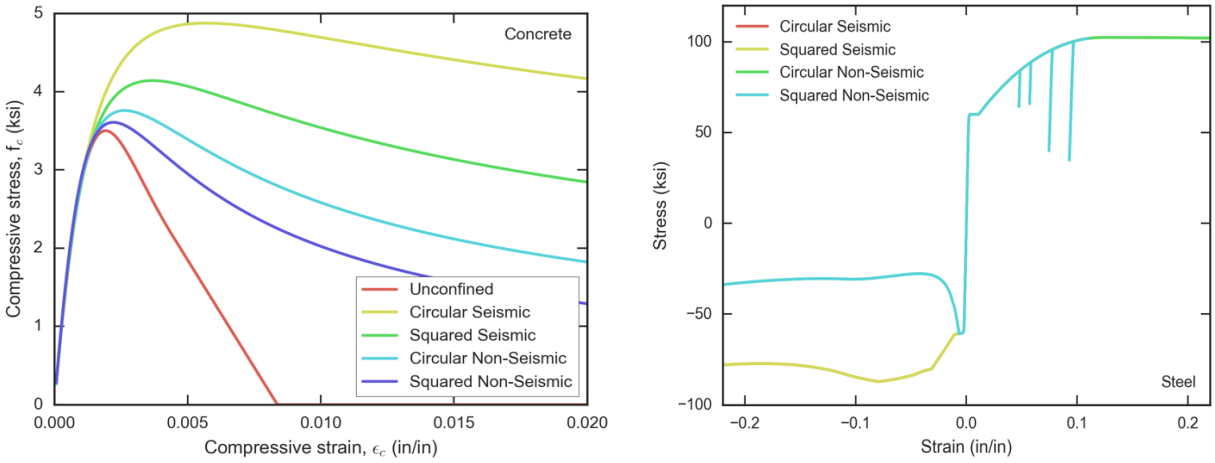

(a) **(b)**

Figure 2.14 – Effects of Various Transverse Reinforcement Spacing on (a) Concrete, and (b) Longitudinal Reinforcement Models.

CHAPTER 3 GEORGIA SEISMIC HAZARD MAPS AND BRIDGE INVENTORY ANALYSIS

To assess the impact of the LRFD Seismic Bridge Design Specifications in Georgia, it is important to determine the potential hazard associated with earthquakes in different parts of the state. Seismic Design Response Spectra and seismic maps based on five site classes, A through E, are developed in this chapter. Additionally, a thorough bridge inventory is conducted to determine the key bridge types to study. This chapter provides an analysis of the bridge inventory for the state of Georgia based on the National Bridge Inventory (NBI) database and specific bridge plans provided by GDOT.

3.1 Georgia Design Response Spectrum and Seismic Zones

Natural hazards can impose severe demands on any type of structure. Seismic detailing has the potential to decrease the probability of damage due to earthquakes during a structure's service life. Hence, design codes and specifications are being continually revised and updated to incorporate any new information gained from experience, research, etc. Bridges should have considerable ductility and deformability to resist earthquake forces. With the idea of performance-based earthquake engineering (PBEE), the latest AASHTO LRFD Bridge Design Specifications [1] recommend that bridges should be designed using displacement-based rather than force-based procedures. PBEE methodology aims at assuring that a desired level of structural performance with definable levels of reliability is achieved when it is subjected to various levels of seismic input. The performance of the structure is measured in terms of engineering demand parameters

(EDPs) such as curvature ductility, displacement, and drift ratio. In this study, such EDPs are employed to measure the damage of various components of the bridge.

Bridges that are in accordance with the LRFD provisions are expected to resist low to moderate seismic loads. In the event of high seismic loads, bridges are expected to suffer significant damage; however, they should have a low probability of collapse. Keeping this performance objective in mind, seismic hazard is defined based on a 1000-year design return period earthquake, which corresponds to 7% probability of exceedance in 75 years.

The AASHTO LRFD Bridge Design Specifications [1] require that the seismic hazard at a location be characterized based on the acceleration spectrum of the location and relevant site factors. There are two procedures for determining the acceleration spectrum given in the code: a) General Procedure, and b) Site-Specific Procedure. The specification lists four conditions as to when the Site-Specific Procedure must be followed. However, as this study focuses on an overall analysis of bridges across the state of Georgia, the General Procedure is followed.

The General Procedure uses the peak ground acceleration coefficient, PGA; short-period spectral acceleration, S_S; and long-period spectral acceleration, S_1, to establish the design spectral acceleration curve. These coefficients can be obtained from the seismic design hazard maps developed by United States Geological Survey (USGS) for the 2007 AASHTO Specifications. For the state of Georgia, the maps for obtaining the ground acceleration coefficient, and short-period and long period accelerations are shown in Figure 3.1. These coefficients are only valid for rock site conditions (Site Class B), which is taken as the reference site class in the specification. Different site class adjustment factors are provided to account for the effects of other site classes.

All of these coefficients are in accordance with performance based on a 1000-year return period and consider performance-based design objectives.

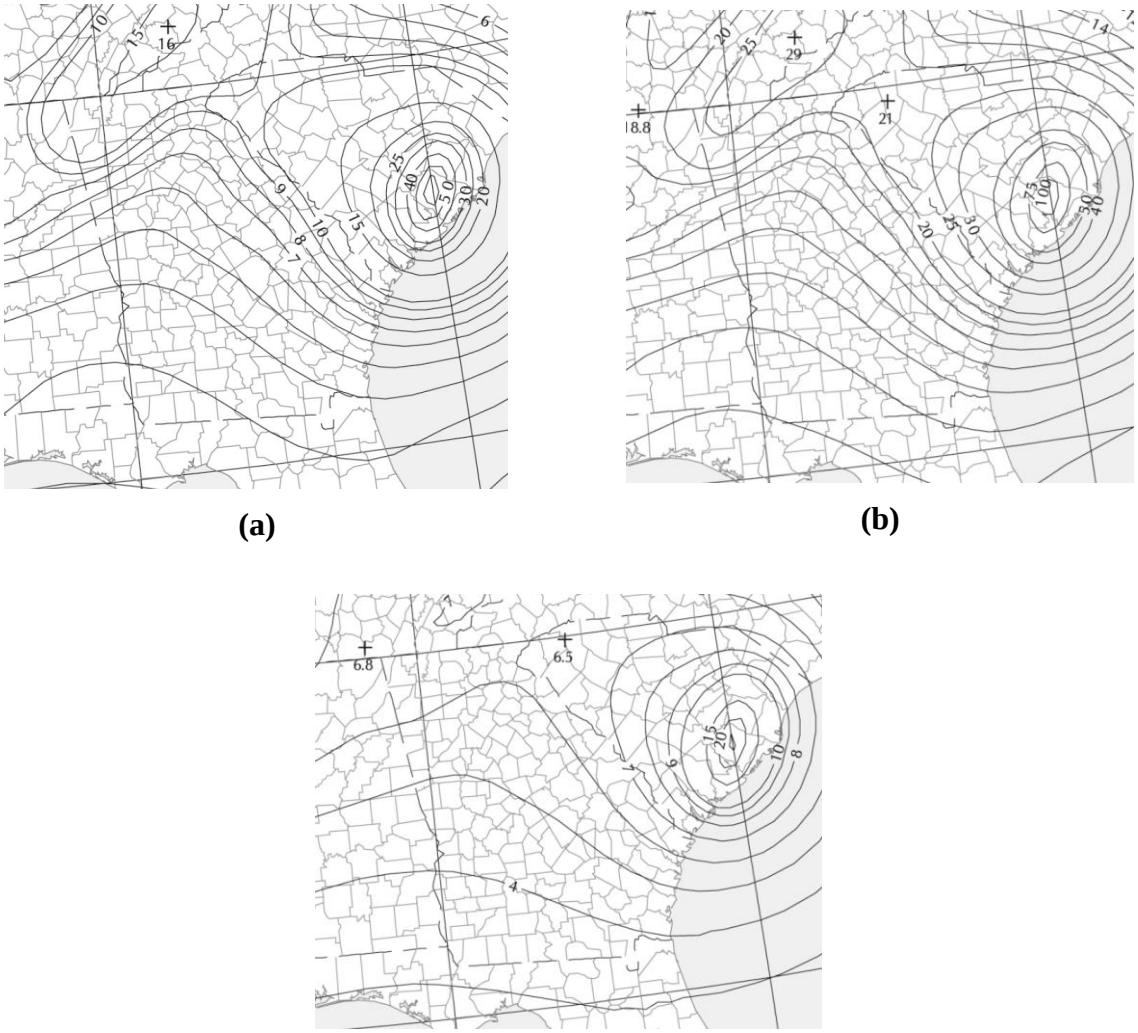

(a) **(b)**

(c)

Figure 3.1 – Map of Georgia Depicting Contour Lines for Seismic Site Class B for (a) Horizontal PGA Coefficient; (b) Horizontal Response Spectral Acceleration Coefficient at Period 0.2 Seconds (S_S); and (c) Horizontal Response Spectral Acceleration Coefficient at Period 1.0 Second (S_1) [1].

The surrounding soil type can have a significant impact on the forces that are transmitted to a structure. To incorporate the site conditions, the specification classifies a site as A through F, per the site class definitions. These site class definitions are based on the type of soil and average

shear wave for the upper 100-ft of the soil profile. Site adjustment factors, F_{PGA} (for PGA) in Table 3-1, F_a (for S_S) in Table 3-2, and F_v (for S_1) in Table 3-3, are used to determine the site-specific acceleration spectrum coefficients, A_S, S_{DS}, and S_{D1}, respectively. These coefficients are then used to plot the design spectral acceleration curve for a region as per Figure 3.2.

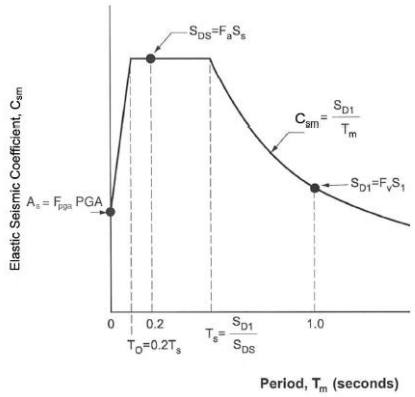

Figure 3.2 – Design Response Spectrum [1].

Table 3-1 – Values of Site Factor, F_{PGA}, at Zero Period on Acceleration Spectrum [1].

Site Class	Peak Ground Acceleration Coefficient				
	PGA < 0.10	PGA = 0.20	PGA = 0.30	PGA = 0.40	PGA =0.50
A	0.8	0.8	0.8	0.8	0.8
B	1.0	1.0	1.0	1.0	1.0
C	1.2	1.2	1.1	1.0	1.0
D	1.6	1.4	1.2	1.1	1.0
E	2.5	1.7	1.2	0.9	0.9

Table 3-2 – Values of Site Factor, F_a, for Short Period Range of Acceleration Spectrum [1].

Site Class	Spectral Acceleration Coefficient at Period 0.2 second				
	$S_S < 0.25$	$S_S = 0.50$	$S_S = 0.75$	$S_S = 1.00$	$S_S > 1.25$
A	0.8	0.8	0.8	0.8	0.8
B	1.0	1.0	1.0	1.0	1.0
C	1.2	1.2	1.1	1.0	1.0
D	1.6	1.4	1.2	1.1	1.0
E	2.5	1.7	1.2	0.9	0.9

Table 3-3 – Values of Site Factor, F_v, for Long Period Range of Acceleration Spectrum [1].

Site Class	Spectral Acceleration Coefficient at Period 1.0 second				
	$S_1 < 0.10$	$S_1 = 0.20$	$S_1 = 0.30$	$S_1 = 0.40$	$S_1 > 0.50$
A	0.8	0.8	0.8	0.8	0.8
B	1.0	1.0	1.0	1.0	1.0
C	1.7	1.6	1.5	1.4	1.3
D	2.4	2.0	1.8	1.6	1.5
E	3.5	3.2	2.8	2.4	2.4

In the present study, Site Classes A to E are examined and the design response spectra for these site classes, using the above-mentioned coefficients, are shown in Figure 3.3. Note S_a is spectral acceleration in units of gravitational acceleration g. All site classes except Site Class F are considered to account for any data collected on soil properties in Georgia. Site Class F requires site-specific investigations to determine the influence of the local site conditions on the structure and a site-specific procedure to determine the design acceleration response spectrum, which were outside the scope of this study.

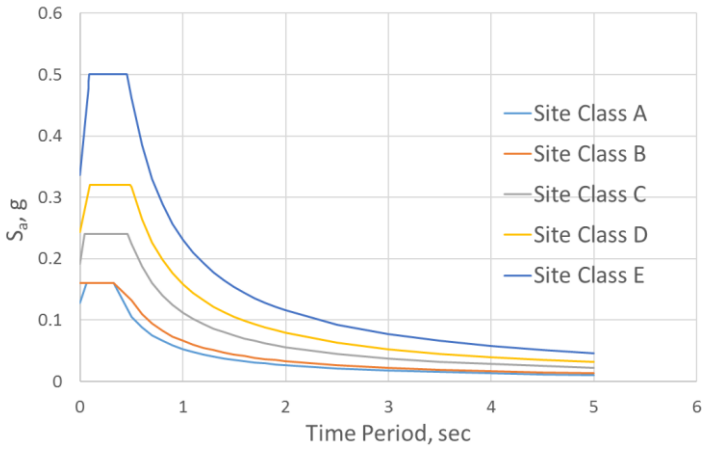

Figure 3.3 – Georgia Design Response Spectra for Site Classes A, B, C, D, and E.

To estimate the seismic vulnerability of highway bridges in Georgia, an appropriate suite of ground motions is essential. Due to unavailability of historic ground motion records, particularly at the intensities required for this research, previous studies have used artificially generated ground motions to study earthquakes in the central and southeastern United States (CSUS). Nielson [8] used Rix and Fernandez-Leon [36] to provide ground motion suites to determine seismic vulnerability of highway bridges in the CSUS. Because Georgia falls in the CSUS region, a suite of 48 Rix and Fernandez-Leon ground motions are used to assess the seismic vulnerability of bridges in this study. Figure 3.4 shows a plot of the spectral acceleration values for a range of structural time periods obtained from these 48 ground motions.

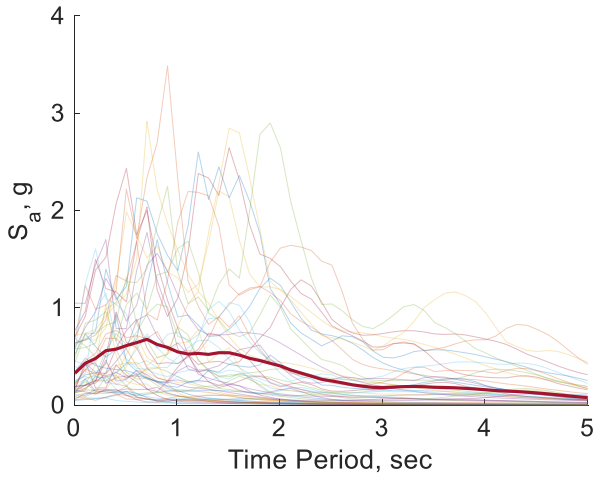

Figure 3.4 – Spectral Acceleration Plot for a Range of Time Periods for the 48 Rix and Fernandez-Leon Ground Motion Suite.

As performance is the main criterion to be followed while designing a bridge using a PBEE methodology, the code suggests classifying the region under study into seismic zones. While designing a bridge for earthquake effects, these zones help the designer determine the type of analysis, detailing requirements, etc., to be used for the bridge. The greater the zone number, the more rigorous the design should be. Table 3-4 shows the boundaries that are used to define these zones; these boundaries are based on the design spectral acceleration coefficient at 1 second, S_{D1}. Although the LRFD code specifies only four zones, Seismic Zone 1 is subdivided into two subzones, Seismic Zones 1-A and 1-B, for this study based on recommendations by GDOT.

Table 3-4 – Seismic Zone Boundaries.

Seismic Zone	Acceleration Coefficient Range
1-A	$S_{D1} < 0.10$
1-B	$0.10 \leq S_{D1} < 0.15$
2	$0.15 \leq S_{D1} < 0.30$
3	$0.30 \leq S_{D1} < 0.50$
4	$S_{D1} \geq 0.50$

As these zone definitions are based on S_{D1}, they incorporate the local seismic and site effects. Therefore, a site with rocky site conditions might fall under a different seismic zone than a nearby site that has soft soil conditions. This concept is elaborated on in the next section, which presents the seismic zone maps for all the site classes for Georgia.

3.2 Georgia Site-Specific Seismic Hazard Maps

Seismic hazard maps are helpful to determine the predicted level of ground motion excitation for a region in consideration. In the present study, the state of Georgia is divided into six regions, as shown in Figure 3.5, based on the expected maximum PGA intensity. The northern region of the state is most susceptible to higher intensity earthquakes.

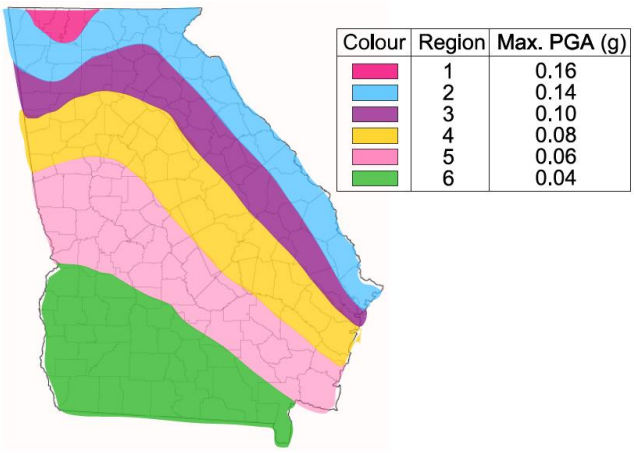

Figure 3.5 – Map of Georgia Showing Six Regions Considered in the Study.

3.2.1 Site Class A Seismic Hazard Map

Site Class A is characterized by very hard rock site conditions where the average shear seismic wave velocity is greater than 5000 ft/sec. The seismic hazard map for this site class for

Georgia is shown in Figure 3.6. The maximum earthquake intensity level for Site Class A is 0.13 g. Hard rocky sites result in large attenuation distances and allow earthquake waves to spread over a vast region, depending on the intensity. The seismic intensity is the lowest compared to the other site classes. Because of the low seismic hazard level, the whole state falls under Seismic Zone 1-A.

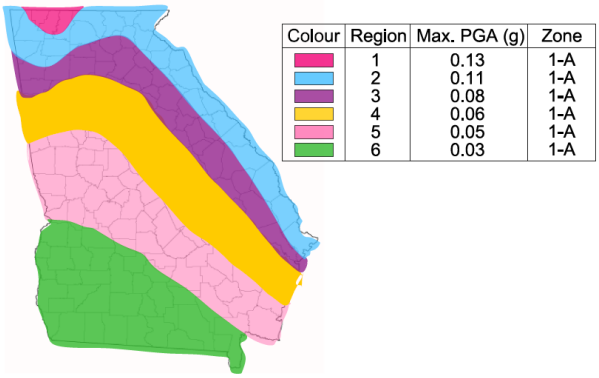

Figure 3.6 – Georgia Seismic Hazard Map for Site Class A.

3.2.2 Site Class B Seismic Hazard Map

Site Class B is characterized by softer rock site conditions than Site Class A with an average seismic wave velocity between 2500 and 5000 ft/sec. As Shown in Figure 3.7, the entire state falls under Seismic Zone 1-A and does not require consideration of rigorous seismic detailing for design. The maximum PGA for Site Class B is 0.16 g.

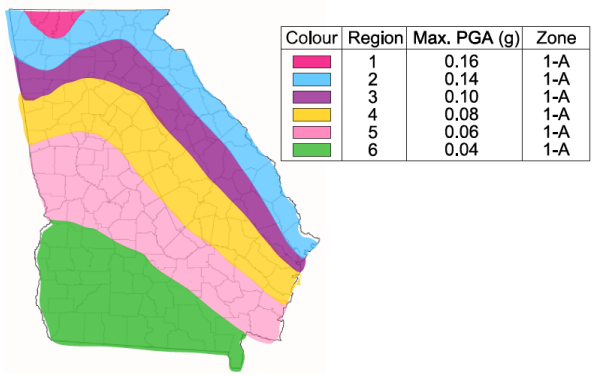

Colour	Region	Max. PGA (g)	Zone
	1	0.16	1-A
	2	0.14	1-A
	3	0.10	1-A
	4	0.08	1-A
	5	0.06	1-A
	6	0.04	1-A

Figure 3.7 – Georgia Seismic Hazard Map for Site Class B.

3.2.3 Site Class C Seismic Hazard Map

Site Class C is characterized by very dense soil or rock where the average shear wave velocity ranges from 600 to 1200 ft/sec. The maximum PGA range for different regions for this site class is 0.05 g to 0.19 g. As depicted in Figure 3.8, Regions 1 and 2 fall in Seismic Zone 1-B for Site Class C, whereas the rest of the state still falls in Seismic Zone 1-A.

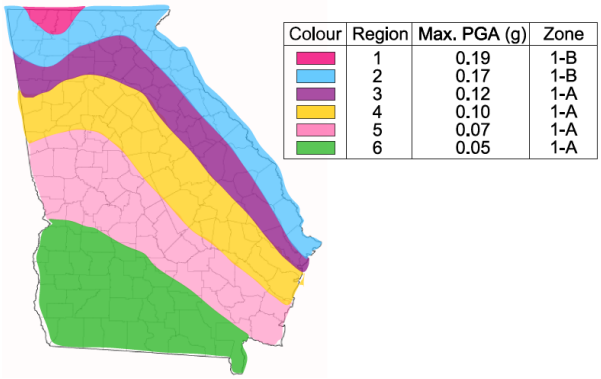

Colour	Region	Max. PGA (g)	Zone
	1	0.19	1-B
	2	0.17	1-B
	3	0.12	1-A
	4	0.10	1-A
	5	0.07	1-A
	6	0.05	1-A

Figure 3.8 – Georgia Seismic Hazard Map for Site Class C.

3.2.4 Site Class D Seismic Hazard Map

Site Class D has softer soil site class conditions compared to Site Class C, leading to amplification of seismic waves, and is characterized by average shear velocity less than 600 ft/sec.

Figure 3.9 shows the seismic hazard map for Georgia for Site Class D. The seismic zone intensity increases from the southern to the northern parts of the state with maximum PGA equal to 0.24 g.

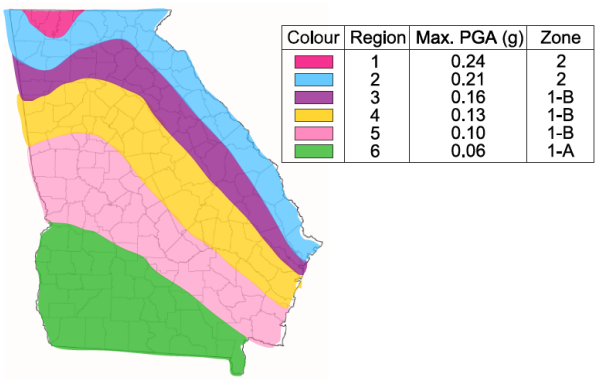

Figure 3.9 – Georgia Seismic Hazard Map for Site Class D.

3.2.5 Site Class E Seismic Hazard Map

Site Class E site conditions are known to be highly reactive to seismic ground motions. The soil composition at these sites mainly consists of clayey or other type of soft soils. Such soils are susceptible to high moisture changes, allowing amplification of the ground motion. The seismic hazard map for Georgia for Site Class E is shown in Figure 3.10. Most of the state falls under Seismic Zone 2 for this site class, with the maximum PGA being 0.35 g in Region 1.

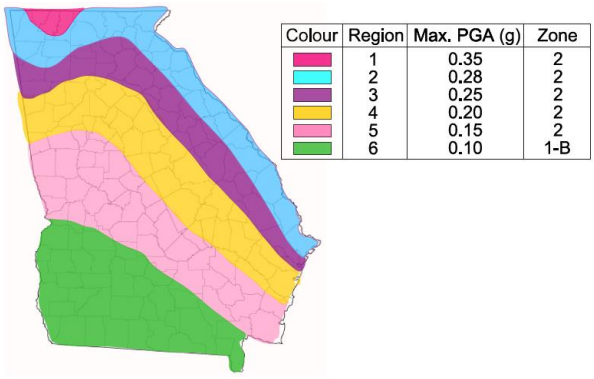

Figure 3.10 – Georgia Seismic Hazard Map for Site Class E.

3.3 Georgia Highway Bridge Inventory Analysis

With 9514 bridges in Georgia, it is computationally infeasible to model and conduct a full detailed analysis of each bridge to obtain a fragility curve and assess its seismic vulnerability. Therefore, bridges are grouped into various classes for analysis. Nielson used this approach to classify bridges based on the type of construction and materials used in the bridges [8]. The present study applies such a classification. It is assumed that bridges within a bridge class behave in a similar way during an earthquake event. Therefore, fragility curves are generated for bridge classes rather than individual bridges.

The National Bridge Inventory database (NBI), maintained by the Federal Highway Administration (FHWA) [37], records the information about all highway structures in the United States. The NBI database provides basic information of 15,122 highway structures in Georgia. Many of these structures are tunnels and culverts, which are assumed to represent a different type of system and therefore, not considered in this study. For the remaining 9514 bridges, a preliminary statistical distribution analysis using two key NBI fields (i.e., material and construction type) was performed to determine a general classification of the inventory. Although detailed bridge characteristics must be studied from the individual bridge plans, the database provides important characteristics such as material type, dimensions, number of spans, skew angle, structural rating, etc.

Table 3-5 shows the distribution of bridges in Georgia based on the construction material type listed in the NBI database [37]. The construction material used in Georgia is predominantly concrete, followed by steel. Similarly, Table 3-6 shows the distribution of bridges in Georgia based on construction types listed in the NBI database [37].

Table 3-5 – Georgia Highway Bridges Classified by Construction Material [37].

Construction Materials	Number of Bridges	Percentage
Concrete	3,227	33.9
Concrete Continuous	124	1.3
Steel	2,501	26.3
Steel Continuous	1,101	11.6
Prestressed Concrete	2,321	24.4
Prestressed Concrete Continuous	116	1.2
Wood or Timber	118	1.2
Masonry	3	0.0
Aluminum, Wrought Iron, or Cast Iron	1	0.0
Other	2	0.0

Table 3-6 – Georgia Highway Bridges Classified by Construction Type [37].

Construction Type	Number of Bridges	Percentage
Slab	1,135	11.9
Stringer/Multi-beam or Girder	5,646	59.3
Girder and Floor Beam System	63	0.7
Tee Beam	2,123	22.3
Box Beam or Girders – Multiple	230	2.4
Box Beam or Girders – Single or Spread	131	1.4
Frame (Culverts Excluded)	24	0.3
Truss – Thru	51	0.5
Arch – Deck	55	0.6
Others	95	0.6

After examination of the NBI database, the research team assigned all the bridges in Georgia to one of seven bridge classes, as given in Table 3-7. The bridges grouped within each class typically would have similar responses to a seismic excitation. Multi-span simply supported

concrete bridges is the most common bridge class in Georgia and represents about 41.03% of bridges in the state. As this study focuses on the impact of seismic transverse spacing and lap splices in bridge columns, only multi-span bridges have been considered hereafter.

Table 3-7 – Georgia Bridge Classes and Their Proportions [37].

Bridge Class	Abbreviation	Number	Percentage
Multi-Span Continuous Steel Girder	MSC Steel	1,065	11.9
Multi-Span Simply Supported Concrete Girder	MSSS Concrete	3,904	41.03
Multi-Span Simply Supported Steel Girder	MSSS Steel	1,516	15.93
Multi-Span Simply Supported Slab	MSSS Slab	951	10.00
Single-Span Concrete Girder	SS Concrete	362	3.80
Single-Span Steel Girder	SS Steel	721	7.58
Other	Other	995	10.46

3.3.1 Bridge Class Statistics

With the bridge classes defined, an examination of key bridge characteristics is necessary to select a representative bridge from each bridge class. Although the NBI database provides the basic bridge characteristics for bridges, detailed information of the representative bridge from each bridge class is obtained from the bridge plans. This step is necessary to generate accurate finite element models of the bridges. The following characteristics, obtained from the NBI database, provide insight into the typical geometric configuration of bridges in each of the four multi-span bridge classes considered:

- Number of spans (presented in Table 3-8)
- Maximum span length (presented in Table 3-9)
- Deck width (presented in Table 3-10)
- Minimum vertical deck width (presented in Table 3-11)

The mode for number of spans for most of the bridge classes in Georgia is 3. Hence, to be able to compare the results across the bridge classes, this study considers only 3-span bridges for each bridge class. Other parameters are chosen as close to the median values of the bridge class depending on the availability of bridge plans.

Table 3-8 – Span Number Statistics for the Four Bridge Classes.

Bridge Class	Mean	Standard Deviation	Median	Maximum	Minimum	Mode
MSC Steel	4.57	3.72	4	41	2	4
MSSS Concrete	5.17	4.49	4	89	2	3
MSSS Steel	3.97	2.27	3	40	2	3
MSSS Slab	5.95	4.16	5	56	2	3

Table 3-9 – Maximum Span Length (ft.) Statistics for the Four Bridge Classes.

Bridge Class	Mean	Standard Deviation	Median	Maximum	Minimum	Mode
MSC Steel	82.22	45.87	83	280	10	27
MSSS Concrete	56.16	30.98	40	187	12	40
MSSS Steel	56.68	28.64	55	252	9	16
MSSS Slab	20.56	5.22	20	88	12	20

Table 3-10 – Deck Width (in.) Statistics for the Four Bridge Classes.

Bridge Class	Mean	Standard Deviation	Median	Maximum	Minimum	Mode
MSC Steel	48.96	31.50	34.70	221.20	10.60	34.00
MSSS Concrete	47.18	25.47	41.30	522.40	12.40	41.30
MSSS Steel	47.28	33.89	34.30	220.10	8.00	25.20
MSSS Slab	28.12	6.69	25.80	96.00	12.00	25.20

Table 3-11 – Minimum Vertical Deck Width (in.) Statistics for the Four Bridge Classes.

Bridge Class	Mean	Standard Deviation	Median	Maximum	Minimum	Mode
MSC Steel	17.62	3.10	16.11	42.09	10.06	16.07
MSSS Concrete	20.48	5.27	19.06	75.01	0.99	16.07
MSSS Steel	18.95	3.70	17.06	43.10	10.08	16.05
MSSS Slab	17.46	3.90	18.07	23.02	10.05	16.05

CHAPTER 4 OVERVIEW OF FRAGILITY CURVES

In recent decades, fragility curves have become an important statistical tool to quantify the potential damage in a structure due to hazards. The first section of this chapter presents the general formulation used in this study to develop the fragility curves. The following sections address the limit states and the probabilistic seismic demand model.

4.1 Analytical Fragility Curve Formulation

A fragility function, F, represents the probability of the demand meeting or exceeding a predefined capacity limit state, given the intensity measure of the hazard. Mathematically, the fragility function can be expressed in terms of a conditional probability as:

$$F = P[D - C \geq 0 | IM = y] \quad (7)$$

where D is the demand of the structural component, C is the capacity of the component, IM is the intensity measure of the hazard, and y is the realization of the hazard intensity. If fragility functions are calculated and plotted over a range of realizations of the chosen intensity measure, they yield a fragility curve. Figure 4.1 shows one such fragility curve obtained for a specified limit state. On the x-axis, this curve represents the considered intensity measure, and on the y-axis, it shows the associated risk. The intensity measure used to evaluate the fragility function in this study is peak ground acceleration.

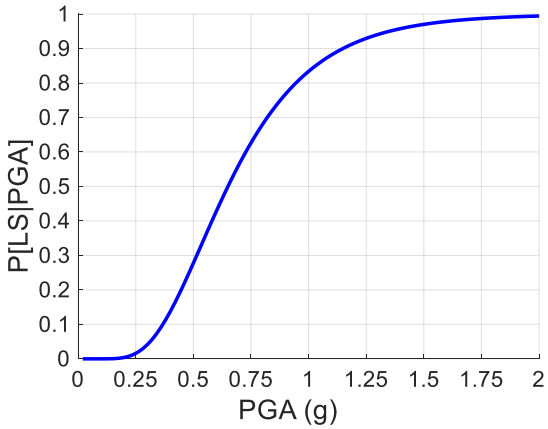

Figure 4.1 – Typical Fragility Curve.

There are three main methods to formulate fragility curves: (1) expert-based, (2) empirical, and (3) analytical. These methods can be combined to obtain more accurate fragility estimation. In fact, the multi-hazard risk analysis tool distributed by the Federal Emergency Management Agency (FEMA), HAZUS-MH, uses this kind of a hybrid approach to determine hazard risk analysis of structures [38]. Another way of obtaining more robust fragility functions is to use advanced statistical techniques, such as Bayesian updating, to combine analytical results obtained from computer simulations and field inspection results. With advancement in structural health monitoring, such hybrid techniques are generally preferred for research purposes.

Expert-based fragility curves were used to estimate the expected behavior of highway bridges in California due to data shortage [39]. This method is no longer popular to quantify fragility functions as there is a high level of uncertainty involved due to subjectivity of the procedure.

Empirical fragility curves rely on the post-hazard assessment of the structure to simulate the demand model. Many researchers used this methodology to formulate fragility functions after the Loma Prieta and Northridge earthquakes [40–42]. This method relies on evaluating fragility

functions through collection of binary pass/fail data from experts for the failure of a structure after the hazard. One could argue that this method should be the most highly favored to estimate damage risk, as the risk is derived from observations of the performance of the structure in the field. However, the major drawback of this method is that it requires an adequate number of structures from a bridge class to quantify the fragility functions. In practice, these data are limited. Moreover, as with the expert-based method, there could be a high level of subjectivity in the post-hazard inspection data, as well.

With computational improvements over the past few decades, analytical fragility curves have become a widespread way to formulate fragility functions. When bridge inspection or ground motion data are not available, numerical simulations are used to quantify the capacity and/or demand of the structure in consideration. Typically, the capacity of the structural component is determined based on experimental tests or its geometric interpretation, and the demand imposed on the component during a hazard is computed through computer simulations. Building an accurate finite element model of the structure and selecting appropriate ground motions are some of the important steps involved in this method.

4.1.1 Component-Level Fragility Curves

An analytical fragility approach is used to estimate the fragility functions for structural components. Due to the variabilities involved, such as geometry, hazard, etc., the capacity and demand models are random variables, rather than deterministic values. If both component capacity and demand models are assumed to follow a lognormal distribution, by the application of the central limit theorem, Equation 7 can be expressed as a lognormal cumulative distribution function in terms of the parameters of the capacity and demand variables as follows:

$$F = \Phi\left(\frac{\ln S_d/S_c}{\sqrt{\beta_d^2 + \beta_c^2}}\right) \quad (8)$$

Where $\Phi(\cdot)$ is the standard normal cumulative distribution function, S_d is the median parameter of the demand random variable, β_d is the lognormal standard deviation of the demand random variable, S_c is the median parameter of the capacity random variable, and β_c is the lognormal standard deviation of the capacity random variable. All of these parameters are defined at each intensity level for which damage fragility is to be determined. From Equation 8, the parameters of the capacity and demand random variables are needed to estimate the fragility function. The techniques used to define these parameters in the function are described in following sections.

4.1.2 System-Level Fragility Curves

Component-level fragility curves can be helpful to determine the most vulnerable links in an overall system. They can also be used to determine appropriate retrofit strategies and component life-cycle cost analyses. However, these curves do not provide information about the vulnerability of the full structure. One component could be more susceptible to a ground motion than another when a complete structure is analyzed. To assess the vulnerability of the structure, the component-level curves must be combined to derive the system-level fragility curves. Under the assumption that the system behaves as a series system, wherein the failure of one component results in the failure of the whole system, these curves can be combined to determine the system-level vulnerability. This assumption has been used by many researchers in the past [8,43]. Either closed-form solutions or numerical solutions can be used to find the system fragility function depending on the number of components and complexity of the failure domains.

In this study, a numerical Monte Carlo simulation approach is used to combine the component-level fragility curves. This process involves generating N random samples from both capacity and demand variable distributions. While generating the samples from the capacity side, the correlation between the limit states is assumed to be equal to 1 to ensure that the numerical samples from each limit state rank in the same order that the limit states are defined. While generating the samples from the demand side, correlations between the bridge components must be incorporated into sampling. After generating the samples, each sample from the demand and capacity side are paired with each other. The paired samples are compared one-to-one to evaluate the failure. If the sample from the limit state side is less than the sample from the demand side, the system is considered to have failed. Following this definition of failure, an indicator function is defined to track the number of failed samples as follows:

$$I_f = \begin{cases} 1 & \text{if } (x_i, x_j) \in F_{ij} \\ 0 & \text{if } (x_i, x_j) \notin F_{ij} \end{cases} \tag{9}$$

where x_i and x_j are the realization of the ith and jth distributions and F_{ij} is defined by the ith and jth limit state.

The indicator function can now be evaluated at equal intervals of a reasonable range of the intensity measure. At each value of the intensity measure, the failure probability can be estimated as:

$$P[LS|IM = y] = \frac{\sum_{i=1}^{N} I_{f_i}}{N} \tag{10}$$

Note that N is number of random sample generated from capacity and demand distributions. It is important to determine a reasonable number of samples to obtain an accurate probability of failure. The results from the sensitivity analysis of the variation of the failure probabilities were plotted with respect to number of samples. Approximately 150,000 samples are enough to stabilize the probability estimates.

4.2 Limit States

As stated in Section 4.1, limit state definitions are required to evaluate the fragility functions. In this study, the limit states of each component are based on either past experimental results or functional interpretation of the component. Engineering Demand Parameters (EDPs) such as displacement, curvature ductility, drift ratio, etc., have been used by researchers to define the limit states of columns. This is in accordance with the performance-based seismic design philosophy in the latest AASHTO LRFD Bridge Design Specifications [1]. These limit states are defined for four damage levels: (1) slight, (2) moderate, (3) extensive, and (4) complete. Table 4-1 describes the definitions adopted for each limit state from HAZUS-MH [38]. Each limit state is assumed to follow a lognormal distribution with the parameters of the distribution obtained from experimental data or past research.

Table 4-1 – HAZUS' Qualitative Limit States [38].

Limit State	Description
Slight	Initial yielding in longitudinal rebars, cracking in column surfaces, minor cracking in plastic hinge regions.
Moderate	Minor spalling at column faces, shear cracks in columns, pile cap damage.
Extensive	Cracks exposing column core; shear failure of columns; flexural failure due to inadequate confinement, anchorage or lap splice; vertical pull of longitudinal reinforcement; ground displacement at column base.
Complete	Buckling of longitudinal rebars, vertical or lap splice failure, column collapse.

The following paragraphs provide descriptions of these limit states for each bridge component considered in the study. Although, in practice, the limit states are expected to vary with the service life of a structure due to aging, corrosion, deterioration, etc., such factors are not considered in this study. Therefore, the limit states are assumed to be constant throughout the service life of the bridge.

Static pushover tests on columns can be used to determine the force-deflection curves and column damage in terms of EDPs. Since the curvature of a structural member is a property of a cross section and is independent of the length of the member, the chosen EDP for this study is curvature ductility. The curvature ductility, $\mu_{\emptyset}$, of a structural member is defined as:

$$\mu_{\emptyset} = \frac{\kappa_{max}}{\kappa_{yield}} \tag{11}$$

where κ_{max} is the maximum curvature observed in the column under seismic shaking, and κ_{yield} is the column yield curvature.

In the present study, the following three cases corresponding to non-seismic and seismic lap splice and transverse reinforcement spacing requirements are considered:

1. No Lap Splice with Non-Seismic Detailing: The lap splice is not provided at the base of the column and a non-seismic transverse reinforcement spacing of 12-in. is used.

2. Lap Splice with Non-Seismic Detailing: The lap splice is provided at the base of the column with transverse reinforcement spacing equal to 12-in.

3. Lap Splice with Seismic Detailing: The lap splice is provided at the base of the column with transverse reinforcement spacing equal to 3-in.

The moment–curvature ductility plots along with the corresponding column limit states for the above-mentioned three cases are shown in Figure 4.2. The column capacities in terms of curvature ductility are adopted from previous experimental test results [18, 44–48] that characterize four limit states characterized by slight, moderate, extensive, and complete damage. Slight damage corresponds to the curvature ductility at the first point of yield in the longitudinal rebar. Moderate damage corresponds to the spalling of cover concrete due to expansive force. Extensive damage corresponds to the exposure of concrete core or yielding of transverse reinforcement, whichever happens first. Complete damage corresponds to the lap splice failure in the case of the lap splice column, or longitudinal rebar buckling in the no lap splice case.

For the three cases of column seismic design considered in this study, the column limit states are presented in Table 4-2. It is assumed that the reduction of transverse reinforcement does

not significantly affect the column capacity. Hence, for the seismic and non-seismic cases, the same limit state values have been assumed.

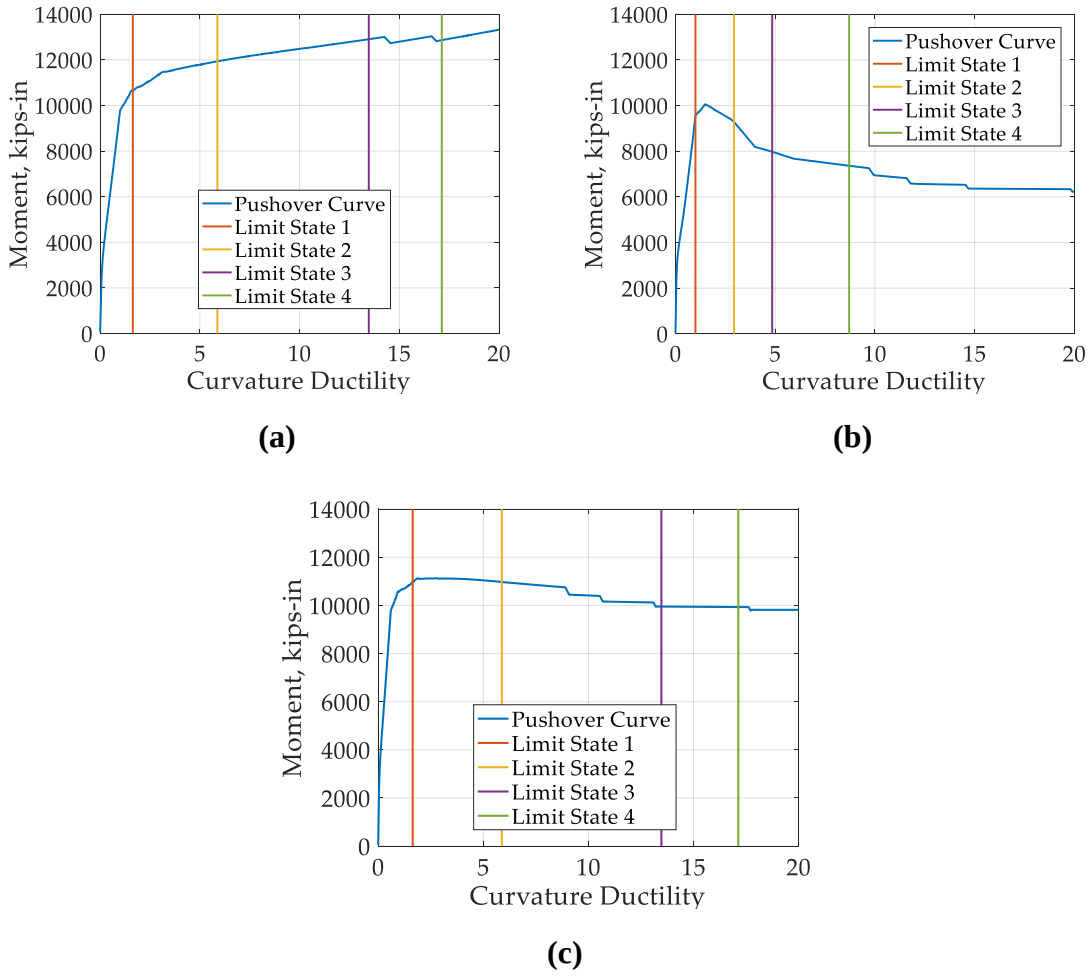

Figure 4.2 – Moment–Curvature Ductility Curves and Limit States for (a) Column with No Lap Splice and Non-Seismic Transverse Detailing; (b) Column with Lap Splice and Non-Seismic Transverse Detailing; and (c) Column with Lap Splice and Seismic Transverse Detailing.

Table 4-2 – Limit State Median Values for Lap-Spliced Column Sections.

Case	Description	Slight	Moderate	Extensive	Complete
1	No Lap Splice & Non-Seismic Detailing	1.64	5.88	13.47	17.13
2	Lap Splice & Non-Seismic Detailing	1.00	2.93	4.85	8.71
3	Lap Splice & Seismic Detailing	1.64	5.88	13.47	17.13

4.3 Probabilistic Seismic Demand Model

In addition to limit states, demand estimates are required to quantify the fragility functions of components. Probabilistic seismic demand models (PSDMs) obtained from analytical seismic analyses of the structure are used for this purpose. PSDMs evaluate the peak structural demand of a component as a function of intensity of ground motions. In this study, the PSDM model is obtained from nonlinear time history analyses by running the suite of 48 ground motions to consider the uncertainty in the structural response. The data points for the peak demands of the components obtained from the nonlinear time history analysis are plotted against the value of PGAs of that ground motion.

Cornell et al. [49] suggested a power function model relation to estimate the median demand from PSDM using the following relation:

$$EDP = a\, IM^{b} \tag{12}$$

where EDP stands for Engineering Demand Parameters, and it refers to median demand in this equation, a and b are the coefficients obtained from the linear regression analysis of the model. To calculate these coefficients, the demand model is transformed into linear space by taking the logarithm of both sides of Equation 12 to obtain the following equation:

$$\ln(EDP) = \ln(a) + b * ln(IM) \quad (13)$$

As stated before, the demand variable is assumed to follow a lognormal distribution in the study. It therefore follows a normal distribution in linear space, with a mean equal to zero and a constant standard deviation, σ.

CHAPTER 5 MODELING AND DETERMINISTIC SEISMIC BRIDGE ANALYSES

This chapter presents bridge characteristics and modeling details that are employed to generate three-dimensional (3-D) finite element models of the representative bridges from each multi-span bridge class in Georgia considered in this study. These 3-D models are useful to evaluate the expected seismic performance of bridges. The lap splice model, as explained in Chapter 2, is incorporated into the analytical bridge models to compare their expected seismic performance for different detailing cases. Column and bearing responses from deterministic bridge analyses performed using a single ground motion are studied to assess the performance degradation due to inadequate lap splice lengths and confining reinforcement. As described in Chapter 1, the analytical fragility curve methodology requires the demand parameters be obtained from these analytical bridge models. This chapter further explains the seismic response of various bridge components obtained from a deterministic nonlinear time history analysis.

5.1 Typical Highway Bridge Components

The typical bridge model used in this study is based on Nielson [8], who conducted research on fragility functions for highway bridges in the CSUS. The most important bridge components for a highway bridge are depicted in Figure 5.1 and can be categorized as follows:

- Superstructure: The components of a bridge that directly receive the live load compose the superstructure. These components typically consist of bridge girders, deck, parapet, etc. In this study, it is assumed that the bridge superstructure remains within the linear

range during an earthquake event. Therefore, its nonlinear properties are not considered.

- Substructure: These are the components that support the bridge and transfer the load from the superstructure and substructure to the surrounding soil. The substructure comprises bents, columns, foundations, and abutments.
- Bearings: Bearings are mechanical devices that allow for the interaction between the substructure and superstructure so that the load from the superstructure can be transferred to the substructure.

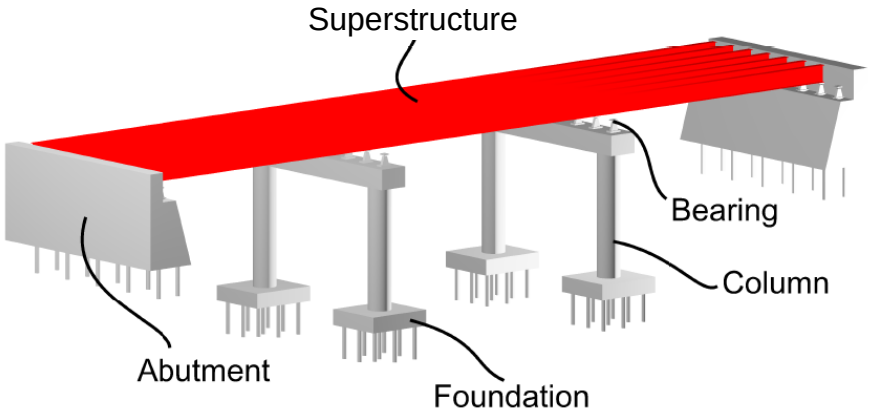

Figure 5.1 – Typical Bridge Configuration.

The 3-D analytical models are generated using the open source finite element package OpenSees [50]. This package is preferred for the study as it permits users a flexibility to generate components with a great degree of accuracy and to evaluate the response of bridge components in detail. The response at the component level is studied in the transverse and longitudinal directions and combined using the square root of the sum of square roots technique (SRSS). The major

components studied are columns and bearings. The following subsections outline the model of the representative bridge for the four multi-span bridge classes.

5.2 Deterministic Seismic Response

Deterministic seismic analysis provides the bridge response at the component level. The Rayleigh damping assumed for all the models is 5%. The deterministic response is evaluated using a single ground motion from Rix and Fernandez-Leon [36] ground motions. Figure 5.2 depicts the acceleration–time history plots of the selected ground motion. This ground motion has a maximum PGA of 0.36 g and duration equal to about 13 seconds. This ground motion is chosen to simulate the effect of the expected maximum PGA for Site Class E in Georgia, which is equal to 0.35 g.

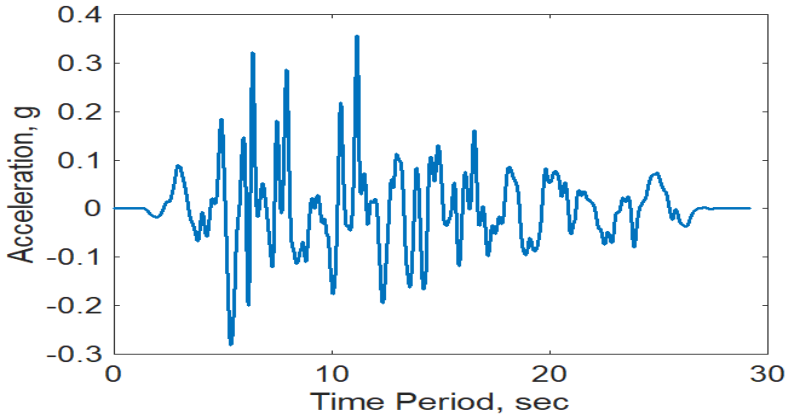

Figure 5.2 – Acceleration–Time Plot for Rix and Fernandez-Leon Ground Motion Selected for Deterministic Bridge Analysis.

5.2.1 Multi-Span Simply Supported Concrete Girder Bridge

5.2.1.1 Superstructure

The multi-span simply supported (MSSS) concrete girder bridge class comprises about 41% of bridges in the state of Georgia. Figure 5.3 presents the basic geometric layout for the MSSS

concrete girder bridge. The bridge has 3 spans, which are 67-ft-6-in., 75-ft, and 67-ft-6-in. long. The deck of the bridge is 43-ft-11-in. wide and uses an 8-in.-thick concrete slab supported by five AASHTO Type III Prestressed Concrete (PSC) beam girders on Spans 1 and 2 and AASHTO Type II PSC beam girders on Span 3. Bridges with other typical deck widths, e.g., 43-ft-3-in., would be expected to exhibit similar performance. The gaps present at the adjacent spans are 4-in., whereas at the abutments, the gaps are equal to 2-in.

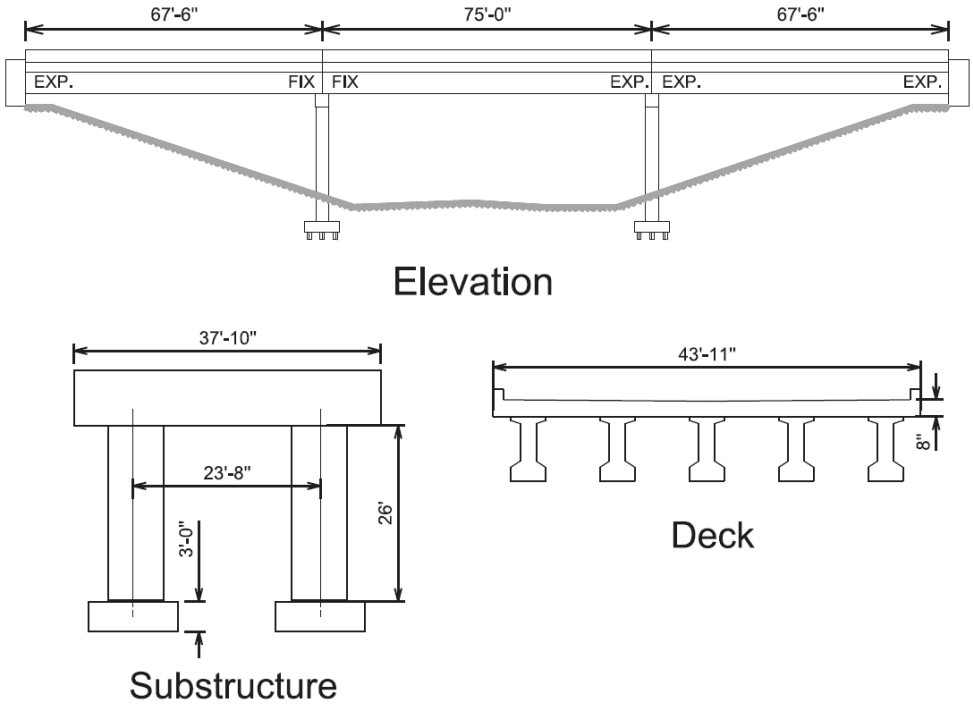

Figure 5.3 – Multi-Span Simply Supported Concrete Girder Bridge Layout.

5.2.1.2 Substructure

The substructure is made of 37-ft-10-in.-wide 2-column concrete bents. As illustrated in Figure 5.4, the bent beam has a square cross section with an edge length of 3-ft-6-in., which is supported by 3-ft by 3-ft square columns. The bent beam uses five equally spaced #11 bars on the top and bottom edges and three equally spaced #5 bars on the side edges with a minimum clear

concrete cover of 2-in. with #4 bars for transverse reinforcement spaced at a maximum distance of 12-in. The two supporting columns for each bent have a center-to-center distance of 23-ft-8-in. and use reinforcement detailing of 12 #11 equally spaced rebars with transverse reinforcement being #4 bars spaced at 12-in. The average height of the columns is 26-ft and the lap splice extends 9-ft from the base of the column. The columns are supported by standard HP 14 × 73 steel H piles.

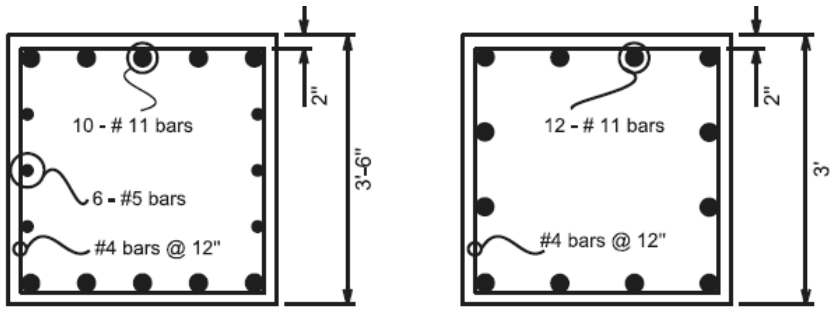

Figure 5.4 – Cross-Sectional Layout for Bent Beam and Column for Multi-Span Simply Supported Concrete Girder Bridge.

5.2.1.3 Bearings

Laminated elastomeric bearings are the most commonly used bearings for the MSSS concrete bridge class. These bearings have a dowel bar embedded in the concrete bent that extends into the bridge girder as shown in Figure 5.5. The elastomeric pad is reinforced using steel plates that are placed in between the layers of elastomer to reduce bulging and shear strains in the pad. Although the steel layers increase the compressive and flexural stiffness of the bearing pad, there is no significant change in the shear stiffness [51]. The behavior of these bearings is characterized by sliding of the girder over the elastomeric pad. Initially, there exists a gap between the girder and dowel bar as illustrated in Figure 5.5. The friction between the elastomer and girder provides the initial stiffness for sliding until the movement is enough to fill the gap between the dowel bar

and girder. At this point, the resistance to the sliding motion is provided by the combined action of the elastomeric pad and the dowel bar.

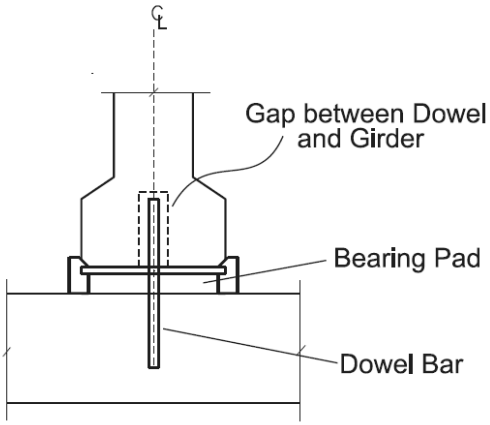

Figure 5.5 – Typical Layout of Elastomeric Bearing.

The initial stiffness provided by the elastomeric pad is modeled as an elastic perfectly plastic material as shown in Figure 5.6(a). Choi proposed a formulation for calculating the initial stiffness, k_0, of the bearing as follows [52]:

$$k_0 = \frac{GA}{h_r} \tag{14}$$

where G is the shear modulus of the elastomer, A is the area of the elastomeric pad, and h_r is the height of the bearing pad. The area and height of the elastomeric pad are dependent on the bearing configuration, and the shear modulus of the elastomer is taken as 131.57 lb/in^2.

The frictional coefficient between the concrete girder and elastomeric pad governs the yield force that can be developed in the bearing pad. Experimental tests conducted on elastomeric bearings have revealed that the coefficient of friction is a function of the normal stress imposed by

the superstructure on the bearing. Based on experimental tests, Scharge proposed an empirical formula to determine the frictional coefficient, μ_f, as follows [53]:

$$\mu_f = 0.05 + \frac{0.4}{\sigma_m} \tag{15}$$

where σ_m is the normal stress on the bearing pad due to the superstructure.

As the gap between the dowel bar and girder is filled, the dowel bar is engaged in the bearing sliding motion. The behavior of the dowel bar can be characterized as lateral force acting on a cantilever. Initially, when the dowel bar is in the elastic range, it is assumed to behave linearly. Under moderate to high lateral loads, the bar follows a nonlinear pattern until the fracturing of the bars, which leads to a sudden drop in the strength. Although the diameter of the dowel bars used for elastomeric bearings in Georgia is 1¼-in., dowel bars in the present study are assumed to be 1-in. diameter due to lack of research on the response of dowel bars. Choi (2002) evaluated the response of 1-in.-diameter dowel bars using an ABAQUS model. The stress–strain behavior of the dowel bar, as shown in Figure 5.6(b), used in the present study is taken from Choi's work with the same stiffness values.

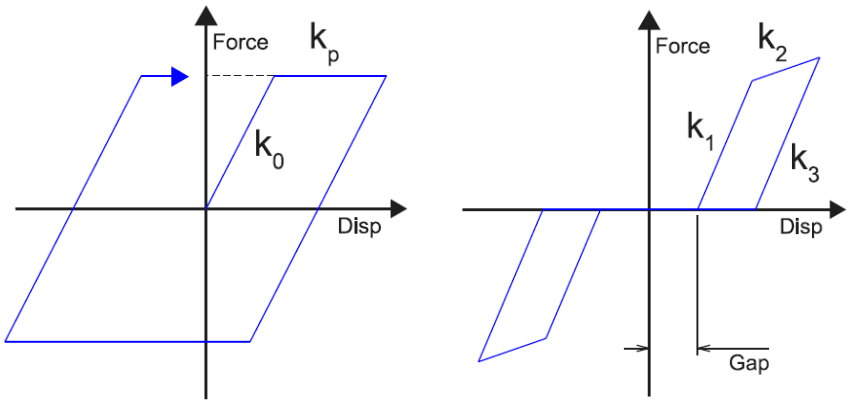

Figure 5.6 – Stress–Strain Model Used for (a) Elastomeric Pad, and (b) Dowel Bar in the Elastomeric Bearing.

Note that the K values shown in Figure 5.6 represent stiffness values of the corresponding branches of the force-displacement curves.

5.2.1.4 Seismic Response

The effect of lap splice and transverse reinforcement spacing on the main components of the bridge is analyzed by nonlinear time history analyses. Due to the presence of a lap splice at the base of the column, more demand is imposed on the bridge columns. The demand is further increased when the lap splice is provided with non-seismic column transverse spacing. This phenomenon is illustrated in Figure 5.7, which shows about 32% increase in the curvature demand when the lap splice is provided with non-seismic transverse reinforcement spacing and about 19% increase when the lap splice is provided with seismic transverse reinforcement spacing.

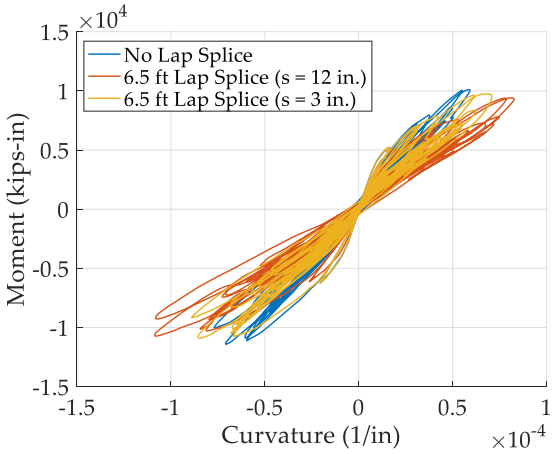

Figure 5.7 – Curvature Demand on Column Base of MSSS Concrete Bridge.

The comparative force–displacement curves for the fixed and expansion laminated elastomeric bearings in the bridge are shown in Figure 5.8. For the fixed bearings, the gap between the dowel bar and elastomeric pad is 0.12-in. Figure 5.8(a) shows the change in stiffness of the force–displacement curve of the fixed elastomeric bearing due to engagement of the dowel bar. Similarly, for the expansion bearing, the gap is 1.0-in., as shown in Figure 5.8(b). The bearing response for all three cases is similar because the chosen ground motion is not of a very high intensity.

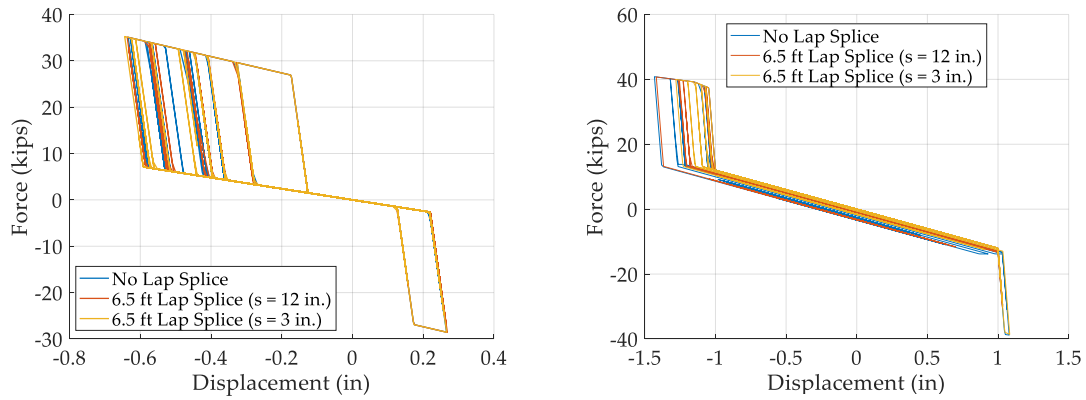

(a) **(b)**

Figure 5.8 – Force–Displacement Curves for (a) Fixed, and (b) Expansion Laminated Elastomeric Bearings Used in MSSS Concrete Bridge.

5.2.2 Multi-Span Continuous Steel Girder Bridge

5.2.2.1 Superstructure

The next bridge class considered in the study was multi-span continuous (MSC) type steel girder bridges. This type of bridge comprises about 11% of bridges in Georgia. The basic geometric configuration for a representative bridge from this bridge class is shown in Figure 5.9. The bridge consists of three spans and is 36-ft-10-in. wide. The span lengths for this bridge are 43-ft, 67-ft, and 43-ft. The deck is a composite steel deck supported by five wide-flange steel girders.

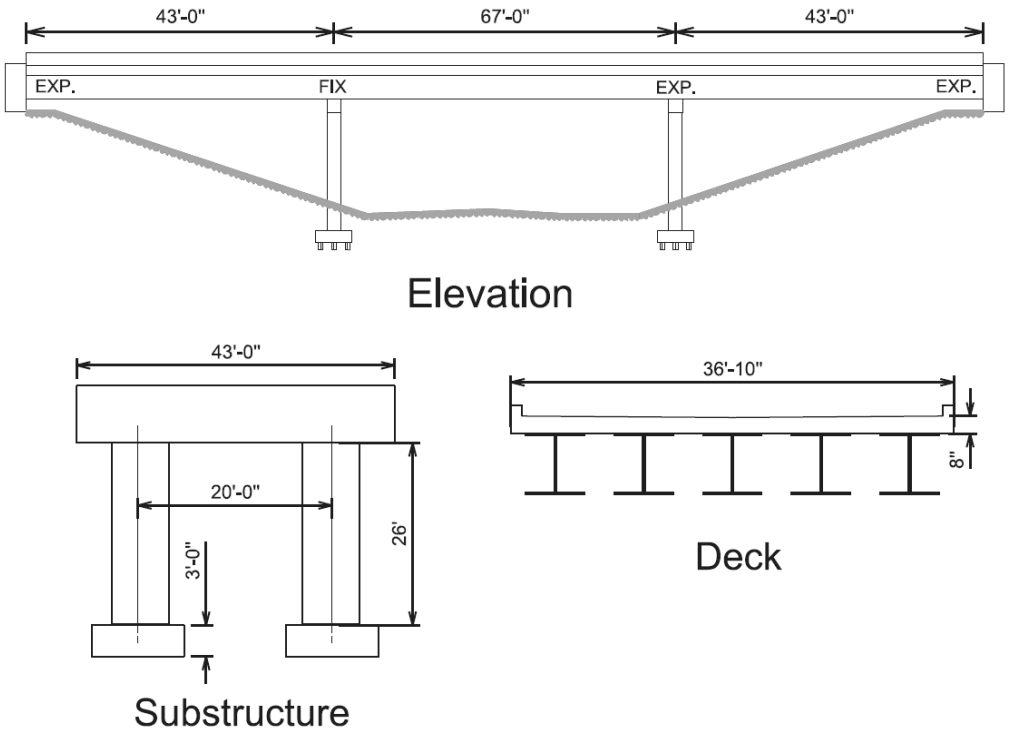

Figure 5.9 – Multi-Span Continuous Steel Girder Bridge Layout.

5.2.2.2 Substructure

Like the previous bridge class, the substructure consists of two-column bents. The average width of the bents is 43-ft and the average height of the columns is 26-ft. The columns are spaced at a distance of 20-ft. The lap splice is present at the base of the column and has a length of 6.5-ft. The cross-sectional layouts for the bent and column are shown in Figure 5.10. The bent has a square cross section with each side equal to 3-ft and is reinforced with seven #11 bars each at the top and bottom edges and two #4 bars on each side. The shear reinforcement for the bents is provided by #5 bars at 12-in. spacing. Likewise, the column has a square cross section with the edge length equal to 3-ft. The column reinforcement consists of 12 #12 equally spaced bars and #4 stirrups spaced at 12 in.

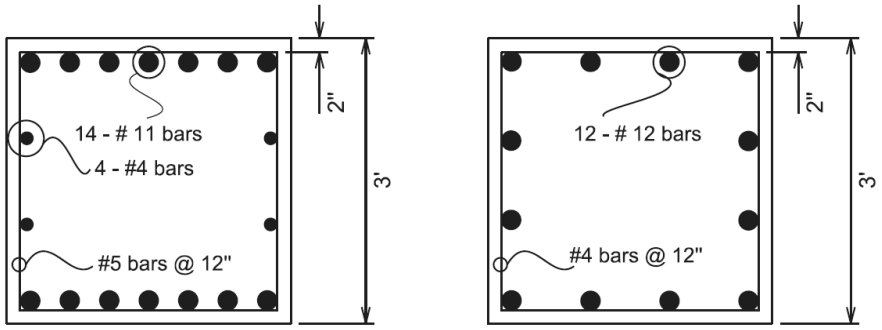

Figure 5.10 – Cross-Sectional Layout for Bent Beam and Column for Multi-Span Continuous Steel Girder Bridge.

5.2.2.3 Bearings

Low-profile steel bearings are the second most commonly used bearings for steel bridges in Georgia. A prototype of a low-profile bridge bearing is shown in Figure 5.11. These bearings are constructed by attaching a masonry plate to the top of the bent or abutment using anchor bolts and a sole plate underneath the girder. For fixed bearings, a curved sole plate and pintles are provided to restrict the translational movements while maintaining the rotational movement. For expansion bearings, no pintles are provided so that free translational movement is permitted to dissipate the energy.

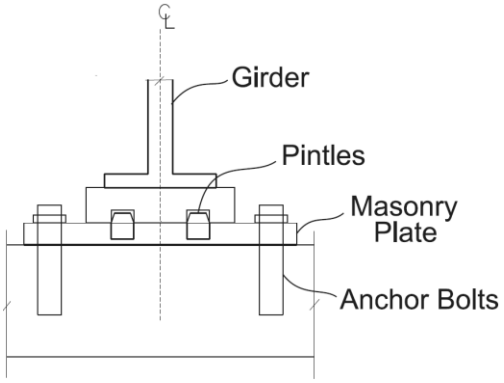

Figure 5.11 – Typical Layout of Low-Profile Steel Fixed Bearing.

The study on analytical modeling of bridge steel bearings was initiated by Mander et al. [54]. However, the test apparatus used by them was not appropriate to simulate field conditions, as the test bearings were mounted to steel assemblies to constrain the damage only to the pintles. This is in contrast with field conditions where the masonry plate is attached to the concrete pedestal by means of anchor bolts. Thus, failure mechanism of either the anchor bolt or pintle, whichever happens first, could lead to the bearing failure. Based on this, Steelman et al. considered two types of low-profile steel fixed bearings: weak anchor and weak pintles [55]. They investigated the cyclic response of these bearings through an improved test apparatus to formulate more accurate analytical models. For the representative MSC steel bridge in Georgia, the diameter of the anchor and pintle is equal to 1-in., however, the effective diameter of the anchor bolts is reduced to 4/5 of the original diameter due to the thread adjustment factor. Due to this, the bearings used in Georgia are considered to be weak anchor bearings and the failure is governed by the rupturing of the anchor bolts.

The fuse capacity, V_{fuse}, for steel bearings can be calculated per the following equation:

$$V_{fuse} = \phi n 0.6 F_u A_{bs} \tag{16}$$

where ϕ is the strength reduction factor (equal to unity), n is the number of shear transfer elements (equal to 2 as there are two anchors), F_u is the ultimate tensile strength of the material, and A_{bs} is the effective cross-sectional area of the shear element.

Along with the fusing action, the bearing interface provides resistance to the translational movement through frictional force. Like elastomeric bearings, frictional resistance is modeled as elastic–perfectly plastic and is coupled with the anchor bolt backbone curve in parallel.

According to the latest AASHTO Specifications (2014), the use of steel bearings is recommended only as fixed bearings, whereas expansion steel bearings have become obsolete. However, as the representative bridge is an older bridge, steel bearings have been used as expansion bearings also. The only difference between fixed and expansion bearings is that there are no pintles to restrict the translational movement in the latter.

5.2.2.4 Seismic Response

Figure 5.12 shows the effect of the 9-ft lap splice and transverse reinforcement spacing on the curvature demand imposed on the MSC steel girder bridge column. As the ground motion is of medium PGA intensity, the column response mostly remains in the linear range. A decrease in the moment capacity and increase in the curvature demand on the column can be observed from the figure when the lap splice is present at the base of the column. The increase in curvature is approximately 12.12% when non-seismic transverse spacing is provided and 3.93% when seismic reinforcement spacing is provided.

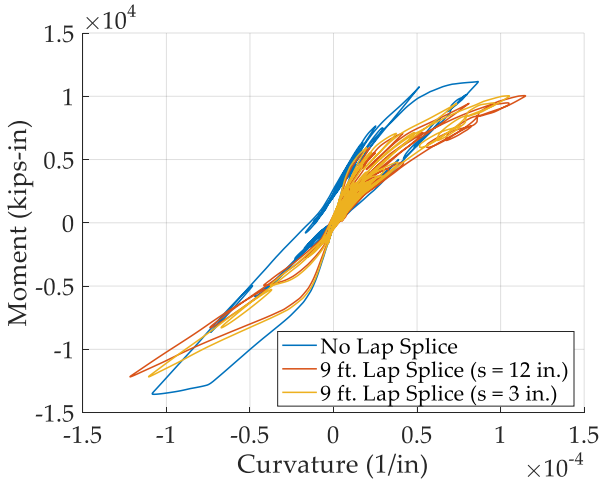

Figure 5.12 – Curvature Demand on Column Base of MSC Steel Girder Bridge.

The force–displacement response for the fixed and expansion steel bearings for MSC steel girder bridges is shown in Figure 5.13(a) and Figure 5.13(b), respectively. The bearing responses are very similar to those of the previous bridge class. The force–displacement response for both types of bearings stays in the linear range, which indicates that there was no rupture in either the pintles or anchors.

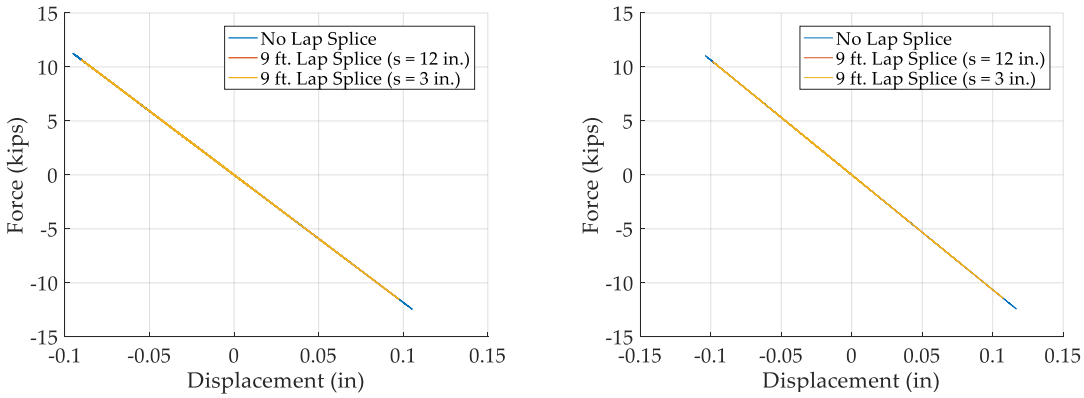

Figure 5.13 – Force–Displacement Curves for (a) Fixed, and (b) Expansion Steel Bearings Used in MSC Steel Girder Bridge.

5.2.3 Multi-Span Simply Supported Steel Girder Bridge

5.2.3.1 Superstructure

The next bridge class considered in the study was MSSS steel girder. The general layout for the representative bridge in this bridge class is shown in Figure 5.14. The bridge has a deck width of 43-ft-3-in. and is supported by five steel girders. The side spans of the bridge are 40-ft long, and the main span is 80-ft long.

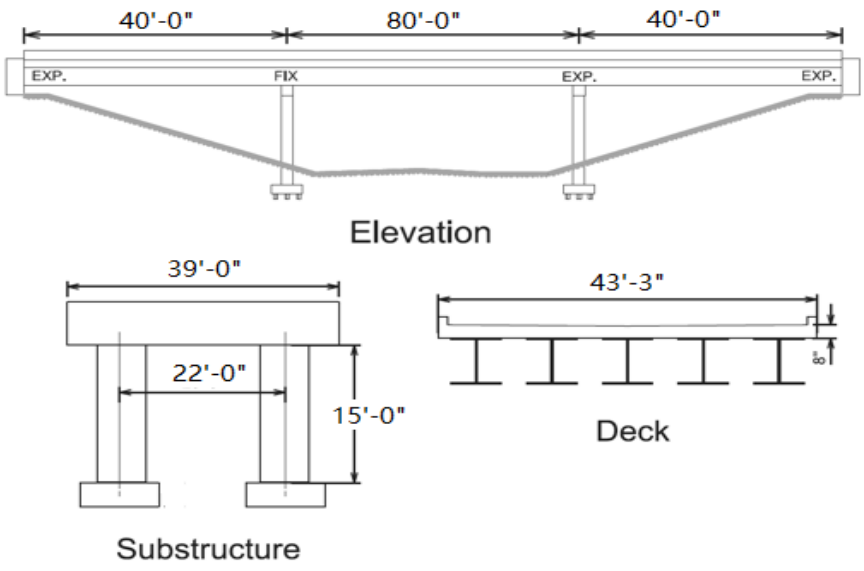

Figure 5.14 – Multi-Span Simply Supported Steel Girder Bridge Layout.

5.2.3.2 Substructure

The substructure for this bridge is supported by two 2-column bents. The width is 39-ft and the average height of the two columns is 15-ft. The bent cross section is a square cross section with width equal to 3-ft-6-in. The bent is reinforced with 14 #11 bars on the top and bottom edges and 2 #6 bars on the side edges. The shear reinforcement comprises #5 bars spaced at 12-in. with a clear concrete cover of 2-in. Figure 5.15 depicts the column cross section, which is a square with the edge length equal to 3.5-ft. The column section is reinforced with eight equally spaced #11 bars with #6 bars providing the shear reinforcement at 6-in. spacing. Lap splice length is taken equal to 9.0-ft.

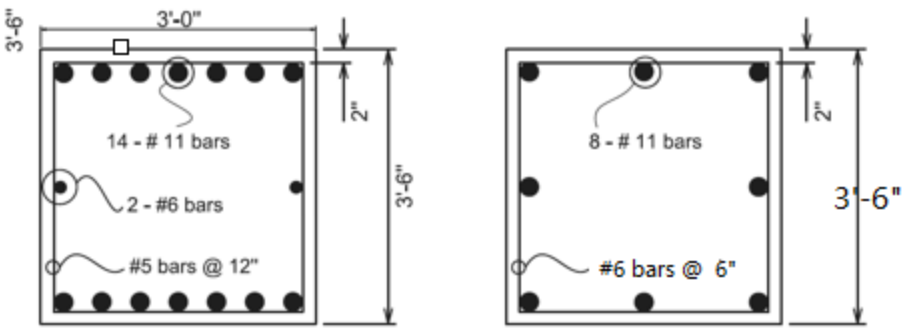

Figure 5.15 – Cross-Sectional Layout for Bent Beam and Column for Multi-Span Simply Supported Steel Girder Bridge.

5.2.3.3 Bearings

As stated in Section 5.2.2.3, the commonly used bearings for steel bridges in Georgia are low-profile steel bearings. This bridge class uses this same type of bearing.

5.2.3.4 Seismic Response

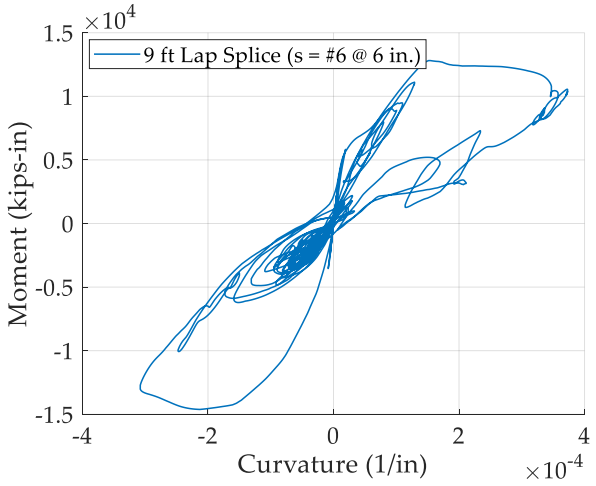

Figure 5.16 – Curvature Demand on Column Base of MSSS Steel Girder Bridge.

For the MSSS steel bridge, there is more displacement demand imposed compared to the MSC steel bridge (see Figure 5.16). This could be the result of more inertial mass in the superstructure of the MSSS steel bridge.

5.2.4 Multi-Span Simply Supported Slab Bridge

5.2.4.1 Superstructure

The final bridge class considered in the study is MSSS slab bridges with pile bents. The general layout for the representative bridge in this bridge class is shown in Figure 5.17. This bridge class does not have columns. Instead, the bents are directly supported by piles. The deck consists of 15 box beams, leading to the deck width of about 46-ft. The end spans of the bridge are 40-ft long, and the middle span is 60-ft long.

5.2.4.2 Substructure

The substructure for this bridge class is pile bents (Figure 5.17). There are four bents in this representative bridge: two bents are located at two ends for abutments, and another two bents are in the middle of the bridge. All bents are supported directly by seven piles. The length of the 14 piles supporting two middle bents is 13.5-ft, measuring from the ground to the bottom of the bents. The piles extend 1.0-ft into the bent caps, as shown in Figure 5.18. The pile cross section is 20-in. diameter with a metal shell of 5/16-in. thickness and 45 ksi strength. The pile section is reinforced with eight equally spaced #10 bars and with #5 bars providing the shear reinforcement at 12-in. spacing. The height and width of the middle bent caps are 3.0-ft and 3.5-ft, respectively. The longitudinal bars in the bent caps consist of four #10 and eight #4, and the stirrups in the bent caps near the piles are #4 @ 6.5-in., and between the piles are #4 @ 10.5-in.

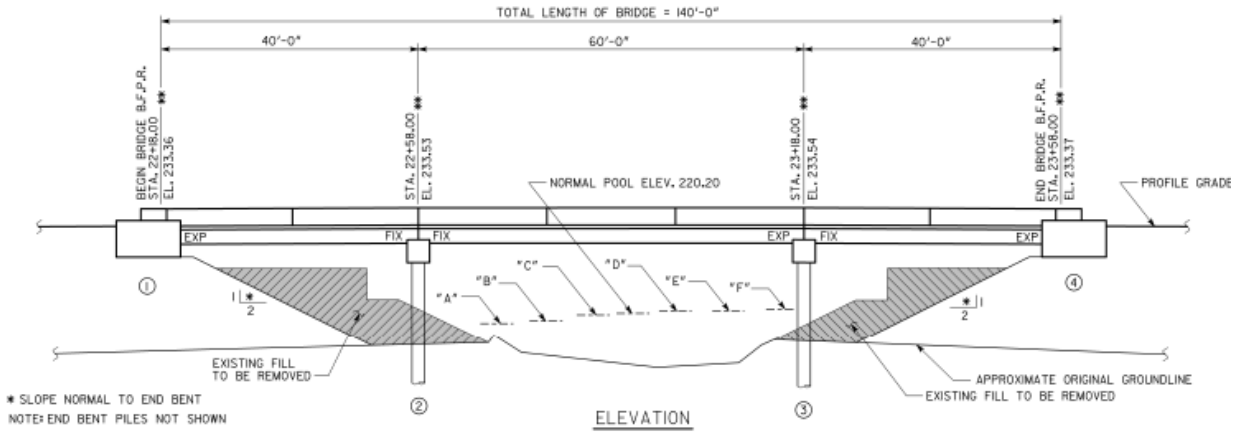

Elevation of the entire bridge

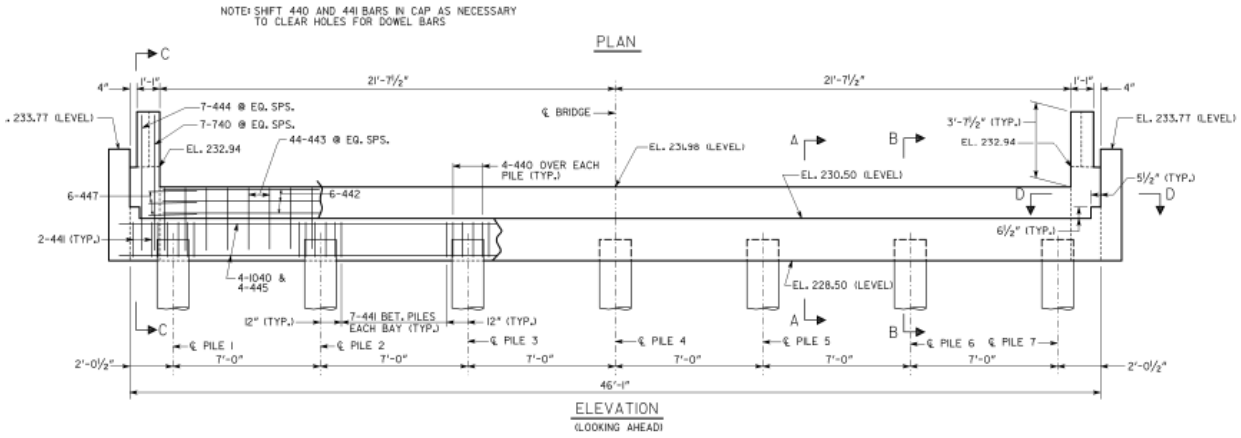

Elevation of the pile bents

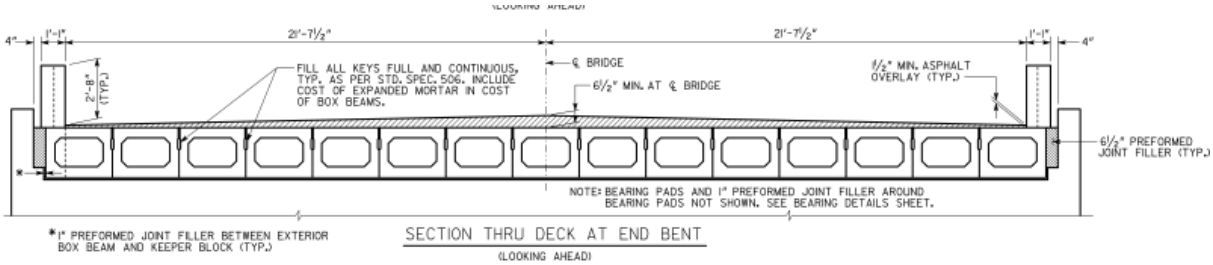

Elevation of the slab consisting of 15 box beams

Figure 5.17 – Multi-Span Simply Supported Slab Bridge Layout.

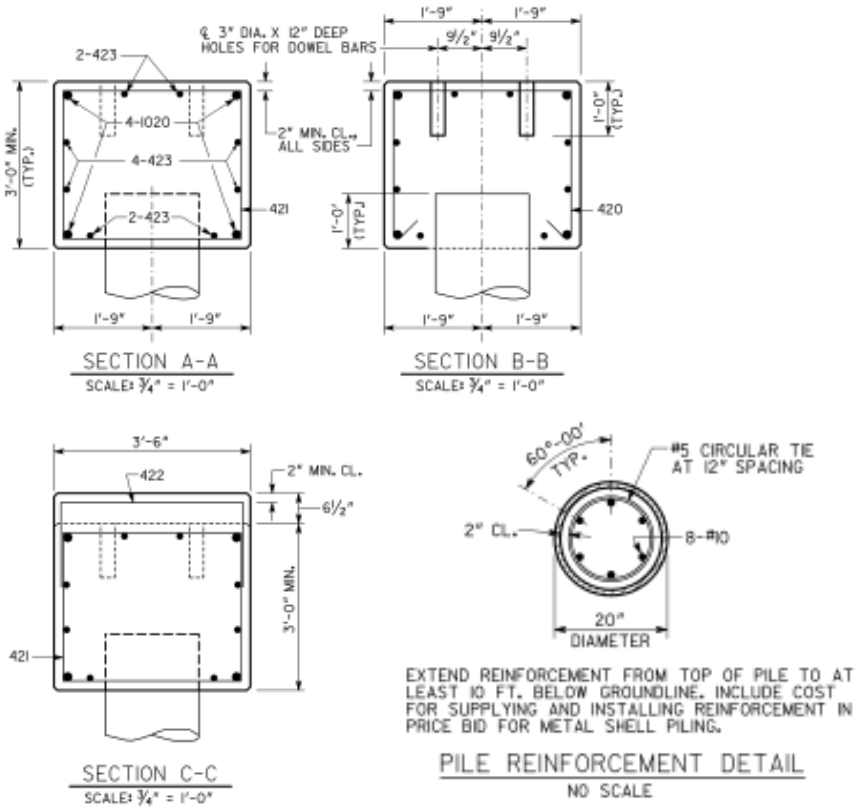

Figure 5.18 – Cross-Sectional Layout for Bent Cap and Pile for Multi-Span Simply Supported Slab Bridge.

5.2.4.3 Bearings

There is a bearing pad below each box beam, as shown in Figure 5.19. Each bearing pad has two holes for two smooth dowel bars 1-in. diameter and 2-ft long. The hole size on the bearing pads for fixed bearings is 1.25-in., and the hole size on the bearing pads for expansion bearings is 2.5-in. The thickness for all the bearing pads is 0.5-in. The bearing model considers the lateral capacities of the elastomeric bearing pad and two dowel bars, as shown in Figure 5.6.

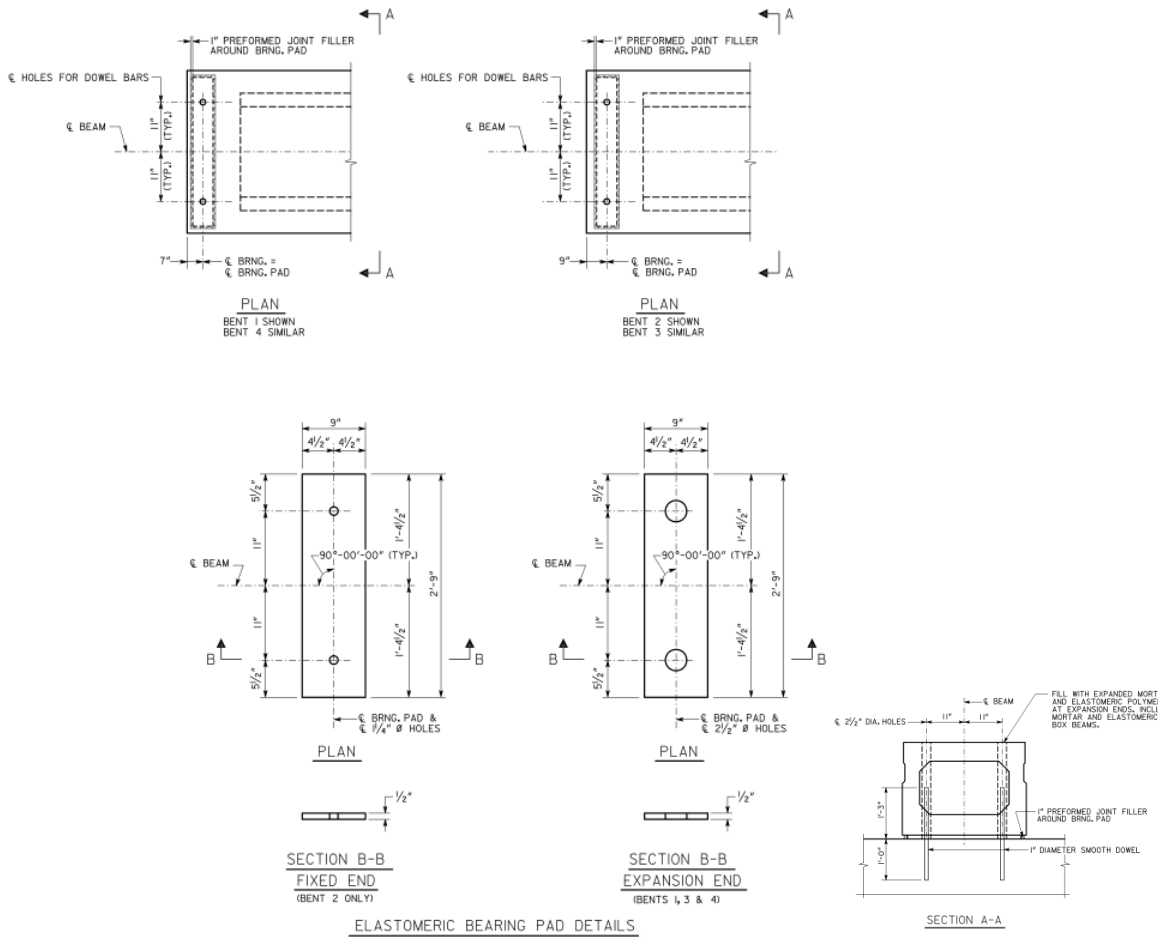

Figure 5.19 –Layout for Fixed and Expansion Bearings for Multi-Span Simply Supported Slab Bridge.

5.2.4.4 Effect of Embedded Pile Length from Piles into Bent Caps (Experimental Results)

Ziehl et al. [56] performed a series of experimental tests to investigate the effect of embedded pile length into bent caps (see Figure 5.20). Four 18-in.-diameter piles were embedded into bent caps with 18-in., 26-in., and 22-in. embedment lengths. The lateral strengths were in a range of 13 to 20 kips. The pile with the longest embedment length (specimen IB-26-1) did not possess the highest strength. In addition, all four piles showed yield plateaus, regardless of the pile embedment length. This conclusion agrees with the provision of at least 12-in. embedment in the latest version of the AASHTO LRFD Bridge Design Specification in 2014 [1].

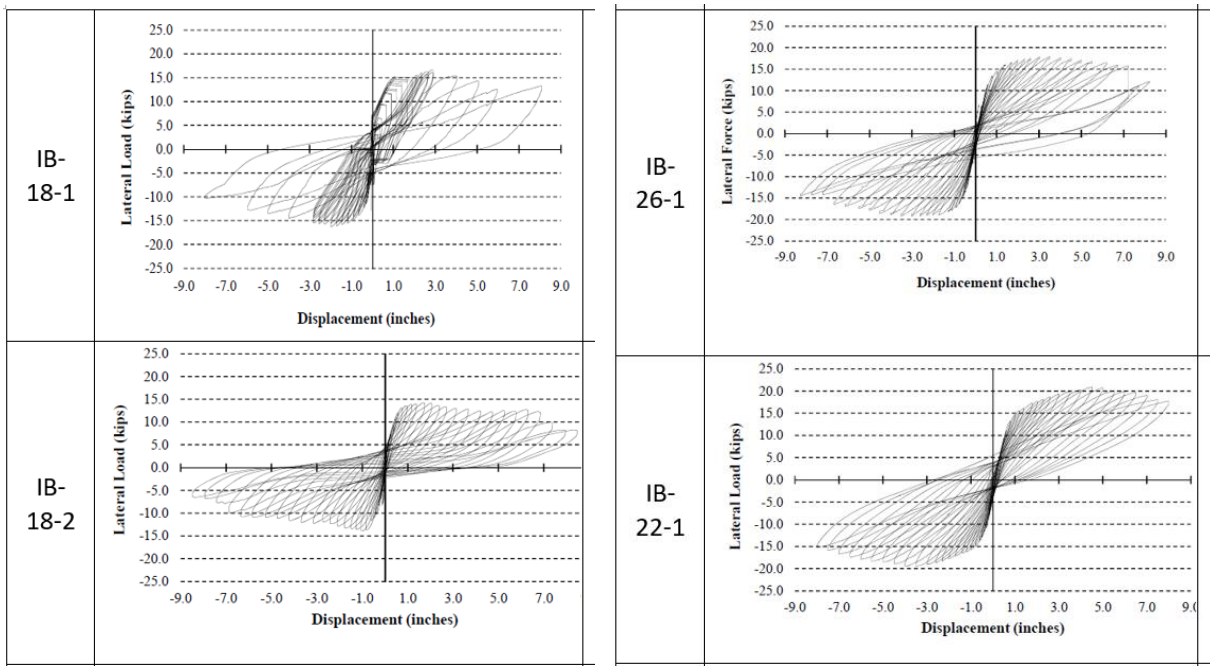

Figure 5.20 – Lateral Strength vs. Lateral Displacement of 18-in. Diameter Piles with 18-in., 26-in., and 22-in. Embedded Length. [56]

CHAPTER 6 SITE-SPECIFIC FRAGILITY CURVES

With the objective of assessing demands imposed on different bridge components, this chapter presents probabilistic seismic demand models (PSDMs) for multi-span highway bridge classes in Georgia. These curves are generated based on nonlinear dynamic analyses under a number of ground motions as a function of peak ground acceleration (PGA) and seismic detailing requirements. Furthermore, fragility curves at the component- and system-level for these bridges are presented in the next subsection. Based on these curves, site-specific seismic damage risk is evaluated for Seismic Classes A, B, C, D, and E. Differences in seismic risk are for the most part described relative to Limit State 1, with some discussions relative to Limit State 2 as relevant. However, all probabilities of reaching the different limit states are provided. Conclusions about risk relative to any of the varying levels of damage represented by the different limit states can be obtained from these values.

6.1 PSDMs for Multi-Span Highway Bridges

As discussed in Section 4.3, PSDMs are generated for columns based on the maximum curvature ductility demands on them. A suite of 48 ground motions is used to assess the demand quantity of interest. PSDMs for various classes of bridges are plotted in Figure 6.1. PSDMs are plotted on a log–log scale with the demand variable on the y-axis and intensity measure on the x-axis. The PSDMs reveal the decrease in seismic performance for all three bridge classes when the logarithm of PGA is greater than −2.

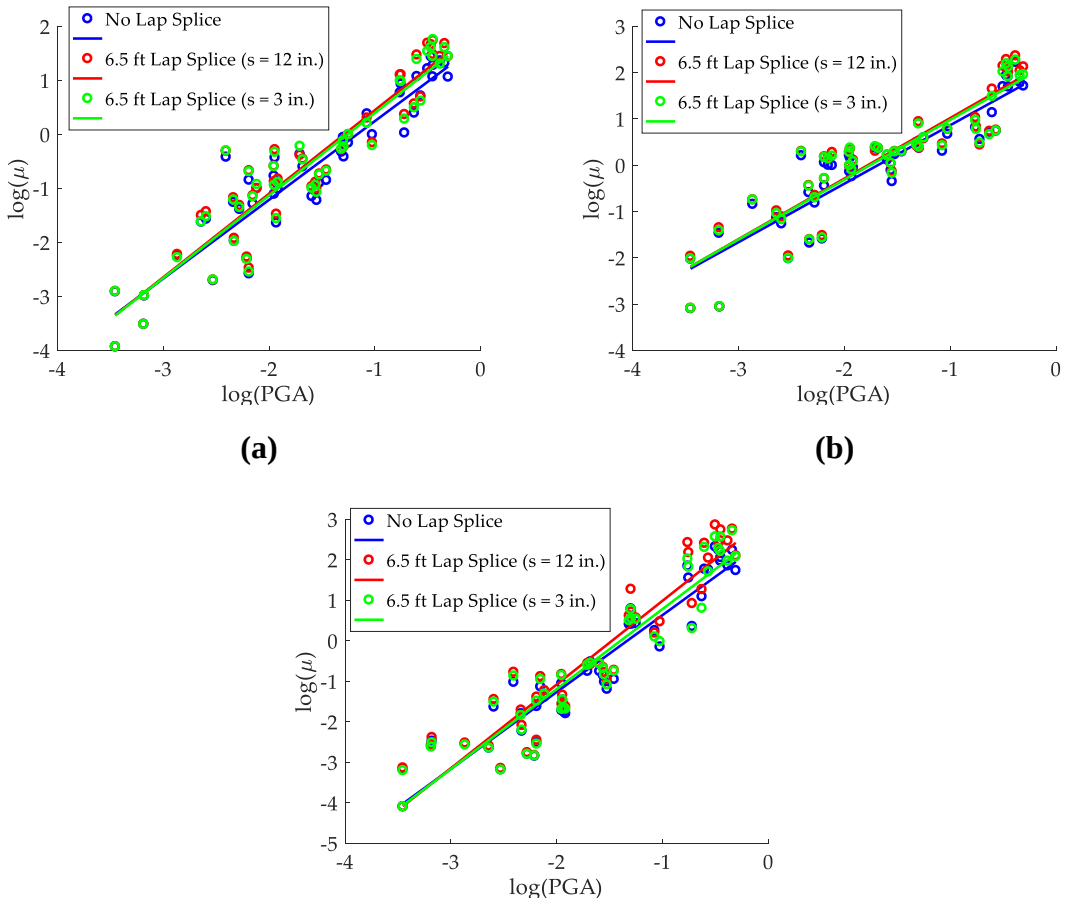

Figure 6.1 – PSDMs for Column Curvature Ductility Demand for (a) MSSS Concrete Bridge, (b) MSC Steel Girder Bridge, and (c) MSSS Steel Girder Bridge.

6.2 Seismic Fragility Curves and Site-Specific Risk Estimates

The following subsections present the column seismic fragility curves for the four limit states considered in this study. These curves are presented for three cases for lap splice and transverse reinforcement spacing: (1) no lap splice, (2) lap splice at the bottom of the column with a non-seismic transverse spacing (12-in. spacing), and (3) lap splice at the bottom of the column with a non-seismic transverse spacing (3-in. spacing).

6.2.1 Multi-Span Simply Supported Concrete Bridges

Figure 6.2 presents the fragility curves for all the limit states for these three cases, and Table 6-1 provides the probability estimates of exceeding the limit states. Note that LS stands for limit state in the figures and tables.

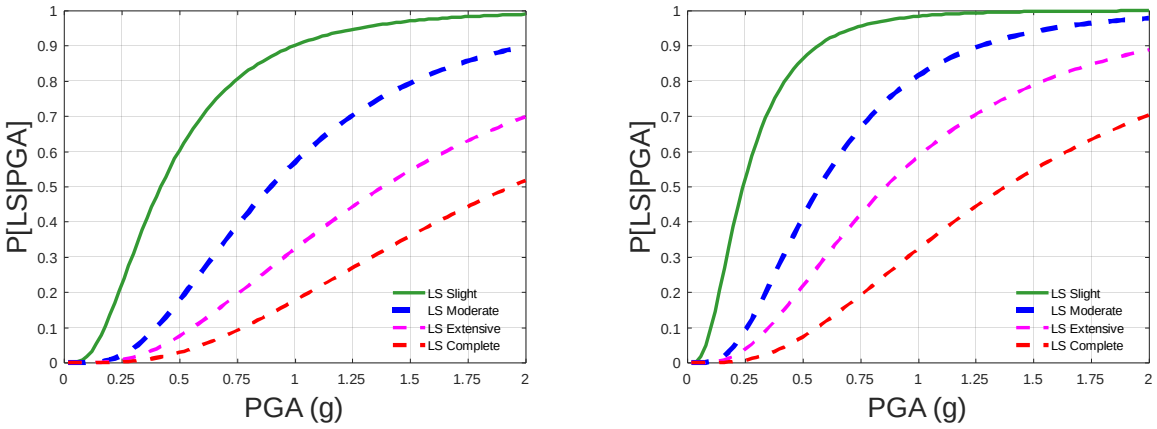

(a) **(b)**

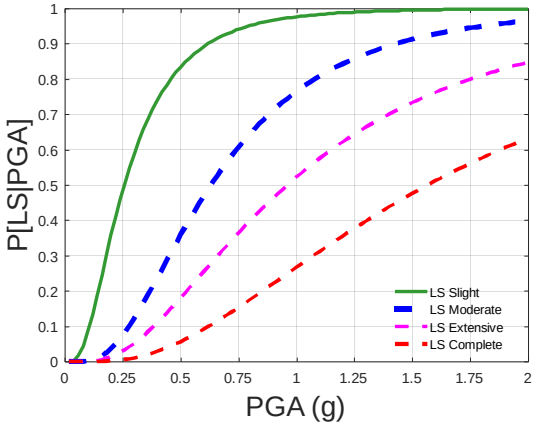

(c)

Figure 6.2 – Seismic Fragility Curves for MSSS Concrete Class for (a) No-Lap Splice with Seismic Spacing (s = 3-in.), (b) Lap Splice with Non-Seismic Spacing (s = 12-in.), and (c) Lap Splice with Seismic Spacing (s = 3-in.).

Table 6-1 – Comparative Probability Estimates of Exceeding Four Limit States for MSSS Concrete Bridges for (a) No-Lap Splice with Seismic Spacing (s = 3-in.), (b) Lap Splice with Non-Seismic Spacing (s = 12-in.), and (c) Lap Splice with Seismic Spacing (s = 3-in.).

(a)

PGA (g)	LS 1	LS 2	LS 3	LS 4
0.05	0.0%	0.0%	0.0%	0.0%
0.10	0.2%	0.0%	0.0%	0.0%
0.15	2.0%	0.0%	0.0%	0.0%
0.20	6.8%	0.2%	0.1%	0.0%
0.25	14.4%	0.7%	0.3%	0.1%
0.30	23.8%	1.9%	0.7%	0.2%
0.35	33.9%	4.0%	1.5%	0.4%

(b)

PGA (g)	LS 1	LS 2	LS 3	LS 4
0.05	0.0%	0.0%	0.0%	0.0%
0.10	2.1%	0.0%	0.0%	0.0%
0.15	11.2%	0.2%	0.1%	0.0%
0.20	26.1%	1.4%	0.5%	0.1%
0.25	42.4%	4.3%	1.6%	0.2%
0.30	56.9%	9.3%	3.7%	0.6%
0.35	68.5%	16.2%	6.8%	1.4%

(c)

PGA (g)	LS 1	LS 2	LS 3	LS 4
0.05	0.0%	0.0%	0.0%	0.0%
0.10	0.4%	0.0%	0.0%	0.0%
0.15	2.9%	0.0%	0.0%	0.0%
0.20	9.3%	0.4%	0.1%	0.0%
0.25	18.9%	1.3%	0.5%	0.1%
0.30	30.1%	3.4%	1.2%	0.3%
0.35	41.4%	6.7%	2.5%	0.8%

6.2.1.1 Site Class A

Table 6-2 presents the failure probabilities of the column reaching or exceeding each limit state. The maximum probability of exceeding Limit State 1 is estimated to be equal to 6.23% in Region 1. As all the probabilities are low, 6.5-ft lap splices with non-seismic transverse spacing are safe to be used for Site Class A.

Table 6-2 – Seismic Risk for MSSS Concrete Bridges for Site Class A when Lap-Splice with Non-Seismic Spacing is Provided.

Region	Zone	PGA (g)	Limit State 1	Limit State 2	Limit State 3	Limit State 4
1	1-A	0.13	6.23%	0.07%	0.03%	0.00%
2	1-A	0.11	3.57%	0.02%	0.01%	0.00%
3	1-A	0.08	0.66%	0.00%	0.00%	0.00%
4	1-A	0.06	0.17%	0.00%	0.00%	0.00%
5	1-A	0.05	0.02%	0.00%	0.00%	0.00%
6	1-A	0.03	0.00%	0.00%	0.00%	0.00%

6.2.1.2 Site Class B

Although for Site Class B, the whole state falls in Seismic Zone 1-A, the earthquake intensities for each region are higher than those for Site Class A. This results in higher probabilities of reaching the limit states for Site Class B compared to Site Class A, as shown in Table 6-3. The maximum probability of exceeding the first limit state is 13.83% in Region 1. Considering this risk, to be on the conservative side, lap splice with seismic reinforcement spacing could be provided for Region 1 for Site Class B. However, for the rest of the state, a lap splice with a non-seismic spacing is sufficient.

Table 6-3 – Seismic Risk for MSSS Concrete Bridges for Site Class B when Lap-Splice with Non-Seismic Spacing is Provided.

Region	Zone	PGA (g)	Limit State 1	Limit State 2	Limit State 3	Limit State 4
1	1-A	0.16	13.83%	0.36%	0.14%	0.01%
2	1-A	0.14	8.76%	0.14%	0.06%	0.00%
3	1-A	0.10	2.11%	0.01%	0.01%	0.00%
4	1-A	0.08	0.66%	0.00%	0.00%	0.00%
5	1-A	0.06	0.11%	0.00%	0.00%	0.00%
6	1-A	0.04	0.01%	0.00%	0.00%	0.00%

6.2.1.3 Site Class C

As observed from Table 6-4(a) when a lap splice with non-seismic spacing is provided at the base of the columns, the probabilities of exceeding Limit State 1 for Seismic Zone 1-B (Regions 1 and 2) are 23.51% and 16.11%. Table 6-4(b) presents the probabilities for Regions 1 and 2 when a lap splice with seismic spacing is provided at the base of the column. When the seismic spacing is provided, the probabilities of exceeding Limit State 1 for Regions 1 and 2 reduce to 8.03% and 4.78%, respectively. Table 6-4(c) presents the probabilities for Regions 1 and 2 when no lap splice is provided at the base of the column. In this case, the probabilities of exceedance further reduce to 5.79% and 3.36%, respectively. Considering these values, for Site Class C, it is recommended that seismic spacing be provided for MSSS concrete bridge class when the bridge is in Seismic Zone 1-B.

Table 6-4 – Seismic Risk for MSSS Concrete Bridges for Site Class C when (a) Lap-Splice with Non-Seismic Spacing is Provided, (b) Lap-Splice with Seismic Spacing is Provided, and (c) No Lap Splice is Provided.

(a)

Region	Zone	PGA (g)	Limit State 1	Limit State 2	Limit State 3	Limit State 4
1	1-B	0.19	23.51%	1.10%	0.42%	0.04%
2	1-B	0.17	16.11%	0.49%	0.19%	0.01%
3	1-A	0.12	4.80%	0.05%	0.02%	0.00%
4	1-A	0.10	1.73%	0.01%	0.00%	0.00%
5	1-A	0.07	0.36%	0.00%	0.00%	0.00%
6	1-A	0.05	0.02%	0.00%	0.00%	0.00%

(b)

Region	Zone	PGA (g)	Limit State 1	Limit State 2	Limit State 3	Limit State 4
1	1-B	0.19	8.03%	0.27%	0.10%	0.02%
2	1-B	0.17	4.78%	0.11%	0.04%	0.01%

(c)

Region	Zone	PGA (g)	Limit State 1	Limit State 2	Limit State 3	Limit State 4
1	1-B	0.19	5.79%	0.13%	0.05%	0.00%
2	1-B	0.17	3.36%	0.05%	0.02%	0.00%

6.2.1.4 Site Class D

For Site Class D, Table 6-5(a) shows that the probabilities of exceeding Limit State 1 are 40.15% and 29.38% for Regions 1 and 2, respectively, when a lap splice and non-seismic spacing are provided. When a lap splice is not provided at the column base as shown in Table 6-5(b), the probability of exceedance for Region 1 has a reduction of 26.99% for Limit State 1. Similarly,

when a lap splice is not provided at the column base, the probability of exceedance for Region 2 has a reduction of 21.31% for Limit State 1. Due to this considerable reduction in the risk, it is recommended that the lap splice should not be provided for Seismic Zone 2 for Site Class D.

For the rest of the state, the risk estimates are low due to lower earthquake intensities even though the regions fall in Seismic Zone 1-B. It is recommended that seismic spacing requirements be followed for Seismic Zone 1-B, particularly for Region 3, which sees a decrease in seismic risk of exceeding Limit State 1 from 13.83% to 3.90%.

Table 6-5 – Seismic Risk for MSSS Concrete Bridges for Site Class D when (a) Lap-Splice with Non-Seismic Spacing is Provided, (b) Lap-Splice with Seismic Spacing is Provided for Seismic Zone 1-B, and No Lap Splice is Provided for Seismic Zone 2.

(a)

Region	Zone	PGA (g)	Limit State 1	Limit State 2	Limit State 3	Limit State 4
1	2	0.24	40.15%	3.76%	1.43%	0.20%
2	2	0.21	29.38%	1.80%	0.68%	0.08%
3	1-B	0.16	13.83%	0.36%	0.14%	0.01%
4	1-B	0.13	6.62%	0.08%	0.04%	0.00%
5	1-B	0.09	1.73%	0.01%	0.00%	0.00%
6	1-A	0.06	0.17%	0.00%	0.00%	0.00%

(b)

Region	Zone	PGA (g)	Limit State 1	Limit State 2	Limit State 3	Limit State 4
1	2	0.24	13.16%	0.60%	0.22%	0.04%
2	2	0.21	8.07%	0.24%	0.09%	0.02%
3	1-B	0.16	3.90%	0.08%	0.03%	0.01%
4	1-B	0.13	1.49%	0.01%	0.01%	0.00%
5	1-B	0.09	0.28%	0.00%	0.00%	0.00%

6.2.1.5 Site Class E

Table 6-6(a) presents the seismic risk estimated for the MSSS concrete bridge class for Site Class E when the lap splice is provided at the base of the column. For most regions, these values are large. Eliminating the lap splice reduces the probability of exceeding Limit State 1 by 34.66% for Region 1. The reduction of risk for other regions can be observed from Table 6-6(b), as well. Therefore, it is recommended to provide no lap splice at the base of the column for Site Class E, particularly for Regions 1–5.

Table 6-6 – Seismic Risk for MSSS Concrete Bridges for Site Class E when (a) Lap-Splice with Non-Seismic Spacing is Provided, (b) Lap-Splice with Seismic Spacing is Provided for Seismic Zone 1-B and No Lap Splice is Provided for Seismic Zone 2.

(a)

Region	Zone	PGA (g)	Limit State 1	Limit State 2	Limit State 3	Limit State 4
1	2	0.35	68.53%	16.19%	6.81%	1.41%
2	2	0.28	51.39%	7.06%	2.76%	0.44%
3	2	0.25	42.37%	4.29%	1.64%	0.23%
4	2	0.20	26.10%	1.38%	0.52%	0.06%
5	2	0.15	11.17%	0.23%	0.09%	0.01%
6	1-B	0.10	2.11%	0.01%	0.01%	0.00%

(b)

Region	Zone	PGA (g)	Limit State 1	Limit State 2	Limit State 3	Limit State 4
1	2	0.35	33.87%	4.02%	1.46%	0.39%
2	2	0.28	19.88%	1.33%	0.48%	0.11%
3	2	0.25	14.36%	0.71%	0.26%	0.05%
4	2	0.2	6.76%	0.17%	0.07%	0.01%
5	2	0.15	2.03%	0.02%	0.01%	0.00%
6	1-B	0.10	0.36%	0.00%	0.00%	0.00%

6.2.2 Multi-Span Continuous Steel Bridges

Seismic analysis of this bridge class is performed using the same set of ground motions and same lap splice cases as for the previous bridge class. Figure 6.3 presents the seismic fragility curves for the MSC steel bridge class.

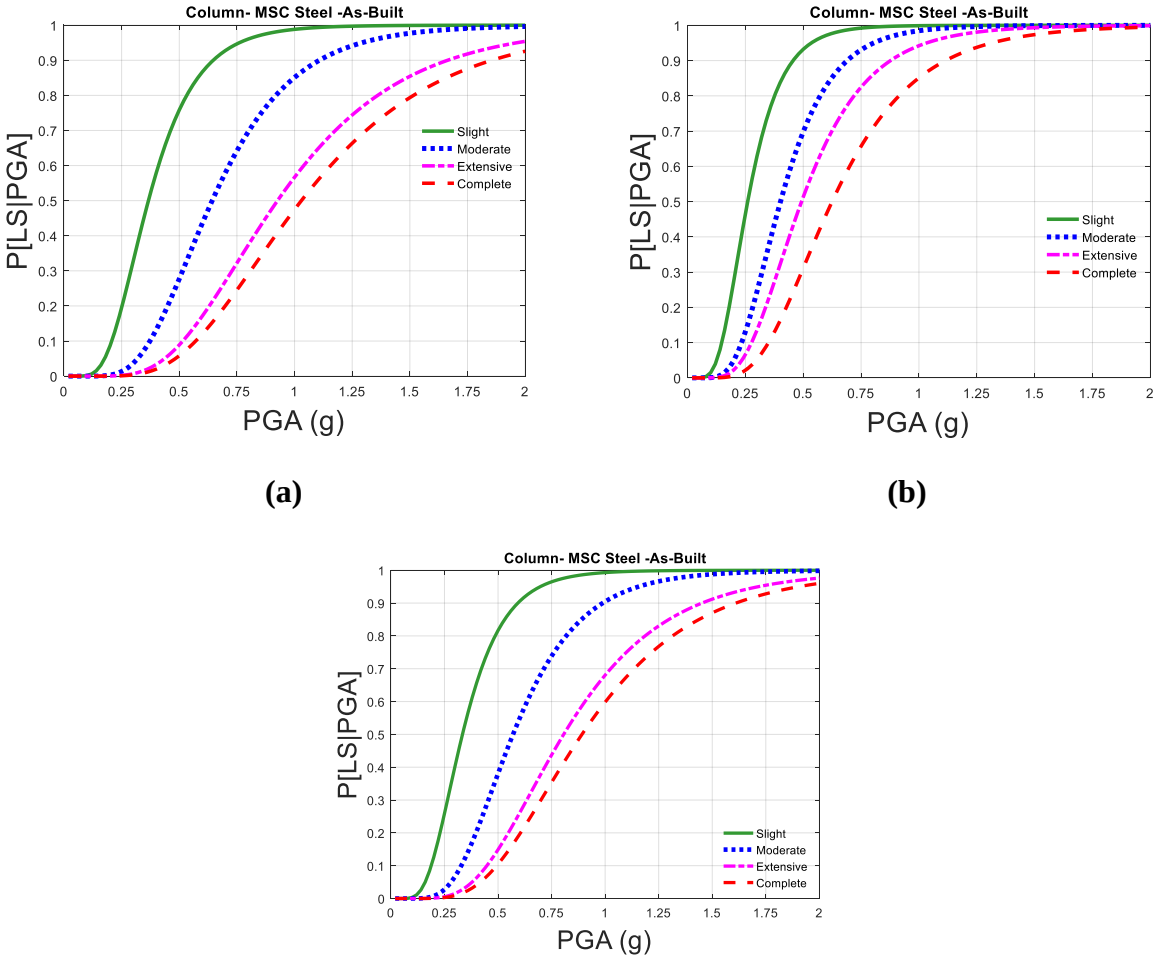

Figure 6.3 – Seismic Fragility Curves for MSC Steel Class for (a) No-Lap Splice with Seismic Spacing (s = 3-in.), (b) Lap Splice with Non-Seismic Spacing (s = 12-in.), and (c) Lap Splice with Seismic Spacing (s = 3-in.).

To facilitate comparison between the bridge classes and varying seismic detail cases, the probability values for seismic risk of exceeding limit states (LS) 1–4 are also presented in Table 6-7. Values are provided up to 0.4 g at intervals of 0.05 g.

Table 6-7 – Comparative Probability Estimates of Exceeding Four Limit States for MSC Steel Bridges for (a) No-Lap Splice with Seismic Spacing (s = 3-in.), (b) Lap Splice with Non-Seismic Spacing (s = 12-in.), and (c) Lap Splice with Seismic Spacing (s = 3-in.).

(a)

PGA	LS1	LS2	LS3	LS4
0.05 g	0.0%	0.0%	0.0%	0.0%
0.1 g	0.2%	0.0%	0.0%	0.0%
0.15 g	2.2%	0.0%	0.0%	0.0%
0.2 g	8.7%	0.3%	0.0%	0.0%
0.25 g	19.5%	1.3%	0.2%	0.1%
0.3 g	32.7%	3.6%	0.7%	0.4%
0.35 g	45.9%	7.6%	1.7%	1.0%
0.4 g	57.9%	13.2%	3.3%	2.0%

(b)

PGA	LS1	LS2	LS3	LS4
0.05 g	0.0%	0.0%	0.0%	0.0%
0.1 g	1.5%	0.0%	0.0%	0.0%
0.15 g	10.5%	1.0%	0.4%	0.1%
0.2 g	27.6%	4.9%	2.3%	0.6%
0.25 g	46.5%	13.1%	6.6%	2.1%
0.3 g	62.8%	24.5%	13.5%	5.2%
0.35 g	75.1%	37.2%	22.4%	10.0%
0.4 g	83.7%	49.6%	32.2%	16.2%

(c)

PGA	LS1	LS2	LS3	LS4
0.05 g	0.0%	0.0%	0.0%	0.0%
0.1 g	0.3%	0.0%	0.0%	0.0%
0.15 g	3.7%	0.1%	0.0%	0.0%
0.2 g	12.6%	0.7%	0.1%	0.1%
0.25 g	25.9%	2.8%	0.5%	0.3%
0.3 g	40.5%	6.8%	1.6%	0.9%
0.35 g	54.2%	12.8%	3.4%	2.1%
0.4 g	65.7%	20.5%	6.3%	4.1%

Note that LS stands for limit state in the tables.

6.2.2.1 Site Class A

For MSC steel bridges in Site Class A, the corresponding probabilities of exceeding Limit States 1–4 for the six regions are shown in Table 6-8. Because the PGA intensities are low, the probabilities of exceeding all the limit states are low, as well. The maximum probability of

exceeding any limit state is in Region 1 and is equal to 5.34%. Thus, providing a long lap splice at the column base with non-seismic transverse spacing is safe for this site class.

Table 6-8 – Seismic Risk for MSC Steel Bridges for Site Class A when Lap-Splice with Non-Seismic Spacing is Provided.

Region	Zone	PGA (g)	Limit State 1	Limit State 2	Limit State 3	Limit State 4
1	1-A	0.13	5.34%	0.34%	0.14%	0.02%
2	1-A	0.11	2.76%	0.12%	0.05%	0.01%
3	1-A	0.08	0.36%	0.01%	0.00%	0.00%
4	1-A	0.06	0.07%	0.00%	0.00%	0.00%
5	1-A	0.05	0.01%	0.00%	0.00%	0.00%
6	1-A	0.03	0.00%	0.00%	0.00%	0.00%

6.2.2.2 Site Class B

For Site Class B, as shown in Table 6-9, the maximum probability of exceeding any limit state is in Region 1 and is equal to 13.47%. This probability is higher than for Site Class A. Therefore, relative to Limit State 1, for Site Class B, if the bridge is in Region 1, it is recommended that seismic transverse spacing be used. If the limit state of interest is Limit State 2, then non-seismic spacing is sufficient. For the rest of the state, for all limit states, long lap splices with non-seismic spacing are safe.

Table 6-9 – Seismic Risk for MSC Steel Bridges for Site Class B when Lap-Splice with Non-Seismic Spacing is Provided.

Region	Zone	PGA (g)	Limit State 1	Limit State 2	Limit State 3	Limit State 4
1	1-A	0.16	13.47%	1.46%	0.62%	0.13%
2	1-A	0.14	7.95%	0.63%	0.26%	0.05%
3	1-A	0.10	1.48%	0.05%	0.02%	0.00%
4	1-A	0.08	0.36%	0.01%	0.00%	0.00%
5	1-A	0.06	0.04%	0.00%	0.00%	0.00%
6	1-A	0.04	0.00%	0.00%	0.00%	0.00%

6.2.2.3 Site Class C

For Site Class C, Table 6-10(a) shows that Regions 1 and 2 show relatively higher probabilities of exceeding the Limit State 1 when a long lap splice with non-seismic spacing is used. However, when lap splice with seismic transverse reinforcement spacing is used, these probabilities reduce significantly from 24.60% to 10.78% for Region 1 and from 16.03% to 6.22% for Region 2, as shown in Table 6-10(b). Hence, for Seismic Zone 1-B in Site Class B, it is recommended to use a lap splice with seismic reinforcement spacing. Again, this is relative to Limit State 1. Considering performance relative to Limit State 2, the probabilities of exceedance may be acceptable for the lap splice and non-seismic spacing. For Seismic Zone 1-A for all limit states, a long lap splice with non-seismic spacing is sufficient.

Table 6-10 – Seismic Risk for MSC Supported Steel Bridges for Site Class C when (a) Lap-Splice with Non-Seismic Spacing is Provided, and (b) Lap-Splice with Seismic Spacing is Provided.

(a)

Region	Zone	PGA (g)	Limit State 1	Limit State 2	Limit State 3	Limit State 4
1	1-B	0.19	24.60%	4.02%	1.81%	0.45%
2	1-B	0.17	16.03%	1.95%	0.01%	0.00%
3	1-A	0.12	3.92%	0.21%	0.09%	0.01%
4	1-A	0.10	1.17%	0.03%	0.01%	0.00%
5	1-A	0.07	0.17%	0.00%	0.00%	0.00%
6	1-A	0.05	0.00%	0.00%	0.00%	0.00%

(b)

Region	Zone	PGA (g)	Limit State 1	Limit State 2	Limit State 3	Limit State 4
1	1-B	0.19	10.78%	0.56%	0.09%	0.04%
2	1-B	0.17	6.22%	0.22%	0.03%	0.01%

6.2.2.4 Site Class D

For Site Class D, Table 6-11(a) shows Limit State 1 probabilities of exceedance of 44.00% and 31.39% for Regions 1 and 2, respectively, when a long lap splice with non-seismic spacing is used. Table 6-11(b) shows the probabilities of exceedance when no lap splice is used for Seismic Zone 2, and lap splice within the plastic hinge region and seismic spacing is used for Seismic Zone 1-B. The probabilities shown in Table 6-11(b) are significantly lower than those in Table 6-11(a), particularly for Regions 1–3 for Limit State 1. Therefore, it is recommended that for Site Class D the lap splice be outside the plastic hinge region for Seismic Zone 2 with seismic spacing if designing for Limit State 1. For Seismic Zone 1-B Region 3, also relative to Limit State 1, the lap splice can be within the plastic hinge region if seismic spacing is provided. Relative to Limit

State 2, it is recommended that lap splice outside the plastic hinge region and seismic spacing be provided for Region 1 to reduce the risk of exceeding Limit State 2 from 11.69% to 1.10%.

Table 6-11 – Seismic Risk for MSC Steel Bridges for Site Class D when (a) Lap-Splice with Non-Seismic Spacing is Provided, and (b) No Lap Splice with 3-in. Spacing for Seismic Zone 2 and Lap-Splice with 3-in. Spacing for Seismic Zone 1-B are Provided.

(a)

Region	Zone	PGA (g)	Limit State 1	Limit State 2	Limit State 3	Limit State 4
1	2	0.24	44.00%	11.69%	5.82%	1.84%
2	2	0.21	31.39%	6.22%	2.91%	0.80%
3	1-B	0.16	13.47%	1.46%	0.62%	0.13%
4	1-B	0.13	5.74%	0.38%	0.15%	0.03%
5	1-B	0.09	1.17%	0.03%	0.01%	0.00%
6	1-A	0.06	0.07%	0.00%	0.00%	0.00%

(b)

Region	Zone	PGA (g)	Limit State 1	Limit State 2	Limit State 3	Limit State 4
1	2	0.24	17.79%	1.10%	0.17%	0.08%
2	2	0.21	10.53%	0.42%	0.06%	0.03%
3	1-B	0.16	4.99%	0.15%	0.02%	0.01%
4	1-B	0.13	1.74%	0.03%	0.00%	0.00%
5	1-B	0.09	0.27%	0.00%	0.00%	0.00%

6.2.2.5 Site Class E

For Site Class E, the corresponding probabilities of exceeding various limit states when lap splice with non-seismic spacing are used are shown in Table 6-12(a). The maximum probability of exceeding Limit State 1 is for Region 1 and is equal to 75.14%. Except for Region 6, which falls in Seismic Zone 1-B, the probabilities of exceeding Limit State 1 for all other regions are above 10%. AASHTO LRFD seismic provisions do not recommend lap splices for

Seismic Zone 2. Table 6-12(b) shows the probabilities of exceeding limit states when the lap splice is outside the plastic hinge region for Seismic Zone 2 and when it is within the plastic hinge region with seismic spacing for Seismic Zone 1-B. There is about a 30% reduction in the probabilities of exceeding Limit State 1 for Regions 1–3, a 20% reduction for Region 4, and a 10% reduction for Region 5 with this seismic detailing. Therefore, it is recommended that, relative to Limit State 1, the lap splice be outside the plastic hinge region with seismic spacing for Seismic Zone 2 in Site Class E. Relative to Limit State 2, the largest reductions in risk are for Regions 1–3. Therefore, it is recommended that the lap splice be outside the plastic hinge region with seismic spacing for Regions 1–3 relative to Limit State 2.

Table 6-12 – Seismic Risk for MSC Steel Bridge Class for Site Class E when (a) Lap-Splice with Non-Seismic Spacing is Provided, and (b) No Lap Splice with 3-in. Spacing for Seismic Zone 2 and Lap-Splice with 3-in. Spacing for Seismic Zone 1-B are Provided.

(a)

Region	Zone	PGA (g)	Limit State 1	Limit State 2	Limit State 3	Limit State 4
1	2	0.35	75.14%	37.22%	22.37%	10.01%
2	2	0.28	56.78%	19.63%	10.46%	3.80%
3	2	0.25	46.51%	13.07%	6.59%	2.14%
4	2	0.20	27.56%	4.93%	2.26%	0.59%
5	2	0.15	10.54%	0.98%	0.41%	0.08%
6	1-B	0.10	1.48%	0.05%	0.02%	0.00%

(b)

Region	Zone	PGA (g)	Limit State 1	Limit State 2	Limit State 3	Limit State 4
1	2	0.35	45.94%	7.61%	1.66%	0.95%
2	2	0.28	27.28%	2.51%	0.44%	0.23%
3	2	0.25	19.51%	1.31%	0.21%	0.10%
4	2	0.2	8.66%	0.30%	0.04%	0.02%
5	2	0.15	2.22%	0.03%	0.00%	0.00%
6	1-B	0.10	0.35%	0.00%	0.00%	0.00%

6.2.3 Multi-Span Simply Supported Steel Bridges

Seismic analysis of this bridge class uses the same set of ground motions and seismic detailing cases as for the previous bridge class. Figure 6.4 presents the seismic fragility curves for the MSSS steel bridge class. To facilitate comparison between the bridge classes and seismic detailing cases, the probability values are also presented in Table 6-13 up to 0.35 g at intervals of 0.05 g. In general, this bridge class shows increased probabilities of exceeding limit states compared to the previously discussed two bridge classes due to the mass of superstructure for MSSS steel bridges being higher than for MSSS concrete bridges. This imposes a greater demand

on the columns, resulting in higher probabilities of reaching the limit states. For MSSS steel bridges, the following results also consider the effect of the number of stirrups in each direction.

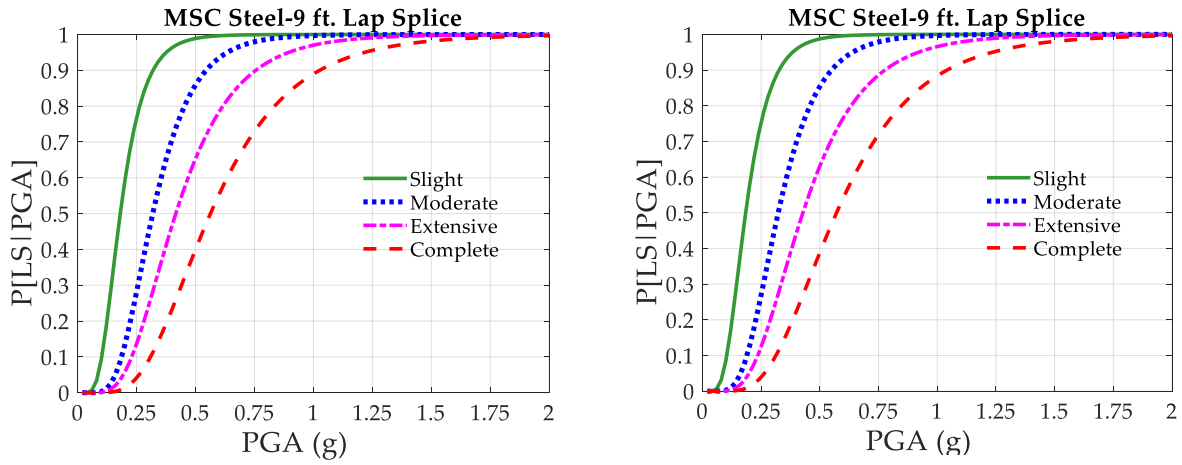

(a) **(b)**

Figure 6.4 – Seismic Fragility Curves for MSSS Steel Bridges with 9-ft Lap Splice at 6-in. Spacing, a) One Stirrup in Each Direction b) Two Stirrups in Each Direction

Table 6-13 – Comparative Probability Estimates of Exceeding Four Limit States for MSSS Steel Bridges for 9-ft Lap Splice with #6 Stirrup at 6-in. Spacing, (a) One Stirrup in Each Direction (b) Two Stirrups in Each Direction

(a)

PGA (g)	Limit State 1	Limit State 2	Limit State 3	Limit State 4
0.05	0.19%	0.00%	0.00%	0.00%
0.10	9.16%	0.26%	0.10%	0.01%
0.15	33.85%	3.51%	1.38%	0.22%
0.20	59.19%	13.19%	5.72%	1.29%
0.25	76.90%	28.11%	13.66%	4.00%
0.30	87.43%	44.44%	24.17%	8.72%
0.35	93.25%	59.17%	35.68%	15.22%

(b)

PGA (g)	Limit State 1	Limit State 2	Limit State 3	Limit State 4
0.05	0.18%	0.00%	0.00%	0.00%
0.10	8.63%	0.25%	0.10%	0.01%
0.15	32.51%	3.31%	1.31%	0.21%
0.20	57.62%	12.56%	5.45%	1.23%
0.25	75.59%	27.01%	13.10%	3.83%
0.30	86.49%	43.03%	23.31%	8.36%
0.35	92.63%	57.68%	34.60%	14.66%

According to the results shown above, two stirrups in each direction (four legs) decrease the probability of exceeding each limit state slightly in comparison with one stirrup in each direction (two legs). This is due to the fact that the combination of the 9-ft lap splice and #6 bar @

6-in. spacing is sufficient to allow the lap splice to develop its flexural yield strength and residual strength. Therefore, the number of stirrups along each direction only marginally strengthens the confinement effect of core concrete.

6.2.3.1 Site Class A

For MSSS steel bridges, as all the regions for Site Class A experience very low earthquake intensities, the risk estimates are within the acceptable range, as shown in Table 6-14. Having two legs or four legs for stirrups in each direction does not make a significant difference in terms of the risk values.

Table 6-14 – Seismic Risk for MSSS Steel Bridges for Site Class A with 9-ft Lap Splice, (a) One Stirrup in Each Direction (b) Two Stirrups in Each Direction

(a)

Region	Zone	PGA (g)	Limit State 1	Limit State 2	Limit State 3	Limit State 4
1	1-A	0.13	21.93%	1.41%	0.55%	0.07%
2	1-A	0.11	14.10%	0.59%	0.23%	0.03%
3	1-A	0.08	3.33%	0.04%	0.02%	0.00%
4	1-A	0.06	0.97%	0.01%	0.00%	0.00%
5	1-A	0.05	0.14%	0.00%	0.00%	0.00%
6	1-A	0.03	0.00%	0.00%	0.00%	0.00%

(b)

Region	Zone	PGA (g)	Limit State 1	Limit State 2	Limit State 3	Limit State 4
1	1-A	0.13	20.91%	1.33%	0.52%	0.07%
2	1-A	0.11	13.36%	0.56%	0.22%	0.02%
3	1-A	0.08	3.11%	0.04%	0.02%	0.00%
4	1-A	0.06	0.90%	0.01%	0.00%	0.00%
5	1-A	0.05	0.13%	0.00%	0.00%	0.00%
6	1-A	0.03	0.00%	0.00%	0.00%	0.00%

6.2.3.2 Site Class B

For Site Class B, although all the regions fall in Seismic Zone 1-A, Table 6-15 shows that Regions 1 and 2 show relatively high risk values (>25%) for Limit State 1. The probabilities of exceedance of Limit State 2 are relatively low. The number of stirrups does not significantly alter the probability of exceedance.

Table 6-15 – Seismic Risk for MSSS Steel Bridges for Site Class B with 9-ft Lap Splice, (a) One Stirrup in Each Direction (b) Two Stirrups in Each Direction

(a)

Region	Zone	PGA (g)	Limit State 1	Limit State 2	Limit State 3	Limit State 4
1	1-A	0.16	39.32%	4.89%	1.96%	0.34%
2	1-A	0.14	28.36%	2.40%	0.94%	0.14%
3	1-A	0.10	9.16%	0.26%	0.10%	0.01%
4	1-A	0.08	3.33%	0.04%	0.02%	0.00%
5	1-A	0.06	0.65%	0.00%	0.00%	0.00%
6	1-A	0.04	0.03%	0.00%	0.00%	0.00%

(b)

Region	Zone	PGA (g)	Limit State 1	Limit State 2	Limit State 3	Limit State 4
1	1-A	0.16	37.88%	4.63%	1.86%	0.32%
2	1-A	0.14	27.15%	2.26%	0.88%	0.13%
3	1-A	0.10	8.63%	0.25%	0.10%	0.01%
4	1-A	0.08	3.11%	0.04%	0.02%	0.00%
5	1-A	0.06	0.60%	0.00%	0.00%	0.00%
6	1-A	0.04	0.03%	0.00%	0.00%	0.00%

6.2.3.3 Site Class C

Similar to Site Class B, Regions 1 and 2 show relatively high risk values greater than 25% for Limit State 1, and low risk values for Limit State 2. Tables 6-16 summarizes the probability of exceedance for each region.

Table 6-16 – Seismic Risk for MSSS Steel Bridges for Site Class C with 9-ft Lap Splice, (a) One Stirrup in Each Direction (b) Two Stirrups in Each Direction

(a)

Region	Zone	PGA (g)	Limit State 1	Limit State 2	Limit State 3	Limit State 4
1	1-B	0.19	55.58%	11.20%	4.77%	1.02%
2	1-B	0.17	43.61%	6.20%	2.52%	0.46%
3	1-A	0.12	17.88%	0.94%	0.36%	0.04%
4	1-A	0.10	7.73%	0.19%	0.08%	0.01%
5	1-A	0.07	1.91%	0.02%	0.01%	0.00%
6	1-A	0.05	0.14%	0.00%	0.00%	0.00%

(b)

Region	Zone	PGA (g)	Limit State 1	Limit State 2	Limit State 3	Limit State 4
1	1-B	0.19	54.01%	10.65%	4.54%	0.97%
2	1-B	0.17	42.11%	5.88%	2.39%	0.44%
3	1-A	0.12	16.99%	0.89%	0.34%	0.04%
4	1-A	0.10	7.28%	0.18%	0.07%	0.01%
5	1-A	0.07	1.78%	0.02%	0.01%	0.00%
6	1-A	0.05	0.13%	0.00%	0.00%	0.00%

6.2.3.4 Site Class D

For Site Class D, Table 6-17 shows that Regions 1-3 have risk values greater than 25% for probabilities of exceeding Limit State 1. The number of stirrups does not significantly alter the probability of exceedance.

Table 6-17 – Seismic Risk for MSSS Steel Bridges for Site Class D with 9-ft Lap Splice, (a) One Stirrup in Each Direction (b) Two Stirrups in Each Direction

(a)

Region	Zone	PGA (g)	Limit State 1	Limit State 2	Limit State 3	Limit State 4
1	2	0.24	74.91%	25.85%	12.36%	3.50%
2	2	0.21	63.40%	15.87%	7.04%	1.68%
3	1-B	0.16	39.32%	4.89%	1.96%	0.34%
4	1-B	0.13	22.98%	1.55%	0.60%	0.08%
5	1-B	0.09	7.73%	0.19%	0.08%	0.01%
6	1-A	0.06	0.97%	0.01%	0.00%	0.00%

(b)

Region	Zone	PGA (g)	Limit State 1	Limit State 2	Limit State 3	Limit State 4
1	2	0.24	73.55%	24.81%	11.84%	3.35%
2	2	0.21	61.86%	15.14%	6.71%	1.60%
3	1-B	0.16	37.88%	4.63%	1.86%	0.32%
4	1-B	0.13	21.92%	1.46%	0.57%	0.08%
5	1-B	0.09	7.28%	0.18%	0.07%	0.01%
6	1-A	0.06	0.90%	0.01%	0.00%	0.00%

6.2.3.5 Site Class E

For Site Class E, most of the state falls in Seismic Zone 2. AASHTO LRFD Design Specifications do not recommend providing a lap splice at the column base for Seismic Zone 2. The probability of exceeding Limit State 1 is more than 25% for Regions 1-5. Regions 1-3 have seismic risk values of 25% or larger for Limit State 2.

Table 6-18 – Seismic Risk for MSSS Steel Bridges for Site Class E with 9-ft Lap Splice, (a) One Stirrup in Each Direction (b) Two Stirrups in Each Direction

(a)

Region	Zone	PGA (g)	Limit State 1	Limit State 2	Limit State 3	Limit State 4
1	2	0.35	93.25%	59.17%	35.68%	15.22%
2	2	0.28	83.92%	37.97%	19.76%	6.59%
3	2	0.25	76.90%	28.11%	13.66%	4.00%
4	2	0.20	59.19%	13.19%	5.72%	1.29%
5	2	0.15	33.85%	3.51%	1.38%	0.22%
6	1-B	0.10	9.16%	0.26%	0.10%	0.01%

(b)

Region	Zone	PGA (g)	Limit State 1	Limit State 2	Limit State 3	Limit State 4
1	2	0.35	92.63%	57.68%	34.60%	14.66%
2	2	0.28	82.83%	36.66%	19.01%	6.32%
3	2	0.25	75.59%	27.01%	13.10%	3.83%
4	2	0.20	57.62%	12.56%	5.45%	1.23%
5	2	0.15	32.51%	3.31%	1.31%	0.21%
6	1-B	0.10	8.63%	0.25%	0.10%	0.01%

6.2.4 Multi-Span Simply Supported Slab Bridges

Seismic analysis of this bridge class is done using the same set of ground motions as for the previous bridge classes. Figure 6.5 presents the seismic fragility curves for the MSSS slab bridge class. For comparison between the embedded pile case and the dowel pile case, the probability values are also presented in Table 6-19 up to 0.35 g at intervals of 0.05 g. In general, this bridge class shows much lower probabilities of damage compared to the other three bridge classes. This can be attributed to the large number of piles in a bent (7 piles in a bent) and the metal

shell on the reinforced concrete piles. In addition, the dowel pile case shows lower probabilities of damage because of the additional dowel bars in the piles. The embedded pile case is similar to the dowel pile case, as both cases have similar lateral capacities. Therefore, the embedded pile and dowel pile cases exhibit similar performance.

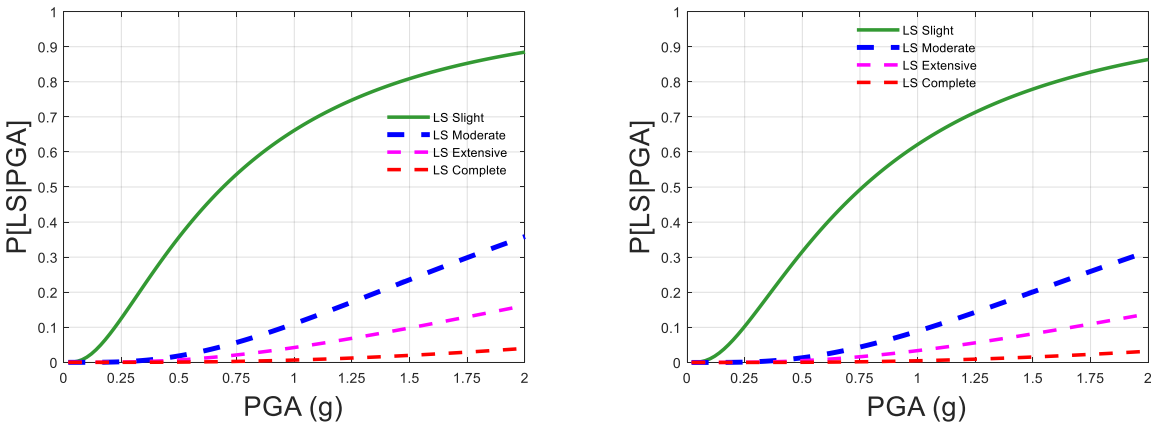

Figure 6.5 – Seismic Fragility Curves for MSSS Slab Bridges with (a) Embedded Piles, and (b) Dowel Piles.

Table 6-19 – Comparative Probability Estimates of Exceeding Four Limit States for MSSS Slab Bridges with (a) Embedded Piles, and (b) Dowel Piles.

(a)

PGA (g)	LS 1	LS 2	LS 3	LS 4
0.05	0.2%	0.0%	0.0%	0.0%
0.10	1.5%	0.0%	0.0%	0.0%
0.15	4.2%	0.0%	0.0%	0.0%
0.20	8.1%	0.1%	0.0%	0.0%
0.25	12.5%	0.2%	0.1%	0.0%
0.30	17.3%	0.3%	0.1%	0.0%
0.35	22.1%	0.6%	0.2%	0.0%

(b)

PGA (g)	LS1	LS2	LS3	LS4
0.05	0.1%	0.0%	0.0%	0.0%
0.10	1.0%	0.0%	0.0%	0.0%
0.15	3.2%	0.0%	0.0%	0.0%
0.20	6.4%	0.0%	0.0%	0.0%
0.25	10.3%	0.1%	0.0%	0.0%
0.30	14.5%	0.2%	0.1%	0.0%
0.35	18.8%	0.4%	0.2%	0.0%

Note that LS stands for limit state in the tables.

CHAPTER 7 ANALYSIS OF COLUMNS WITH VARIOUS TRANSVERSE REINFORCEMENT SPACINGS IN PLASTIC HINGES

The provisions 5.10.11.4.1d and e in the 2014 AASHTO LRFD Bridge Design Specifications [1] specify the transverse reinforcement area and spacing in the plastic hinge region. These are intended to support the axial load carried by the column core and to ensure that buckling of the longitudinal reinforcement is prevented. Thus, the spacing of the confining reinforcement is an important parameter to consider. In addition, there are impacts on constructability for varying spacing of the transverse reinforcement. Current specifications indicate that the vertical spacing of hoops cannot exceed 4.0-in., which is more rigorous than the 6.0-in. spacing in the 2011 AASHTO Guide Specifications for LRFD Seismic Bridge Design. To investigate the differences between the 4-in. and 6-in. spacings for bridges in Georgia subject to seismic hazard (the maximum PGA occurring in Site Class E is 0.34 g), the column responses and seismic risks are compared in the following paragraphs.

First, section analyses of seismically designed columns (#5 bars @ 4-in. o.c. transverse reinforcement) compared to non-seismically designed columns (#4 bars @ 12-in. o.c. transverse reinforcement) in both square and circular configurations were performed, as shown in Figure 7.1. The columns used are based on typical Georgia bridges, with concrete strength of 3500 psi and steel yield strength of 60,000 psi. The columns are 16-ft in height (Figure 2.14) and were modeled to have periods at approximately 0.6 second. The higher performance of the seismically designed columns (#5 bars @ 4-in. o.c. transverse reinforcement) compared to the non-seismically designed columns (#4 bars @ 12-in. o.c. transverse reinforcement) in terms of post-yield strength is seen in Figure 7.1.

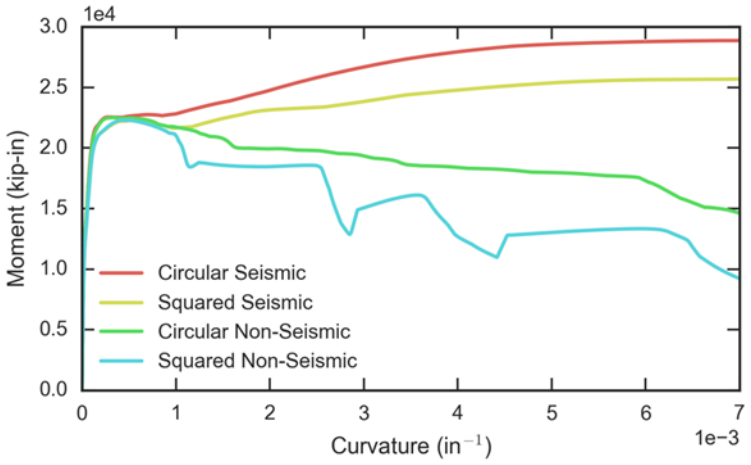

Figure 7.1 – Section Analysis.

A study using a single ground motion from the Rix suite was completed, scaling its maximum PGA between 0.1 and 0.65 g. By scaling the PGA, researchers can determine under what magnitude ground motion the transverse reinforcement becomes a critical factor in the response of the column. A summary of the effect of the column section properties versus ground motion PGA is shown in Figure 7.2. The figure indicates that transverse reinforcement is not a significant factor until reaching PGA values greater than 0.3 g. It is evident that the seismic circular column performs best, as expected.

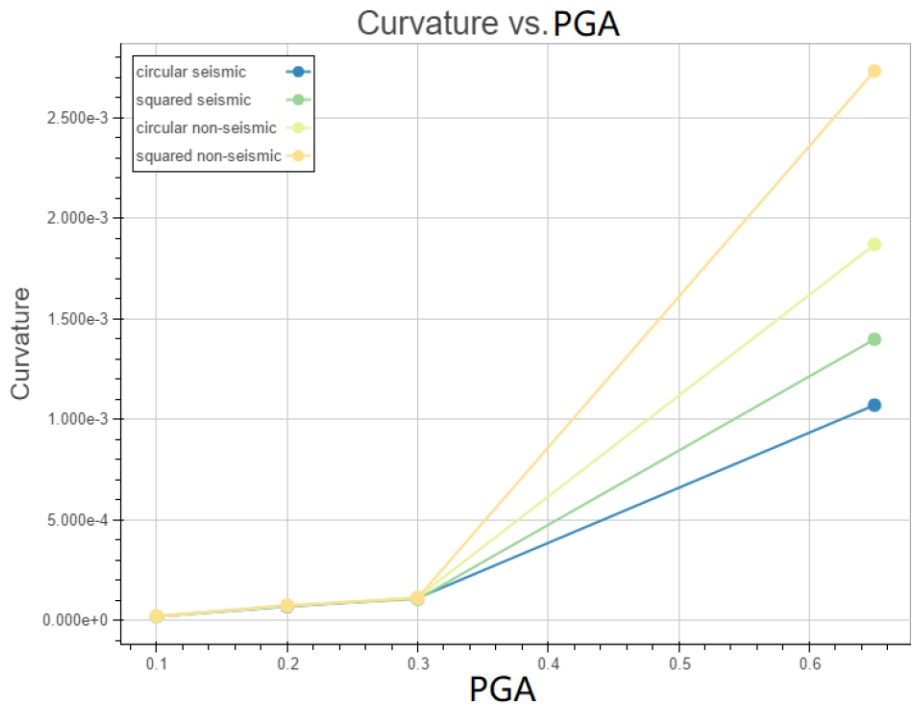

Figure 7.2 – Rix Ground Motion Scaling Summary Comparison.

Detailed comparisons of the seismic responses under varying values of PGA (0.1, 0.2, 0.3, and 0.65 g) are shown in Figures 7.3–7.6, respectively. These plots exhibit that at PGAs of 0.3 g and lower, the responses of all columns are very similar. Although Figure 7.2 shows that under a higher PGA (0.65 g), the column curvature responses are different, the column drifts are similar. Furthermore, the maximum factored PGA in Georgia is only 0.35 g, below the level where there is a difference in response.

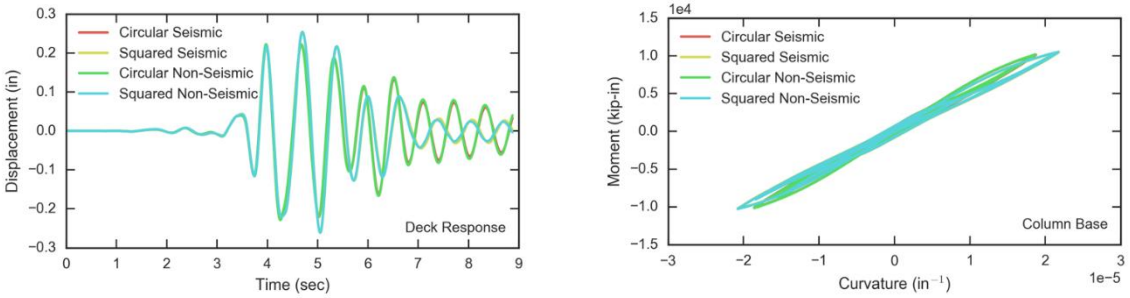

Figure 7.3 – Rix Ground Motion Scaling Responses at 0.1 g.

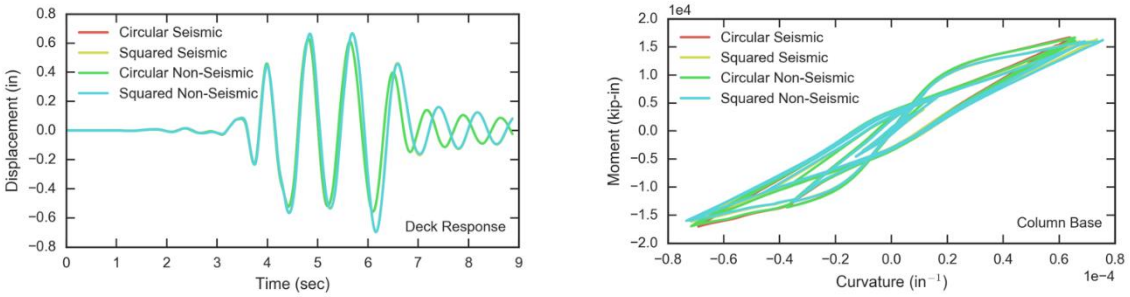

Figure 7.4 – Rix Ground Motion Scaling Responses at 0.2 g.

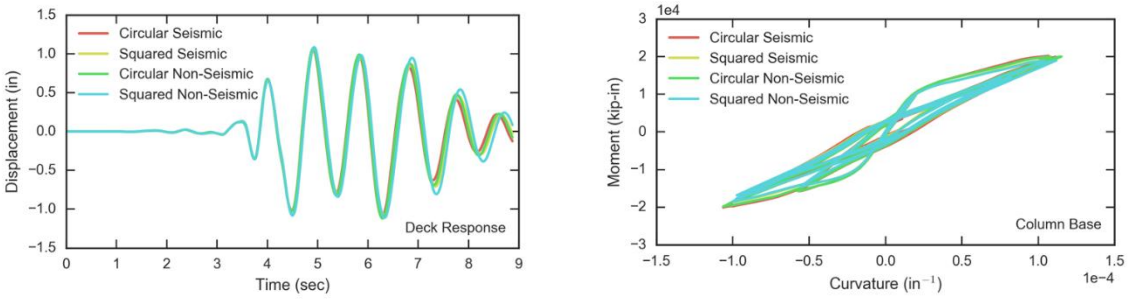

Figure 7.5 – Rix Ground Motion Scaling Responses at 0.3 g.

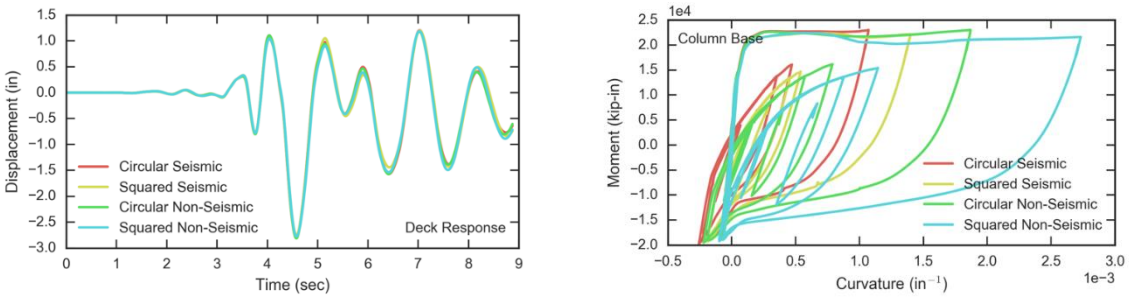

Figure 7.6 – Rix Ground Motion Scaling Responses at 0.65 g.

Since the maximum transverse reinforcement spacing specified in the latest AASHTO LRFD Bridge Design Specifications was reduced to 4-in., the small spacing raises an issue that it is difficult for the concrete to uniformly and smoothly flow through reinforcement gaps. Thus, a spacing of 6-in. for #6 transverse reinforcement is more constructible. This spacing is studied compared to #3 @ 3-in. and #6 @ 4-in. to investigate the estimated differences in seismic risk. As shown in Figure 7.7(a), both #6 @ 6-in. and #6 @ 4-in. provide greater strength and ductility than #3 @ 3-in. From the reinforcement aspect, the smaller spacing has the increased capacity to prevent reinforcement buckling (Figure 7.7(b)). However, for the overall section behavior shown in Figure 7.7(c), the performance of the three cases, #3 @ 3-in., #6 @ 4-in., and #6 @ 6-in., is similar. In addition, the seismic risk probabilities for the #3 @ 3-in. and #6 @ 6-in. cases are similar, with at most a 5% difference in exceeding limit states, as shown in Table 7.1. This is the case for all PGAs studied up to 0.4 g and for all limit states.

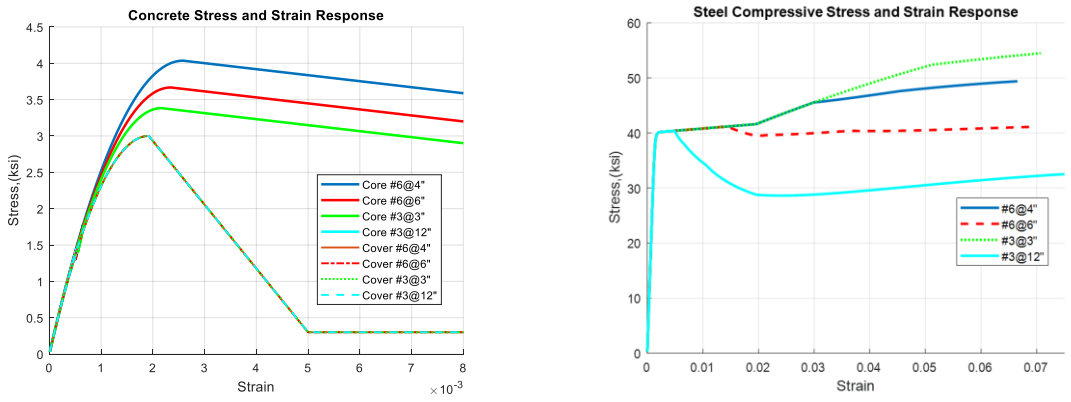

(a) **(b)**

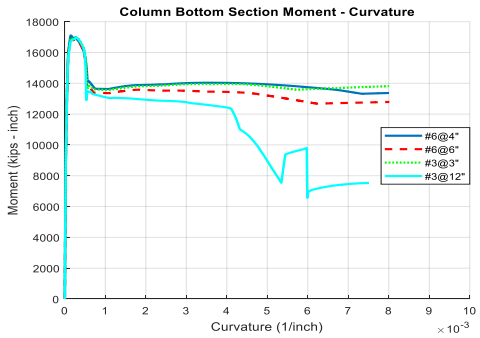

(c)

Figure 7.7 – Effects of Transverse Reinforcement Spacings at 3-in., 4-in., and 6-in. for (a) Concrete, (b) Longitudinal Reinforcement, and (c) Moment vs. Curvature.

Table 7.1 – Comparative Probability Estimates of Exceeding Four Limit States for Columns with: (a) #3 @ 3-in., and (b) #6 @ 6-in.

(a)

PGA	LS1	LS2	LS3	LS4
0.05 g	0.0%	0.0%	0.0%	0.0%
0.1 g	0.2%	0.0%	0.0%	0.0%
0.15 g	2.2%	0.0%	0.0%	0.0%
0.2 g	8.7%	0.3%	0.0%	0.0%
0.25 g	19.5%	1.3%	0.2%	0.1%
0.3 g	32.7%	3.6%	0.7%	0.4%
0.35 g	45.9%	7.6%	1.7%	1.0%
0.4 g	57.9%	13.2%	3.3%	2.0%

(b)

PGA	LS1	LS2	LS3	LS4
0.05 g	0.0%	0.0%	0.0%	0.0%
0.1 g	2.6%	0.0%	0.0%	0.0%
0.15 g	3.0%	0.1%	0.0%	0.0%
0.2 g	10.8%	0.5%	0.1%	0.0%
0.25 g	23.0%	2.1%	0.4%	0.2%
0.3 g	37.0%	5.4%	1.2%	0.7%
0.35 g	50.5%	10.6%	2.7%	1.6%
0.4 g	62.3%	17.4%	5.0%	3.2%

Note that LS stands for limit state in the tables.

CHAPTER 8 CONCLUSIONS AND RECOMMENDATIONS

Because the state of Georgia is identified as a region with low to moderate seismic activity, prior to adoption of LRFD design specifications, few bridges were designed with seismic detailing. However, recent specifications, including integration of seismic provisions from AASHTO LRFD Bridge Design Specifications [1] into Georgia's Bridge and Structures Design Manual [4], have increased the number of Georgia bridges requiring seismic design. This study investigates the impact of the most recent seismic detailing requirements on estimated seismic risk for bridges in Georgia. Based on the results, recommendations on seismic design for bridges in Georgia by bridge type and site class are provided to GDOT.

The first part of the study focuses on a literature review of previous research on seismic detailing, highlighting the importance of providing adequate lap splice length and transverse reinforcement to increase the strength and ductility of columns, especially in the case of cyclic loading. To analyze the effect of lap splices, a lap splice force transfer mechanism used in this study is presented. The model based on this mechanism depends on various factors, including the length of the lap splice, the transverse reinforcement spacing, the steel strength, and the steel rebar diameter. A parametric study investigating the impact of these variables on the lap splice stress–strain is conducted to determine the extent of influence of the factors.

To study the impact of the most recent AASHTO LRFD Bridge Design Specifications [1] on seismic performance, it is necessary to identify the potential seismic hazard in the state of Georgia. This is accomplished by dividing the state into six regions based on maximum PGA for Site Classes A, B, C, D, and E. It is found that the northern region of Georgia for each site class is

most susceptible to potential earthquakes. The maximum PGA in the state is expected for Site Class E in the northern region of Georgia and is equal to 0.34 g.

The seismic detailing parameters, including lap splice and varying transverse reinforcement spacing values, are incorporated into 3-D finite element bridge models using the software OpenSees. These models are used to estimate the demand imposed on bridge columns through running nonlinear time history analyses. Four classes of highway bridges, namely MSSS concrete girder bridges, MSC steel girder bridges, MSSS steel girder bridges, and MSSS slab bridges, are analyzed to evaluate their seismic risk first based on a deterministic response analysis. The ground motion for the deterministic analysis is chosen such that its maximum acceleration matches the expected maximum PGA in Georgia. The deterministic nonlinear time history analyses show the increase in the curvature demand when a lap splice is provided with non-seismic detailing for the northern regions of Georgia.

A probabilistic analysis is then conducted using a representative bridge from each bridge class. A suite of 48 ground motions is used to account for seismic uncertainty. The capacity and demand imposed on the columns are compared in terms of curvature ductility to evaluate their risk of damage. The probabilities of exceeding four limit states are found. These four limit states correspond to: curvature ductility at the first point of yield in the longitudinal rebar; spalling of cover concrete due to expansive force; exposure of concrete core or yielding of transverse reinforcement, whichever happens first; and lap splice failure in the case of a lap-spliced column, or longitudinal rebar buckling in the no lap splice case. The following are the main conclusions drawn from the probabilistic analyses:

1. For MSSS concrete girder bridges, it is recommended that 6.5-ft lap splice can be provided at the base of the columns with 12-in. spacing for Seismic Zone 1-A irrespective of the site class. For Site Class B, given a probability of exceedance of Limit State 1 of 13.83% for Region 1 with a PGA equal to 0.16 g, a transverse reinforcement spacing of 3-in. could be provided. For the rest of the state, lap splice with non-seismic spacing is sufficient (refer to Sections 6.2.1.1 and 6.2.1.2).

   For Site Class C, Regions 1 and 2 with PGAs 0.19 g and 0.17 g, respectively, fall in Seismic Zone 1-B. For these cases, it is recommended that seismic spacing of 3-in. be provided to reduce the risk of exceeding Limit State 1 from 23.51% and 16.11% to 8.03% and 4.78%, for Regions 1 and 2, respectively. The 6.5-ft lap splice can be at the base of the column for this site class (refer to Section 6.2.1.3).

   For Site Class D, Regions 3–5 fall in Seismic Zone 1-B. Of these, seismic spacing is recommended for Region 3 to reduce the risk of exceeding Limit State 1 from 13.83% to 3.90% (refer to Section 6.2.1.4).

   Regions 1 and 2 for Site Class D and Regions 1–5 for Site Class E fall in Seismic Zone 2. For Seismic Zone 2, it is recommended that the lap splice not be provided at the base of the column, irrespective of the site class (refer to Section 6.2.1.5).

2. For MSC steel girder bridges, it is recommended that 9-ft lap splice can be provided at the base of the columns with 12-in. spacing for Seismic Zone 1-A, irrespective of the site class. For Site Class B, given a probability of exceedance of Limit State 1 of 13.47% for Region 1 with a PGA equal to 0.16 g, a transverse reinforcement spacing of 3-in. could be provided. For the rest of the state, lap splice with non-seismic spacing is sufficient (refer to Sections 6.2.2.1, 6.2.2.2, and 6.2.2.3).

For Seismic Zone 1-B for Site Classes C and D, the 9-ft lap splice could be provided at the base of the column with transverse reinforcement spacing recommended equal to 3-in. to reduce the risk of exceeding Limit State 1 by approximately 10%. Relative to Limit State 2, the probabilities of limit-state exceedance may be acceptable for the lap splice and non-seismic spacing (refer to Sections 6.2.2.3 and 6.2.2.4).

For Seismic Zone 2, if designing for Limit State 1, it is recommended that the lap splice not be provided at the base of the column, irrespective of the site class D or E (refer to Sections 6.2.2.4 and 6.2.2.5).

3. For MSSS steel girder bridges, the results of the analysis show that the increase of legs from two to four for stirrups in each direction does not significantly reduce the probability of exceeding defined limit state (refer to Section 6.2.3). Site Class A does not require seismic detailing, as the seismic risk values are within the acceptable range (refer to Section 6.2.3.1). However, risk values are larger than 25% of exceeding Limit State 1 for Regions 1 and 2 (Site Class B and C), Regions 1-3 (Site Class D) and Regions 1-5 (Site Class E). Moreover, Region 1 in Site Class D has a probability of 25.85% of exceeding Limit State 2, and in Site Class E a probability of exceedance of 35.68% for Limit State 3.

4. For multi-span simply supported slab bridges, the conventional practice is to support the bridge superstructure on piles. The pile-bent connection is created such that the pile is embedded into the bent cap a certain distance. In Georgia, the typical practice is to extend the pile 1-ft into the cap if the pile diameter is 20-in. or less.

   Specification 10.7.1.2 in the latest AASHTO LRFD Bridge Design Specifications (2014) suggests that the pile should extend at least 12-in. into the cap, which is the only

requirement in Seismic Zone 1. This specification is in agreement with the experimental results by Ziehl et al. [56] in 2012 (refer to Section 5.2.4.4). The pile embedment length does not significantly affect the pile lateral strength.

Additionally, according to Specification 5.13.4.6.2 [1], for Seismic Zone 2, piles may be used to resist both axial and lateral loads. The minimum depth of embedment and axial and lateral pile resistances required for seismic loads must be determined by design criteria established by site-specific geological and geotechnical investigations. Concrete piles are to be anchored to the pile footing or cap by either embedment of reinforcement or anchorages to resist uplift forces. Dowel bars designed as per the development length criterion must be provided between the pile and bent to resist uplift forces.

The MSSS slab bridge class shows much lower limit state exceedance probabilities compared to the other three bridge classes (refer to Section 6.2.4). This can be attributed to a large number of piles in a bent (i.e., 7 piles in a bent) and the metal shell on the reinforced concrete piles. In addition, the dowel pile case shows a slightly lower probability because of the additional dowel bars in the piles. The embedded pile case is similar to the dowel pile case, as both cases have similar lateral capacities. Therefore, the embedded pile and dowel pile cases exhibit similar performance.

5. Both 4-in. and 6-in. spacings of transverse reinforcement provide the same confinement capacity for longitudinal lap-spliced bars in plastic hinge regions, with a small difference in the core concrete ductility (refer to Chapter 7). From the obtained results of bridge column responses, the comparisons of no lap-spliced columns with transverse spacings of 12-in. versus 3-in. show that the responses are similar, with only a slight decrease (see Figures 7.2–7.5). Thus, for the level of seismic hazard present in the state of Georgia,

there is not a significant increase in performance for columns with tight transverse reinforcement spacing. From the results of the seismic risk assessment, the risk probabilities for the #3 @ 3 in., #6 @ 4-in., and #6 @ 6-in. cases for Georgia bridges are similar, with a difference of approximately 5% under the maximum factored PGA of 0.35 g in Georgia (see Table 7.1). Thus, for Georgia bridges, 6-in. maximum transverse reinforcement spacing is acceptable.

REFERENCES

1. AASHTO. 2014. *AASHTO LRFD Bridge Design Specifications*. American Association of State Highway and Transportation Officials, Washington, D.C.
2. Biryol, C.B., L.S. Wagner, K.M. Fischer, and R.B. Hawman. 2016. "Relationship between Observed Upper Mantle Structures and Recent Tectonic Activity across the Southeastern United States." *Journal of Geophysical Research: Solid Earth* 121 (5): 3393–414. doi:10.1002/2015JB012698.
3. Hite, M.C. 2007. "Evaluation of the Performance of Bridge Steel Pedestals under Low Seismic Loads." Ph.D. dissertation, Georgia Institute of Technology. https://smartech.gatech.edu/bitstream/handle/1853/14485/hite_monique_c_200705_phd.pdf .
4. Georgia DOT (GDOT). 2017. "Georgia Department of Transportation Bridge and Structures Design Manual." Oct. 2005. http://www.dot.ga.gov/PartnerSmart/DesignManuals/BridgeandStructure/GDOT_Bridge_and_Structures_Policy_Manual.pdf.
5. Jaradat, O.A., D.I. McLean, and M.L. Marsh. 1998. "Performance of Existing Bridge Columns under Cyclic Loading – Part 1: Experimental Results and Observed Behavior." *ACI Structural Journal* 95 (6): 695–704.
6. Lin, Y., and N.M. Hawkins. 1996. *Seismic Behavior of Bridge Pier Column Lap Splices*. Ph.D. dissertation, University of Illinois at Urbana–Champaign.
7. Mander, J.B., and N. Basöz. 1999. "Seismic Fragility Curve Theory for Highway Bridges." In *Technical Council on Lifeline Earthquake Engineering Monograph, Proceedings of the*

1999 5th U.S. Conference on Lifeline Earthquake Engineering: Optimazing Post-Earthquake Lifeline System Reliability: 31–40. ASCE.

8. Nielson, B.G. 2005. “Analytical Fragility Curves for Highway Bridges in Moderate Seismic Zones.” *Civil and Environmental Engineering*. Georgia Institute of Technology.
9. Nielson, B.G., and R. DesRoches. 2007. “Analytical Seismic Fragility Curves for Typical Bridges in the Central and Southeastern United States.” *Earthquake Spectra* 23 (3): 615–33.
10. Ghosh, J., and J.E. Padgett. 2010. “Aging Considerations in the Development of Time-Dependent Seismic Fragility Curves.” *Journal of Structural Engineering* 136 (12): 1497–1511.
11. Zhiqiang, W., and G.C. Lee. 2009. “A Comparative Study of Bridge Damage due to the Wenchuan, Northridge, Loma Prieta and San Fernando Earthquakes.” *Earthquake Eng & Eng Vib* 8 (8): 251–61. doi:10.1007/s11803-009-9063-y.
12. Mylonakis, G., C. Syngros, and G. Gazetas. 2006. “The Role of Soil in the Collapse of 18 Piers of Hanshin Expressway in the Kobe Earthquake.” *Earthquake Engineering & Structural Dynamics* 35 (5): 547–75. doi: 10.1002/eqe.543.
13. Orangun, C.O., J.O. Jirsa, and J.E. Breen. 1977. “A Reevaluation of Test Data on Development Length and Splices.” *ACI Journal Proceedings* 74 (3): 114–22.
14. Sozen, M.A., and J.P. Moehle. 1990. *Development and Lap-Splice Lengths for Deformed Reinforcing Bars in Concrete: A Report to the Portland Cement Association, Skokie, IL, and the Concrete Reinforcing Steel Institute, Schaumburg, IL*. Portland Cement Association, 109 pp.
15. Cairns, J., and P.D. Arthur. 1979. “Strength of Lapped Splices in Reinforced Concrete

Columns." *ACI Journal Proceedings* 76 (2): 277–96. doi:10.14359/6947.

16. Paulay, T., T.M. Zanza, and A. Scarpas. 1981. *Lapped Splices in Bridge Piers and in Columns of Earthquake Resisting Reinforced Concrete Frames*. University of Canterbury, Department of Civil Engineering, 117 pp.
17. Lynn, A.C., J.P. Moehle, and S.A. Mahin. 1996. "Seismic Evaluation of Existing Reinforced Concrete Building Columns." *Earthquake Spectra* 12 (4): 715–39.
18. Melek, M., and J.W. Wallace. 2004. "Cyclic Behavior of Columns with Short Lap Splices." *ACI Structural Journal* 101 (6): 802–11. doi:10.14359/13455.
19. Cho, J.Y., and J.A. Pincheira. 2004. "Nonlinear Modeling of RC Columns with Short Lap Splices." *13th World Conference on Earthquake Engineering,* Paper No. 1506, Vancouver, B.C.
20. Harajli, M.H., B.S. Hamad, and A.A. Rteil. 2005. "Effect of Confinement on Bond Strength between Steel Bars and Concrete." *ACI Structural Journal* 101 (S58): 595–603.
21. Wu, C., G.C. Jeffery, S. Volz, R.K. Brow, and M.L. Koenigstein. 2013. "Global Bond Behavior of Enamel-Coated Rebar in Concrete Beams with Spliced Reinforcement." *Construction and Building Materials* 40: 793–801. doi:10.1016/j.conbuildmat.2012.11.076.
22. Hamad, B.S., and S. Najjar. 2002. "Evaluation of the Role of Transverse Reinforcement in Confining Tension Lap Splices in High Strength Concrete." *Materials and Structures* 35 (4). Kluwer Academic Publishers: 219–28. doi:10.1007/BF02533083.
23. El-Azab, M.A., H.M. Mohamed, and A. Farahat. 2014. "Effect of Tension Lap Splice on the Behavior of High Strength Self-Compacted Concrete Beams." *Alexandria Engineering Journal* 53 (2): 319–28. doi:10.1016/j.aej.2014.01.009.
24. Mabrouk, R.T.S., and A. Mounir. 2017. "Behavior of RC Beams with Tension Lap Splices

Confined with Transverse Reinforcement Using Different Types of Concrete under Pure Bending." *Alexandria Engineering Journal*. In press. doi:10.1016/j.aej.2017.05.001.

25. Aboutaha, R.S., M.U. Engelhardt, J.O. Jirsa, and M.F. Kreger. 1996. "Retrofit of Concrete Columns with Inadequate Lap Splices by the Use of Rectangular Steel Jackets." *Earthquake Spectra* 12 (4): 693–714. doi:10.1193/1.1585906.
26. Biskinis, D., and M.N. Fardis. 2007. "Effect of Lap Splices on Flexural Resistance and Cyclic Deformation Capacity of RC Members." *Beton- Und Stahlbetonbau* 102 (S1). WILEY-VCH Verlag: 51–9. doi:10.1002/best.200710105.
27. Harajli, M.H., and F.Dagher. 2008. "Seismic Strengthening of Bond-Critical Regions in Rectangular Reinforced Concrete Columns Using Fiber-Reinforced Polymer Wraps." *ACI Structural Journal* 105 (1): 68–77.
28. Hannewald, P. 2013. "Seismic Behavior of Poorly Detailed RC Bridge Piers." Ph.D. thesis, *École Polytechnique Fédérale de Lausanne*.
29. Priestley, M.J.N., F. Seible, and G.M. Calvi. 1996. *Seismic Design and Retrofit of Bridges*.
30. Tariverdilo, S., A. Farjadi, and M. Barkhordary. 2009. "Fragility Curves for Reinforced Concrete Frames with Lap-Spliced Columns." *International Journal of Engineering – Transactions A: Basics* 22 (3): 213.
31. Canbay, E., and R.J. Frosch. 2005. "Bond Strength of Lap-Spliced Bars." *ACI Structural Journal* 102 (4): 605–14..
32. MacKay, B., D. Schmidt, and T. Rezansoff. 1989. "Effectiveness of Concrete Confinement on Lap Splice Performance in Concrete Beams under Reversed Inelastic Loading." *Canadian Journal of Civil Engineering*, 16 (1). NRC Research Press Ottawa, Canada : 36–44. doi:10.1139/l89-005.

33. Paulay, T. 1982. “Lapped Splices in Earthquake-Resisting Columns.” *ACI Journal Proceedings* 79 (6): 458–69. doi:10.14359/10920.

34. Abdel-Kareem, A.H., and H. Abousafa. 2013. “Effect of Transverse Reinforcement on the Behavior of Tension Lap Splice in High-Strength Reinforced Concrete Beams.” *World Academy of Science, Eng. & Technol. Intern. Journal of Bioeng. & Life Sciences* 7 (12): 989–96.

35. Mander, J.B., M.J.N. Priestley, and R. Park. 1988. “Theoretical Stress–Strain Model for Confined Concrete.” *Journal of Structural Engineering* 114 (8): 1804–1826. doi:10.1061/(ASCE)0733-9445(1988)114:8(1804).

36. Rix, G.J., and J.A. Fernandez-Leon. 2004. “Synthetic Ground Motions for Memphis, TN.”

37. FHWA. 2002. “National Bridge Inventory.”

38. FEMA. 2003. “HAZUS. Earthquake Model, Technical Manual.” Federal Emergency Management Agency, Washington D.C.

39. Rojahn, C., and R.L. Sharpe. 1985. *Earthquake Damage Evaluation Data for California.* ATC-13, Applied Technology Council, Redwood City, Calif., 492 pp.

40. Basoz, N., and A.S. Kiremidjian. 1999. “Development of Empirical Fragility Curves for Bridges.” *Technical Council on Lifeline Earthquake Engineering Monograph*, No. 16. ASCE: 693–702.

41. Der Kiureghian, A. 2002. “Bayesian Methods for Seismic Fragility Assessment of Lifeline Components.” In *Acceptable Risk Processes, Lifelines and Natural Hazards,* ed. C. Taylor and E. Vanmarcke (ASCE Monograph No. 21): 61–77.

42. Shinozuka, M., M.Q. Feng, H. Kim, T. Uzawa, and T. Ueda. 2003. “Statistical Analysis of Fragility Curves.” *Multidisciplinary Center for Earthquake Engineering Research,*

MCEER-03-0002.

43. Ghosh, J. 2013. “Parameterized Seismic Reliability Assessment and Life-Cycle Analysis of Aging Highway Bridges.” Ph.D. dissertation, Rice University, Houston, Tex. http://hdl.handle.net/1911/71955.

44. ChaiI, Y.H., M.J.N. Priestley, and F. Seible. 1991. “Seismic Retrofit of Circular Bridge Columns for Enhanced Flexural Performance.” *ACI Structural Journal* 88 (5): 572–84. doi:10.14359/2759.

45. Sun, Z., M.J.N. Priestley, and F. Seible. 1993. “Diagnostics and Retrofit of Rectangular Bridge Columns for Seismic Loads.” University of California, Dept. of Applied Mechanics & Engineering Sciences, San Diego, Calif.

46. Lehman, D.E. 2000. “Seismic Performance of Well-Confined Concrete Bridge Columns.” Berkeley: Pacific Earthquake Engineering Research Center.

47. Calderone, A., D.E. Lehman, and J.P. Moehle. 2001. “Behavior of Reinforced Concrete Bridge Columns Having Varying Aspect Ratios and Varying Lengths of Confinement.” Berkeley: Pacific Earthquake Engineering Research Center.

48. Brown, W.A., D.E. Lehman, and J.F. Stanton.. 2006. “Bar Buckling in Reinforced Concrete Bridge Columns.” PEER Report 2007/11. Pacific Earthquake Engineering Research Center, Berkeley.

49. Cornell, C.A., F. Jalayer, R.O. Hamburger, and D.A. Foutch. 2002. “Probabilistic Basis for 2000 SAC Federal Emergency Management Agency Steel Moment Frame Guidelines.” *Journal of Structural Engineering* 128 (4): 526–33. doi:10.1061/(ASCE)0733-9445(2002)128:4(526).

50. Mazzoni, S., F. Mckenna, M.H. Scott, and G.L. Fenves. 2006. “Open System for

Earthquake Engineering Simulation (OpenSees): OpenSees Command Language Manual." University of California, Berkeley.

51. Roeder, C.W., and J.F. Stanton. 1983. "Elastomeric Bearings: State-of-the-Art." *Journal of Structural Engineering* 109 (12): 2853–71. doi:10.1061/(ASCE)0733-9445(1983)109:12(2853).
52. Choi, E. 2002. "Seismic Analysis and Retrofit of Mid-America Bridges." Georgia Institute of Technology.
53. Scharge, L. 1981. "Anchoring of Bearings by Friction, Joint Sealing and Bearing Systems for Concrete Structures." *World Congress on Joints and Bearings*.
54. Mander, J.B., D.K. Kim, S.S. Chen, and G.J. Premus. 1996. "Response of Steel Bridge Bearings to Reversed Cyclic Loading." National Center for Earthquake Engineering Research, State University of New York, Buffalo.
55. Steelman, J.S., E.T. Filipov, L.A. Fahnestock, J.R. Revell, J.M. Lafave, J.F. Hajjar, and D.A. Foutch. 2013. "Experimental Behavior of Steel Fixed Bearings and Implications for Seismic Bridge Response." *Journal of Bridge Engineering* 19 (8) [A4014007].
56. Ziehl, P.H., J.M. Caicedo, D. Rizos, T. Mays, A. Larosche, M.K. ElBatanouny, and B. Mustain. 2012. "Behavior of Pile to Bent Cap Connections Subjected to Seismic Forces. " SCDOT Research Project No. 672. FHWA Federal Project No. FHWA-SC-12-03.
57. SC DOT. 2006. "SC DOT Bridge Design Manual." South Caroliina Department of Transportation. http://www.scdot.org/doing/technicalPDFs/structuralDesign/bd_manual.pdf